INSTITUT FÜR HYDROLOGIE
ALBERT-LUDWIGS-UNIVERSITÄT FREIBURG I.BR.

Stefan Eppert

Development and application of an event-based model using the GIUH approach for simulation of discharge and solutes

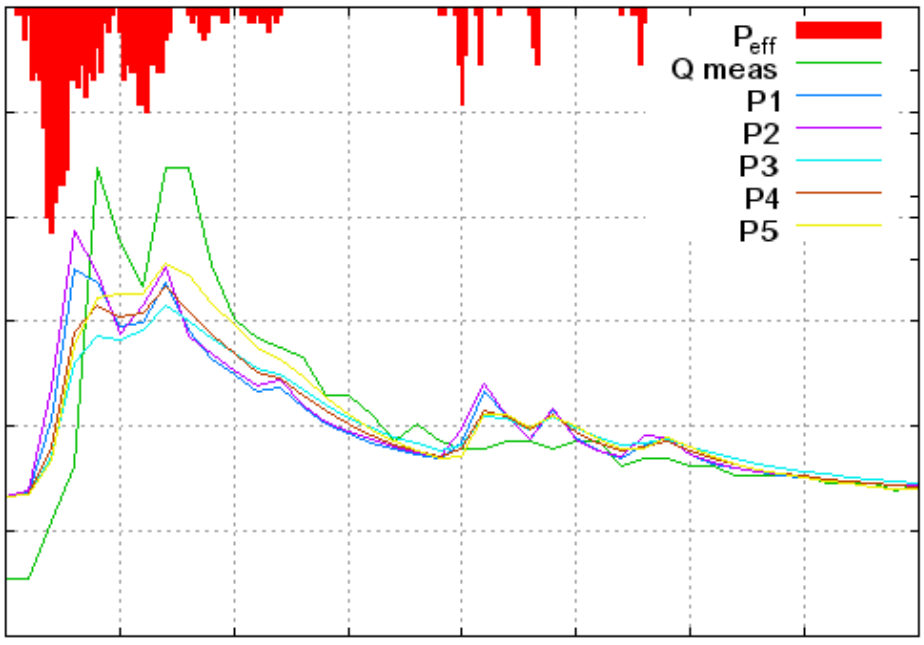

Diplomarbeit unter Leitung von PD Dr. S. Uhlenbrook
Freiburg i. Br., März 2005

INSTITUT FÜR HYDROLOGIE
ALBERT-LUDWIGS-UNIVERSITÄT FREIBURG I.BR.

Stefan Eppert

Development and application of an event-based model using the GIUH approach for simulation of discharge and solutes

Referent: PD Dr. Stefan Uhlenbrook
Koreferent: Dr. Jens Lange

Diplomarbeit unter Leitung von PD Dr. S. Uhlenbrook
Freiburg i. Br., März 2005

Preface

First of all, I would like to thank my parents for enabling me to study. For discussion, proof-reading and help with technical problems, I thank Gunter Adolph, Andrea Schmitz, Laurin Wissmeier, Kiran Majer and Suse Osthoff.

Contents

List of figures

List of tables

List of Abbreviations

τ	time	(sec)
$h(\tau)$	response function	
$\bar{x}$	arithmetic mean of the x_i	
$\bar{y}$	arithmetic mean of the y_i	
^{16}O	oxygen 16	
^{18}O	oxygen 18	
^{1}H	hydrogen 1	
^{2}H	deuterium	
ADE	Advection Dispersion Equation	
A_i	area contributing to a reach or a path	(km^2)
a_{ij}	weight of class j in hill FPD i	
ANN	Artificial Neural Network	
A_{tot}	total area of a catchment	(km^2)
A_ω	average catchment area	
c	concentration	(mg/l)
CE	Calibration Event	
const	pattern of effective precipitation using a constant runoff coefficient	
c_p	concentration of precipitation	(mg/l)
D	dispersion coefficient	(m^2/s)
D8	Deterministic-8 single flow algorithm	
DEM	Digital Elevation Model	
DFG	Deutsche Forschungsgesellschaft (German Research Foundation)	
EMMA	end member mixing approach	
Eq.	equation	
exp	pattern of effective precipitation using an exponential decrease of losses	
FPD	Flow Path Distribution	
GIS	Geographical Information System	
GIUH	Geomorphological Instantaneous Unit Hydrograph	
GLA	Geologisches Landesamt (Geological Survey of Baden-Württemberg)	
GUH	Geomorphological Unit Hydrograph	
GUHmod	Geomorphological Unit Hydrograph Model	
H	water height	(mm)
$h(L_\gamma,t)$	travel time distribution for a path of length L_γ	
H_4SiO_4	silicic acid	
HBV	a conceptual rainfall-runoff model	

HHQ	highest measured discharge	(m^3/s)
HRU	Hydrological Response Unit	
IAEA	International Atomic Energy Agency	
IUH	Instantaneous Unit Hydrograph	
JVM	Java Virtual Machine	
K	mean residence time in a linear store	
k_f	saturated hydrologic conductivity	(m/s)
L_γ	path length	(m)
L_ω	average length of reaches of order ω	
L_Ω	length of the highest order reach in the network	
M	number of hill FPDs	
MHQ	mean high discharge	(m^3/s)
MNQ	mean low discharge	(m^3/s)
MQ	mean discharge	(m^3/s)
N	number of stores	
n	number	
N	number of parameter	
n(x)	width of the network	
NNQ	lowest measured discharge	(m^3/s)
n_R	number of simulation runs	
N_{reach}	total number of reaches in the network	
N_ω	stream number	
P	precipitation	(mm)
p (γ)	probability for path in Γ	
P_D	dispersion parameter	
P_e	Peclet Number	
P_{eff}	effective precipitation	(mm)
Q	runoff	(m^3/s)
q(t)	volume of hillslope response at time t	(m^3)
R^2	coefficient of determination	
R_A	area ratio	
R_B	bifurcation ratio	
R_C	Combined model efficiency for runoff and silica modelling	
R_{eff}	Nash – Sutcliffe model efficiency	
R_L	length ratio	
R_{sample}	ratio of isotopes in the sample	
$R_{standard}$	ratio of isotopes in the standard	
Si	Silica	
t	Time	(sec)
t_0	Mean holding time	(sec)
TAC	Tracer Aided Catchment model	
TAC^D	Tracer Aided Catchment model, distributed	
TIN	Triangular Irregular Network	

TK	topographical map	
u	Water velocity	(m/s)
UH	Unit Hydrograph	
v	average stream velocity	
V - SMOW	Vienna Standard Mean Ocean Water	
vc	channel wave celerity	(m/10 min)
vhf	wave celerity of fast hillslope component	(m/10 min)
vhs	wave celerity of slow hillslope component	(m/10 min)
v_t, v_{H2}, v_{H1}	wave celerity	(m/time step)
w(x)	weight function	
x	path length	(m)
x_i	measured value at time i	
y_i	simulated value at time i	
z	Conversion factor	
α	dispersivity	(m)
β	modified residence time	
γ	path in Γ	
Γ(N)	gamma function	
Γ_p	set of path	
δ	delta value	(‰)
Δt	time step	(sec)
π	Pi	
ω	stream order (Strahler)	

Summary

In this study an event-based semi-distributed rainfall-runoff model is developed. It uses the Geomorphological Instantaneous Unit Hydrograph approach with a representation of catchment topography by Flow Path length Distributions (FPDs) derived from a Digital Elevation Model. Hillslope response is divided into a fast and a slow component, each represented by a FPD and a characteristic wave celerity. These are added and routed through the channel network. At the end the baseflow, which is held constant during the event, is added to catchment response.

Silica concentrations are modelled assuming a fixed silica concentration for each runoff component. The natural isotopes $^{18}0$ and ^{2}H are modelled using an input function for precipitation and a fixed δ-value for baseflow. It is supposed that no fractionation processes take place during routing.

Besides the model, routines for evaluation Monte Carlo simulations and visualization of model outputs and a graphical user interface have been written. The programme is platform independent as it is written in Java.

The model has been applied to the meso-scale Brugga catchment in the Black Forrest in Germany, and to its subcatchment St. Wilhelmer Talbach. The delineation of dominating runoff processes used in the catchment model TAC^{D} is aggregated to two classes and used to determine source areas of the fast and slow hillslope component. Values for wave velocities of the hillslope components and the channel network have been determined by Monte Carlo simulations. In total, 72,000 model runs were made for four events used in calibration. For all events parameter sets exist, that yield Nash-Sutcliffe model efficiencies higher than 0.8 for runoff and higher than 0.6 for silica modelling. Despite the parsimonious parameterization, equifinality complicates the unambiguous determination of validation parameter sets.

Two methods to determine effective precipitation are compared to each other. One assumes a constant runoff value and the other an exponential decrease of losses. Similar results have been achieved with both methods. For each type of effective precipitation and each catchment parameter sets have been determined regarding goodness of runoff prediction, and one parameter set regarding runoff and silica concentrations of the Brugga. This multi-criteria calibration narrowed the parameter space to slower wave celerities which are closer to measured values.

Four events are used for model validation. The best results are obtained with the parameter set determined by multi-criteria calibration, yielding model efficiencies of 0.8 for two events and 0.5 for the third. The fourth event is a rain-on-snow event and cannot be modelled successfully with any validation parameter set.

Isotope modelling does not yield close fits to modelled data, because the large influence of pre-event water is not accounted for in the model concept. For further studies, it is possible to add another parameter to the model which gives a constant or variable fraction of pre-event water for each runoff component to overcome this problem.

The model works successful for events without snow-melt if precipitation data represent area rainfall. For spatially inhomogeneous precipitation events, the regionalisation of data from several rain gauges clearly improves model performance. The model is not as versatile as more complex models like TAC^{D}. But its application in arid regions or ungauged basins seems promising, if limited data availability does not permit the use of its more complex counterparts.

Keywords:
Geomorphological Instantaneous Unit Hydrograph, event-based model, solutes, natural isotopes, multi-criteria calibration, Monte-Carlo simulations

Zusammenfassung

Gegenstand der vorliegenden Arbeit ist die Entwicklung eines Niederschlags-Abfluss-Modells unter Benutzung des *Geomorphological Instantaneous Unit Hydrograph* (GIUH) – Ansatzes. Es werden Abfluss und Stofftransport von Silikat und natürlichen Isotopen auf der Ereignisskala simuliert. Die Topographie des Einzugsgebiets wird durch Fließweglängenverteilungen beschrieben. Schnelle und langsame Abflusskomponenten werden getrennt modelliert und im Gerinnenetz zusammengeführt. Jeder Abflusskomponente werden eine Fließweglängenverteilung und eine charakteristische Fließgeschwindigkeit zugewiesen. Der Basisabfluss wird während des Ereignisses konstant gehalten.

Zur Stofftransportmodellierung wird von einer konstanten Silikatkonzentration für jede Abflusskomponente ausgegangen. Für die natürlichen Isotope ^{2}H und ^{18}O werden eine Input-Funktion der Isotopensignatur des Niederschlags und ein konstanter δ-Wert des Basisabflusses verwendet.

Neben dem eigentlichen Modell wurden Routinen zur Durchführung von Monte Carlo – Simulationen, zur Evaluation und zur Darstellung der Ergebnisse, sowie eine graphische Benutzeroberfläche entwickelt. Das Programmpaket ist in Java geschrieben, dadurch kann es unter allen gängigen Betriebssystemen verwendet werden.

Das Modell wurde im mesoskaligen Bruggaeinzugsgebiet im Schwarzwald und einem Teileinzugsgebiet, dem St. Wilhelmer Talbach angewendet. Die Ausweisung der Herkunftsräume der schnellen und langsamen Abflusskomponenten basiert auf der Raumgliederung nach dominanten Abflussprozessen des TAC^{D}-Modells. Die Fließgeschwindigkeiten der Hangkomponenten und des Gerinnenetzwerks wurden mit Monte Carlo-Simulationen kalibriert. Insgesamt wurden 72.000 Modelldurchläufe für vier Kallibrierungsereignisse berechnet. Für alle Ereignisse konnten Parametersätze gefunden werden, mit denen sich Nash-Sutcliffe-Modelleffizienzen von mindestens 0,8 für die Abfluss- und 0,6 für die Silikatmodellierung erzielen lassen. Trotz der geringen Anzahl an Kallibrierungsparametern erschwert Equifinalität die Identifikation eines eindeutigen Parametersatzes.

Für die Berechnung des Effektivniederschlags werden zwei Methoden verwendet, zum einen ein zeitlich konstanter Abflussbeiwert und zum anderen eine exponentielle Abnahme der Verlustrate. Beide liefern vergleichbar gute Ergebnisse. Für die Einzugsgebiete und die zwei Arten der Effektivniederschlagsberechnung wurden Parametersätze aufgrund der Güte der Abflusssimulation bestimmt. Ein weiterer Parametersatz wurde unter Betrachtung der Güte von Abfluss- und Silikatmodellierung im Bruggaeinzugsgebiet bestimmt. Diese *multi-criteria*-Kallibrierung stellt ein wirkungsvolles Mittel zur Einschränkung des Wertebereichs der erfolgreichen

Parametersätze dar. Die so ermittelten Fließgeschwindigkeiten liegen näher an den in Tracerexperimenten gemessenen Werten.
Vier Ereignisse wurden zur Modellvalidierung verwendet. Die besten Ergebnisse sind mit dem mittels *Multi-criteria*-Kallibrierung gewonnenen Parametersatz erzielt worden. Für die Abflusssimulation wurden bei zwei Ereignissen Modeleffizienzen von 0,8 und bei einem Ereignis von 0,5 erreicht. Das vierte Ereignis ist durch Schneeschmelze beeinflusst und lässt sich mit keinem Parametersatz zufrieden stellend nachbilden.

Bei der Isotopenmodellierung konnte der Deuteriumgehalt im Abfluss nicht erfolgreich simuliert werden, da der nicht zu vernachlässigende Einfluss von *pre-event*-Wasser im Modellkonzept nicht berücksichtigt ist. In späteren Studien kann dies durch die Einführung eines zeitlich konstanten oder variablen Parameters geändert werden, der den Anteil von *pre-event*-Wasser im Abfluss der einzelnen Komponenten angibt.

Das Modell liefert gute Ergebnisse für nicht schneebeeinflusste Ereignisse, wenn die Niederschlagsdaten den Gebietsniederschlag gut wiedergeben. Für Ereignisse mit hoher räumlicher Variabilität verbessern sich die Modellergebnisse deutlich, wenn die Niederschlagsmesswerte mehrerer Stationen auf das Gebiet regionalisiert werden. Das entwickelte Modell ist nicht so vielseitig einsetzbar wie komplexere Modelle (z.B. TAC^D), bietet sich aber an, wenn diese aufgrund fehlender Daten nicht einsetzbar sind. Dies trifft auf viele aride und ungemessene Gebiete zu.

Schlüsselwörter:
Geomorphological Instantaneous Unit Hydrograph, Ereignisskale, Stofftransport, natürliche Isotope, Multi-criteria-Kallibrierung, Monte-Carlo-Simulationen

1 Introduction

Rainfall-runoff modelling deals with the prediction of stream discharge for known or assumed pattern of effective precipitations. Due to the increased computer power available, physics-based distributed models have become very popular in the last decade. They work successfully and allow e.g. the investigation of internal processes in the catchment, solute modelling and predictions on the effects of landuse change. The drawback is that their huge data requirements limit their sound application to well-known micro-scale catchments.

To scale up model application a simpler process description is needed. In the project "runoff generation and catchment modelling", funded by the German Research Foundation (DFG), numerous studies have taken place in the Brugga catchment to discover and quantify runoff generation processes. The distributed conceptual model TAC^D has been developed for process-oriented modelling at the meso-scale. Due to its simplified but well-founded process representation, meso-scale catchment behaviour can be reproduced successfully.

However, data requirements are still high and application to other catchments is laborious.

1.1 Objective

The objective of this study is to develop a parsimonious semi-distributed event-based model and to check if it can compete with more complex models. The Geomorphological Instantaneous Unit hydrograph (GIUH or GUH, RODRIGUEZ-ITURBE AND VALDES 1979) approach is used in this study. Catchment topography is described with flow path length distributions (SNELL AND SIVAPALAN 1994) derived from digital terrain models. It can be resorted to the diploma thesis of ARMBRUSTER (1997) who applied the GIUH to one event in the St. Wilhelmer Talbach catchment using flow velocities measured by tracer experiments. Also, for the first time, modelling silica concentrations and natural isotopes is approached by use of the GIUH. This provides data for multi-criteria calibration.

This work follows the rationale of SIVAPALAN (2003), that the known process complexity at hillslope scale is difficult to scale up to watershed scale, and that therefore simplifications have to be made to filter out unnecessary details while keeping the essential aspects of watershed heterogeneity.

Hillslope response is split into a fast and a slow component, based on the delineation of runoff processes used by TAC^D (UHLENBROOK 1999, ROSER 2001). Other aspects like data preprocessing where kept to a minimum to check the potential of simple operations for runoff prediction.

Thus minimum data requirements are precipitation data, a digital terrain model of the catchment and some measured events for calibration. A classification of sources of fast and slow runoff components is advisable, especially for silica modelling.

These requirements are easily met, even for ungauged basins, if a temporal runoff gauging station can be installed.

1.2 Proceeding

Based on the Turbo Pascal programme of ARMBRUSTER (1997), a modelling environment is developed, consisting of the modelling routine, a parameter sampling module for Monte Carlo simulations, an evaluation tool to get quantitative measures for goodness of fit, a Graphical User Interface (GUI) and a visualization routine based on the freeware programme Gnuplot. It is written in Java to be platform independent.

This model, GUHmod (Geomorphological instantaneous Unit Hydrograph model), is applied to two nested meso-scale catchments, the Brugga and the St. Wilhelmer Talbach in the Black Forrest in south-western Germany.

Monte Carlo simulations are conducted to determine validation parameter sets from for events. This is done for both catchments and for two methods to determine effective precipitation. One parameter set is determined using multi-criteria calibration, namely discharge and silica concentrations in runoff of the Brugga at Oberried.

Four events are used for model evaluation. Validation parameter sets are transferred from one catchment to the other to check for the influence of catchment size.

2 Study Site

2.1 Position and Topography

GUHmod, the model developed in this study, is applied to the Brugga basin in the Black Forest in southwest Germany. A sub-basin in the south-east of the catchment, the St. Wilhelmer Talbach, is also explicitly modelled.

The Brugga catchment covers an area of 40 km², the St. Wilhelmer Talbach covers 15.4 km². So both may be classified as meso-scale catchments, which range from 10^1 to 10^3 km² according to BLÖSCHL (1996).

The Brugga basin is mountainous with a maximum height of 1492 m above mean sea level at the Feldberg and a minimum height of 434 m at the outlet in Oberried. Mean slope is 19.5°, relief intensity is high. Steep forested hillslopes make up 75% of the catchment, valley floors 5% and hilly uplands 20% (GÜNTNER ET AL. 1999). Urban settlements cover only 2% of the area.

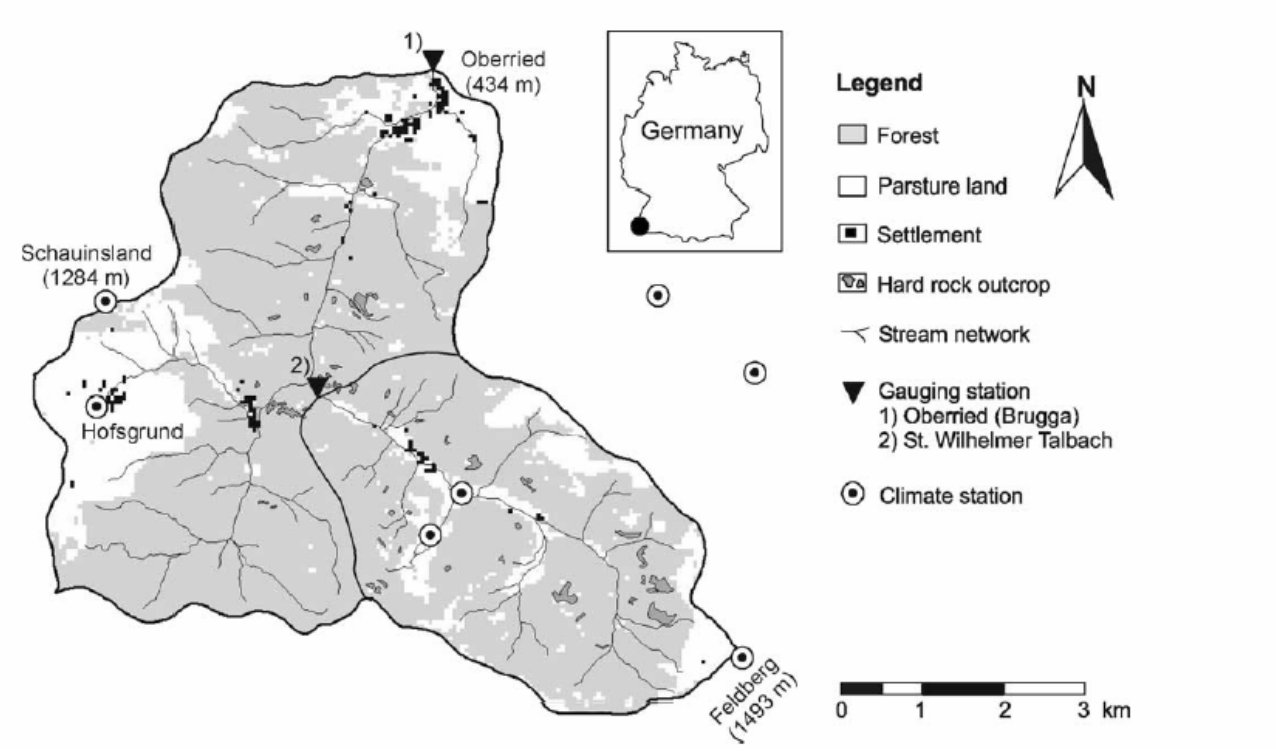

Figure 2.1: The Brugga catchment with monitoring network (UHLENBROOK ET AL. 2002).

The St. Wilhelmer Talbach basin ranges in elevation from 636 to 1496 m. It was reshaped by glacial erosion in the quaternary. The valley is a glacial trough, periglacial blocks and debris and moraines are abundant.

2.2 Climate

Mean annual precipitation amounts to 1750 mm in the Brugga and 1850 mm in the St. Wilhelmer Talbach basin. Maximum precipitation occurs from June to August. Spatial variability of precipitation is high (TETZLAFF AND UHLENBROOK 2005). Temperature is height-dependant with a gradient of -0.6° C per 100 m, mean temperature is 7.7° C.

2.3 Hydrogeology

The study area is underlain by different metamorphic and intrusive rocks. This bedrock material is mostly covered by brown soils developed in the glacial and periglacial drift covers, and is exposed on steep slopes (WENNINGER ET AL. 2004). Steep boulder fields with very high hydraulic conductivities (10^{-2}–10^{-1} m s^{-1}) and flow velocities of several metres per hour often occur below these outcrops (MEHLHORN 1998). As the bedrock permeability is low (between 10^{-10} and 10^{-5} m s^{-1}) (STOBER 1995), the most important area for runoff generation is the drift cover (GLA 1981; UHLENBROOK ET AL. 2002). The drift cover was mainly formed in the Pleistocene during widely periglacial conditions by solifluction processes. Three layers were identified. The bedrock and the autochthon weathering zone is overlain by the first periglacial layer, the so-called base layer. A tile-like orientation of the coarse material is characteristic for this layer. The matrix is compact and consolidated, and hydraulic conductivity is low. Above this is the main layer, with a larger amount of fine material, higher water and air storage capacity, and without any regular orientation of the coarse material. The top layer consists of coarse material due to frost and melting processes (HÄDRICH AND STAHR 1997) and washout of fine soil material. At the lower parts of the hillslopes, the periglacial hillslope layers and the fluvioglacial material of the valley floor are interlocked, often in cones of accumulated material or alluvial fans. Here the hydraulic conductivity can be assumed to be high due to deposition of coarse material. The depth to bedrock is about 1–4 m at the slopes, up to 10 m at the foot of the hillslopes, and unknown on the valley floor (GLA 1981).

2.4 Hydrology

Both streams show a nivo-pluvial regime due to snowmelt in spring (Figure 2.1). The secondary peak in December can be explained by intrusion of warm air and rain-on-snow effects (UHLENBROOK ET AL. 2002). The Brugga discharges into the Dreisam, which is also shown in Figure 2.2.

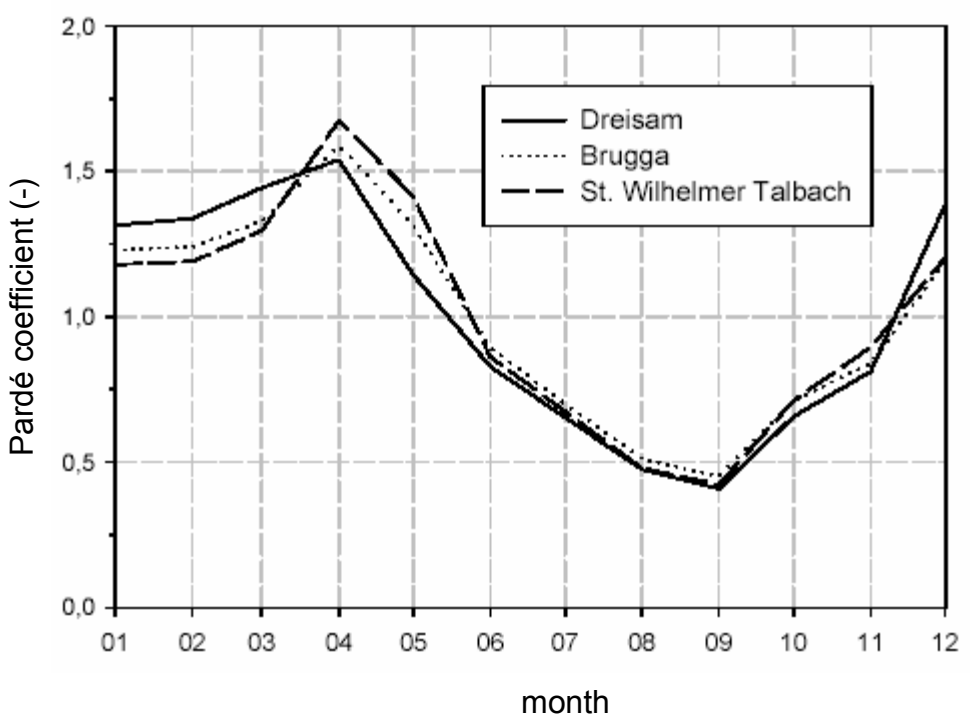

Figure 2.2: Runoff regimes (Period 1972-1992).

The big difference between mean discharge MQ and mean high discharge MHQ (Table 2.1) shows the small storage capacity of the crystalline catchments and stress the importance of fast runoff components (UHLENBROOK 1999).

Table 2.1: Runoff characteristics (LfU 1996 in Roser 2001, edited).

	Brugga	**St. Wilhelmer Talbach**
Time series	1934-1994	1955-1994
HHQ (m^3/s)	55.1 (23/11/44)	11.6 (22/12/91)
MHQ (m^3/s)	15.75	6.6
MQ (m^3/s)	1.54	0.66
MNQ (m^3/s)	0.37	0.13
NNQ (m^3/s)	0.19 (03/09/64)	0.07 (02/09/55)

2.5 Conclusions

The Brugga basin is a mountainous, mostly forested meso-scale catchment. Precipitation and temperature are highly heterogeneous in space and time. The catchment is underlain by crystalline rock with small storage capacity.

3 Theory and State of the Art

Mathematical models in hydrology aim at representing natural processes using equations. The modelled entity (catchment, hillslope etc.) is seen as a system with a defined relationship between inputs and outputs, the transfer function. Thus rainfall-runoff-modelling deals with finding the runoff produced by precipitation events.

3.1 Model Classification

There are several approaches to classify models. Considering model complexity, BECK (1991) distinguishes between metric, conceptual and physics-based models. Regarding spatial discretisation, one can divide them into lumped, semi-distributed and distributed (TODINI 1988). Models may be either predictive or investigative (O'CONNEL 1991). The former give answers to a specific question ("How much runoff will there be?"), while the latter are used to confirm one's perceptional model of a catchment ("What are the dominant processes?").

Metric models treat the system as a *black box*, disregarding the controlling processes. A certain type of transfer function is assumed, and parameters are chosen to fit measured calibration data. In general, these models are lumped (disregarding catchment structure), simple, and fast to apply. Given a time series of rainfall-runoff data long enough for proper calibration, metric models can provide good estimations of runoff and are still used in flood prediction (YOUNG 2002). Recently, artificial neural networks (ANNs) have become quite popular metric models as they are capable of identifying nonlinear relationships between input and output data (DAWSON & WILBY 2001). Metric models are also called empirical, analytical or parametric models.

Physics-based models try to model catchment response as realistic as possible. They are distributed, representing the catchment by a grid of cells. Water flux from cell to cell is modelled solving differential equations. These models are powerful and versatile, but requiring many parameters. This limits their application to well-known, micro-scale catchments. Mike-She (REFSGAARD AND STORM 1995) is an example for physics-based models.

Conceptual models are positioned in between these extremes. In contrast to metric models, they try represent dominant processes in the catchment. Using analogies and simplifications, their complexity and need for parameters is small compared to physics-based models. Conceptual models may be lumped, distributed or semi-distributed, dividing the catchment into functional units called hydrotopes or hydrological response units (HRUs). HBV (BERGSTRÖM 1992) is an example for conceptional models.

3.2 Theory of Unit Hydrograph

The unit hydrograph (SHERMAN 1932) is a lumped, discrete routing method to transfer rainfall to runoff at the basin outlet. It is linear and time-invariant, i.e. two units of precipitation will produce twice as much runoff as one unit and the same amount of precipitation causes the same amount of runoff at any time. A uniform distribution of precipitation in the catchment is assumed.

The linearity assumption has proved to work better for effective than for total precipitation. Therefore, runoff is separated into baseflow and storm runoff (also called direct runoff), only the latter being influenced by the precipitation event. The part of rainfall that transforms into storm runoff is called effective rainfall, the ratio of storm runoff to total runoff is called runoff coefficient. Effective precipitation is used as input data, output data represents storm runoff.

Assuming a uniform distribution of precipitation may be a gross simplification, especially for convective events and in areas with pronounced topography.

First, the catchment response to a normalized *unit* input of a certain length is calculated. Then for each time-step during an event, this response is multiplied by the actual amount of input and the resulting curves are superponed:

$$Q_D(t) = \sum_{\tau=1}^{t} P_{eff}(t-\tau+1)\, h(\tau) \tag{3.1}$$

where t denotes time, Q_D storm runoff, P_{eff} effective precipitation and $h(\tau)$ the response function. For a detailed description of the unit hydrograph and methods to derive response functions, see DYCK AND PESCHKE (1989, pp. 315-333).

The unit hydrograph is a well-understood and frequently used concept. It has been subject to many enhancements. DOOGE (1959) reformulated it to process instantaneous (Dirac) impulses, changing Eq. (3.1) to the convolution integral

$$Q_D(t) = \int_0^t P_{eff}(t)\, h(t-\tau)dt \tag{3.2}$$

and using the response function

$$h(t) = \frac{1}{K}\exp(-\frac{t}{K}) \tag{3.3}$$

where K is a time, which can be interpreted as the mean residence time in a linear store. As this approach only considers the dynamic response of the catchment, residence time equals response time.
This approach is called instantaneous unit hydrograph (IUH).

NASH (1959) introduced a cascade of linear stores in series for modelling hydrograph shape, using two parameters to determine the response function:

$$h(t) = \left(\frac{t}{K}\right)^{N-1} \frac{\exp(-t/K)}{K\,\Gamma(N)} \tag{3.4}$$

where N is the number of stores and K the mean residence time. Γ(N) is the gamma function.

The unit hydrograph is still used as a routing method, e.g. in the IHACRES model (JAKEMAN ET AL. 1990).

3.2.1 Geomorphological Instantaneous Unit Hydrograph based on Horton ratios

RODRIGUEZ-ITURBE AND VALDES (1979) introduced the geomorphological instantaneous unit hydrograph (GIUH), also called geomorphological unit hydrograph (GUH), to link hydrograph shape to channel network characteristics:

> "The convergence of overland flow is a major cause of the growth upslope of the channels making up the network, but, on the other hand, hollows are a cause of the occurrence of overland flow. From this point of view the drainage network itself may be seen as a reflection of the runoff-producing mechanisms occurring in the basin. (...) The objective is then to explicitly derive the IUH through its connection with the (...) Horton Laws of basin composition." (RODRIGUEZ-ITURBE 1993)

The channel network is described using the STRAHLER (1957) ordering scheme for classifying its reaches. Streams which start from a spring are assigned the first order. At each confluence of reaches of the same order ω, the downstream reach is assigned an order of ω+1 (Figure 3.1).

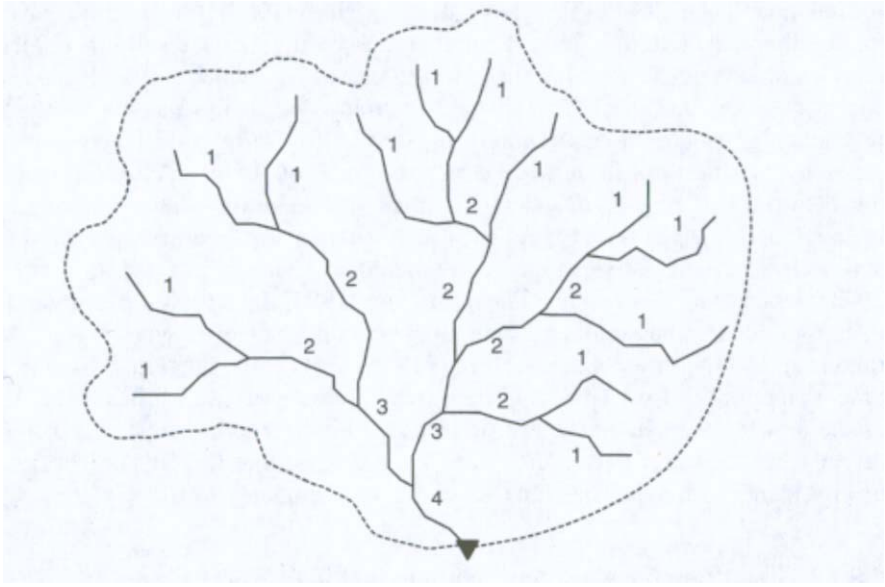

Figure 3.1: Strahler ordering of a river network (*BEVEN *2001a, p. 101).

Based on the stream orders, Horton defined a set of parameters to describe network geometry, known as Horton laws or Horton ratios:

$$R_B = \frac{N_\omega}{N_{\omega+1}} \tag{3.5}$$

$$R_A = \frac{\overline{A}_\omega}{\overline{A}_{\omega-1}} \tag{3.6}$$

$$R_L = \overline{L}_\omega - \overline{L}_{\omega-1} \tag{3.7}$$

where R_B is called bifurcation ratio, R_A area ratio and R_L length ratio, N_ω denotes the number, $\overline{A}_\omega$ the average catchment area and $\overline{L}_\omega$ the average length of reaches of order ω.

The general idea of the GIUH is define a set Γ_P of possible paths γ a *raindrop* may take to reach the catchment outlet. A travel time distribution, representing the catchment response, is set up according to the length of the paths and a characteristic velocity.

The original GIUH is probabilistic, using Markov chains to derive the pathway probabilities p(γ) for the paths in Γ_P. The *raindrop* remains a random time (with an exponential probability distribution) in each reach (called *stat*e) on its path γ, before it passes to a higher order reach.

Subsequent work by GUPTA ET AL. (1980), GUPTA AND WAYMIRE (1983) and others aimed at simplifying the theory. GUPTA ET AL. (1980) give the GIUH f(t) for a unit input as

$$f(t) = \sum_{\gamma \in \Gamma} p(\gamma) \cdot h(L_\gamma, t) \tag{3.8}$$

where t is time, L_γ is the path length and $h(L_\gamma,t)$ is a travel time distribution for a path of length L_γ.

ROSSO (1984) showed, that the GIUH can be fitted to a Nash cascade (Eq. 3.4), with the parameters

$$N = 3.29\left[\frac{R_A}{R_B}\right]^{0.78} R_L \tag{3.9}$$

$$K = 0.70\left[\frac{R_A}{R_B R_L}\right]^{0.48} L_\Omega v^{-1} \tag{3.10}$$

where R_A, R_B and R_L are the Horton ratios as defined in (Eq. 3.5) to (Eq. 3.7), L_Ω is the length of the highest order reach in the network and v is average stream velocity (with v and L_Ω in corresponding units).

SHAMSELDIN AND NASH (1998) claim that, as there is no causal link between the Horton Laws and catchment response, the GIUH has little advantage over other regression techniques for determining the parameters of a Nash cascade.

3.2.2 GIUH based on Width or Area Functions

The use of geomorphological characteristics to determine catchment response is appealing, especially for ungauged basins with lack of calibration data. Therefore many approaches exist which use the same rationale as RODRIGUEZ-ITURBE AND VALDES (1979) cited above.

ROSS (1921) proposed to split the catchment into zones of equal travel time of runoff to the outlet, weighting the runoff produced in each zone with its proportion of catchment area, thus creating a time-area diagram. CLARK (1945) used a similar approach. However, in those days it was difficult to estimate travel times and runoff producing areas (BEVEN 2001a, pp. 26-28).

The network width function (Figure 3.2), is built by counting the number of reaches in a certain discretised distance from the outlet. Like in the GIUH, network morphology is used to characterise catchment response, but use of Horton Laws is avoided. Assumptions are uniform hillslope contribution for each reach and time-invariant flow velocity.

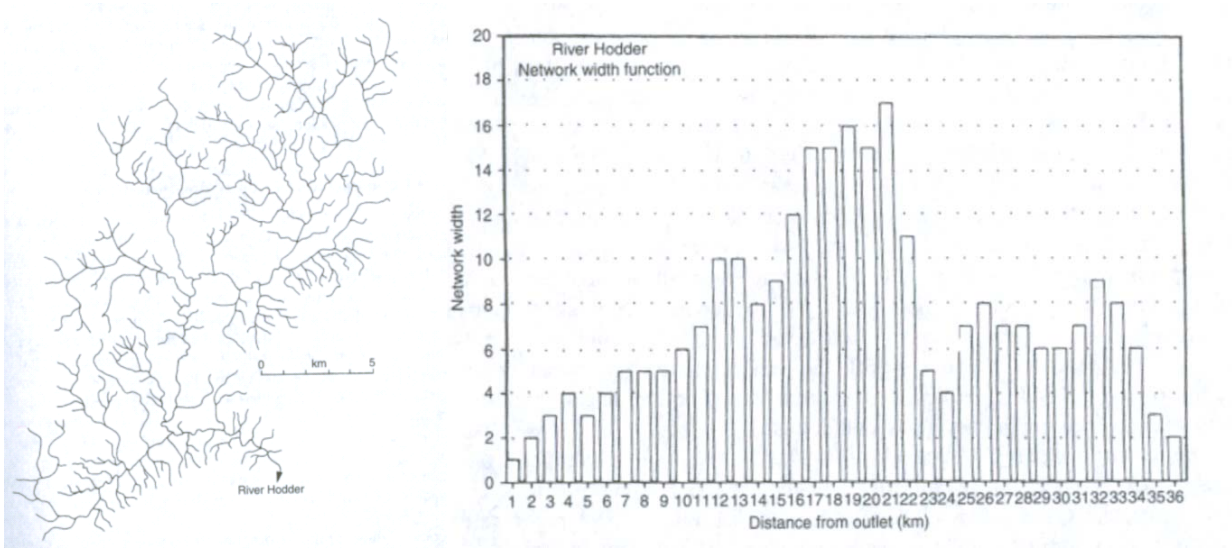

Figure 3.2: Network (left) and Network width function (right) for River Hodder catchment (*BEVEN *2001a, p. 99).

Defining a weight function

$$W(x) = \frac{n(x)}{N_{Reach}} \tag{3.11}$$

where x is the distance to the outlet, n(x) the width of the network and N_{Reach} the total number of reaches in the network, yields a catchment response f(t) to an unit input as

$$f(t) = \int_0^\infty W(x) \cdot h(x,t)dx \tag{3.12}$$

where h(x,t) is the response function for an input at distance x to the outlet (MESA AND MIFFLIN 1986).

A weighting function which avoids the assumption of uniform contribution to each reach is the area function

$$W(x) = \frac{A_i}{A_{tot}} \tag{3.13}$$

where A_i is the area contributing to a reach or a path, depending on the concept, and A_{tot} is the total area of a catchment.

Using network structure to model catchment response works fine for large catchments, where travel time to the catchment outlet is determined mostly by channel travel time. In catchments smaller than about 50 km² hillslope travel times are dominating (KIRKBY

1993). Hence hillslope response should be incorporated in model used in catchments of the micro- and meso scale.

MESA AND MIFFLIN (1986) conceptualized hillslope response as a fast and a slow component. Most of the runoff is contributed by the slow component. Triangular approximations of hydrograph shape are used to model hillslope response f_h. Basin response f_b is derived by coupling f_h with network response f_n:

$$f_b(t) = \int_0^t f_n(t-\tau) f_h(\tau) dz \tag{3.14}$$

where t and τ denotes times in arbitrary units.

With the availability of Digital Elevation Models (DEMs) it is possible to create width functions for hillslopes as well (see chapter 3.3). Therefore hillslope response may be modelled using detailed representations of the geomorphological basin structure. Again a set of paths may be defined which represents flow lengths from hillslope to channel and from the channel reaches to the basin outlet, constituting a flow path distribution (FPD).

3.2.3 Response Function

As the unit hydrograph is a routing technique without losses, a response function h(x,t) needs to yield the same output as input:

$$\int_0^\infty h(x,t) dt = 1 \tag{3.15}$$

where t is time. For example (Eq. 3.4) fulfils this condition. Another important issue is parameterisation. The more degrees of freedom a response function has, the easier it can be fitted to a measured hydrograph, but parametrization uncertainty may be higher.

Furthermore a physical interpretation of parameters is desirable. Water flow is a complex turbulent three-dimensional process, which cannot be described analytically. A simplified way to describe wave propagation along a channel is the one-dimensional advection dispersion equation (ADE):

$$\frac{\partial Q}{\partial t} = D \frac{\partial^2 Q}{\partial x^2} - v_t \frac{\partial Q}{\partial x} \tag{3.16}$$

where Q is discharge (m^3/s), v_t wave celerity (m/s), x a path length (m) and D the dispersion coefficient (m^2/s). The ADE, also known as diffusive wave approach (DYCK AND PESCHKE, 1989, p. 337), is a simplification of the St.-Venant-Equations, neglecting the

acceleration terms. A wave propagates downstream according to its celerity and at the same time disperses due to friction and turbulence. While these causes for dispersion are called 'hydrodynamic dispersion', there is also dispersion due to different path lengths of water 'packets'. This is called geomorphological dispersion.
Wave celerity v and water velocity u can be linked by

$$v = \frac{5}{3}u \tag{3.17}$$

(DINGMAN 2002, p. 551).

A solution to the ADE is the inverse Gaussian function (also known as Green's function). This two-parameter function is also used by MESA AND MIFFLIN (1986), and SNELL AND SIVAPALAN (1994), ARMBRUSTER (1997) and others:

$$h(t) = \frac{1}{\sqrt{t^3 4\pi/(Pe \cdot t_0)}} \exp\left(-\frac{(1 - t/t_0)^2}{4t/(Pe \cdot t_0)}\right) \tag{3.18}$$

where t_0 is mean holding time and P_e is the dimensionless Peclet-Number defined as

$$Pe = \frac{x}{\alpha} = \frac{1}{PD} \tag{3.19}$$

where x is flow path length in meters and α is dispersivity in meters. PD, the reciprocal value of P_e, is known as dispersion parameter.

3.2.4 Solute Modelling

Solutes transport modelling normally is the domain of physics-based distributed models. For ideal tracers, i.e. substances flowing in accordance with the water without retardation or resorption (KÄSS 1992, p. 10), application of simpler models is possible.

BARNES AND BONNELL (1996) used a hydrograph approach to model stable isotopes (see chapter 3.4.2). Streamflow concentrations of solutes are linked to discharge via

$$Q_D(t)\,c(t) = \int_0^\infty P_{eff}(t-\tau)\,c_p(t-\tau)\,h(\tau)\,d\tau \tag{3.20}$$

where Q_D is direct runoff, c(t) is the concentration of solutes in runoff, c_P is the concentration of solutes in precipitation, h(τ) is the response function and t and τ are times.

The response function used is

$$h(\tau) = \beta \exp(-\beta\tau) \tag{3.21}$$

with

$$\beta = \frac{P}{K}\left(P + \frac{H}{K}\right)^{-1} \tag{3.22}$$

where P is a constant precipitation rate, K the mean residence time as in Eq. 3.3 and H is a water height (mm), representing 'dead water', i.e. water which does not take part in runoff generation, but mixes with the water contributing to stormflow, thus changing its isotope signature. Water flow is described using Eq. 3.2 and 3.3. Note, that mean residence time and response time are decoupled for solute flow modelling by Eq. 3.21. Modelled deuterium concentrations show a good fit to measured data but quantitative measures are not given

WEILER ET AL. (2003) use isotope signatures in precipitation and streamflow to determine for each time step the *event water* fraction of runoff, i. e. the water that precipitates during the event in contrast to pre-event water stored in the catchment from prior precipitation. Two different transfer functions for event and pre-event water are used to calculate catchment response with the IUH. Application to two events in a micro-scale catchment yield model efficiencies (see chapter 3.5.1) up to 0.94 for discharge and 0.92

3.3 Deriving Flow Path Distributions from Digital Elevation Models

Flow paths within a catchment can be derived from its topography, assuming that water flows downslope along the steepest gradient. This seems reasonable for surface and near surface flow processes (QUINN ET AL. 1991), but may be wrong if preferential flow does not follow surface topography, e.g. in karst areas.

To do this a Geographic Information System (GIS), which is a data base application to process spatial data, and a Digital Elevation Model (DEM), a digital representation of catchment topography, are needed. PCRaster, a grid-based freeware GIS, was used for this study.

Elevation data is available in three common formats: digitized contour lines (also called cartometric DEM (WALKER AND WILLGOOSE 1999)), irregular point elevation data forming a Triangular Irregular Network (TIN) and point elevation data in a regular grid (photogrammetric DEM). The first may be digitized from topographic maps, the second is suitable if measurements are made in the field and is very efficient in describing catchment topography with few points (BAND 1993). The third is especially handy for data

gathered by remote sensing using satellites or airplanes, widely available and addressed in the following. Derivation of flow paths from contour lines is described by O'LOUGHLIN (1986). See GANDOY-BERNASCONI AND PALACIOS-VELEX (1990) for using TINs.

To characterise a landscape as a regular grid of cells, a representative elevation value is assigned to each cell. Of course the grid resolution should be fine enough to display catchment topography adequately, as intra-cellular heterogeneities cannot be accounted for.

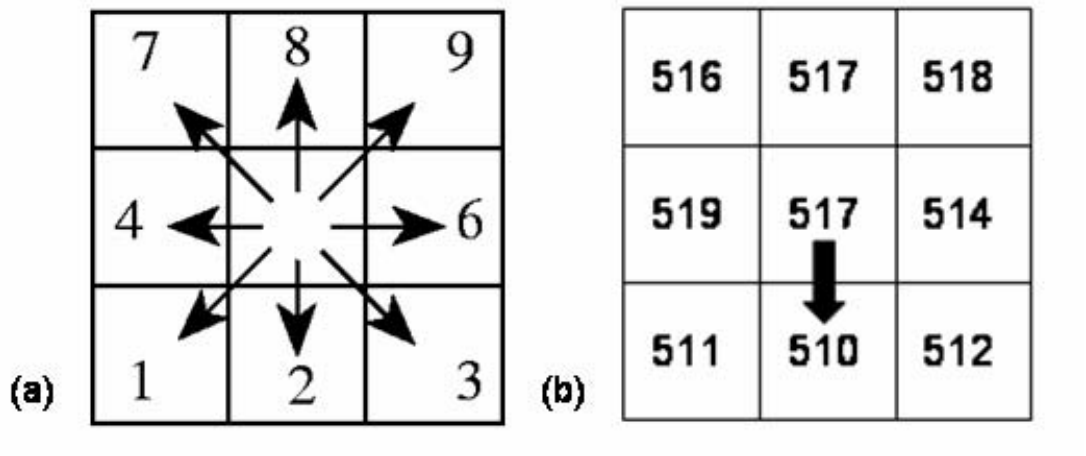

Figure 3.3: D8- Algorithm for derivation of flow direction. (a) Nomenclature of adjacent cells (PCRASTER MANUAL 2001***). (b) Example of flow direction.***

Flow directions can be determined using the Deterministic 8 (D8) single flow algorithm (O'CALLAGHAN AND MARK 1984). Water flows to the one of the eight surrounding cells, which has the steepest slope (Figure 3.3). Distances are calculated from cell centre to cell centre, resulting in a distance of one cell length l to cells 2, 4, 6 and 8 and a distance of $\sqrt{2}$ l to the diagonal cells 1, 3, 7 and 9. A value of 5 denotes a sink, i.e. a cell without outlet, for example a well or the catchment outlet. Due to inaccuracies in the DEM sinks may occur in regions without pronounced topography. They have to be removed in order to construct flow direction maps. Most GIS software provides algorithms to do this automatically.

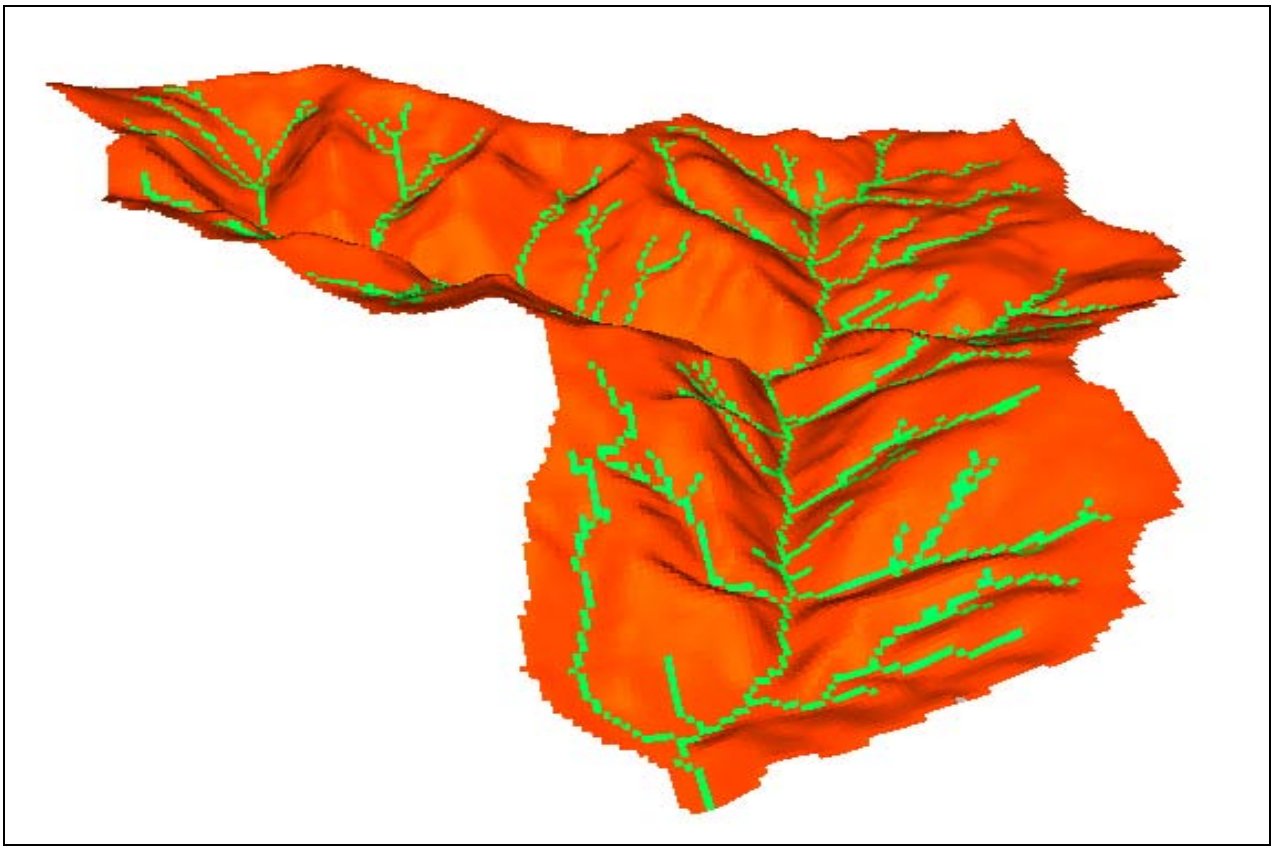

Figure 3.4: 3-D Visualization of Brugga DEM (viewed from outlet).

Figure 3.4 shows the DEM of the Brugga catchment and the channel network. Figure 3.5 shows a section of the corresponding flow map. Flow directions are coded in a map as numbers, but visualised as lines.

The channel network can be digitized from a map or created from the flow direction map. In the latter case each cell is assigned an 'accumulative flux', i.e. the number of 'upstream' cells from which water flows to this cell. All cells that have a number of contributing cells higher than a predefined threshold value are considered channel cells.

This method is very sensitive to the threshold value chosen and to grid resolution (SNELL AND SIVAPALAN 1994). Another problem is that photogrammetric DEMs often do not represent ground elevation but canopy or building height. Therefore a channel network constructed from a DEM should be checked on consistency with nature.

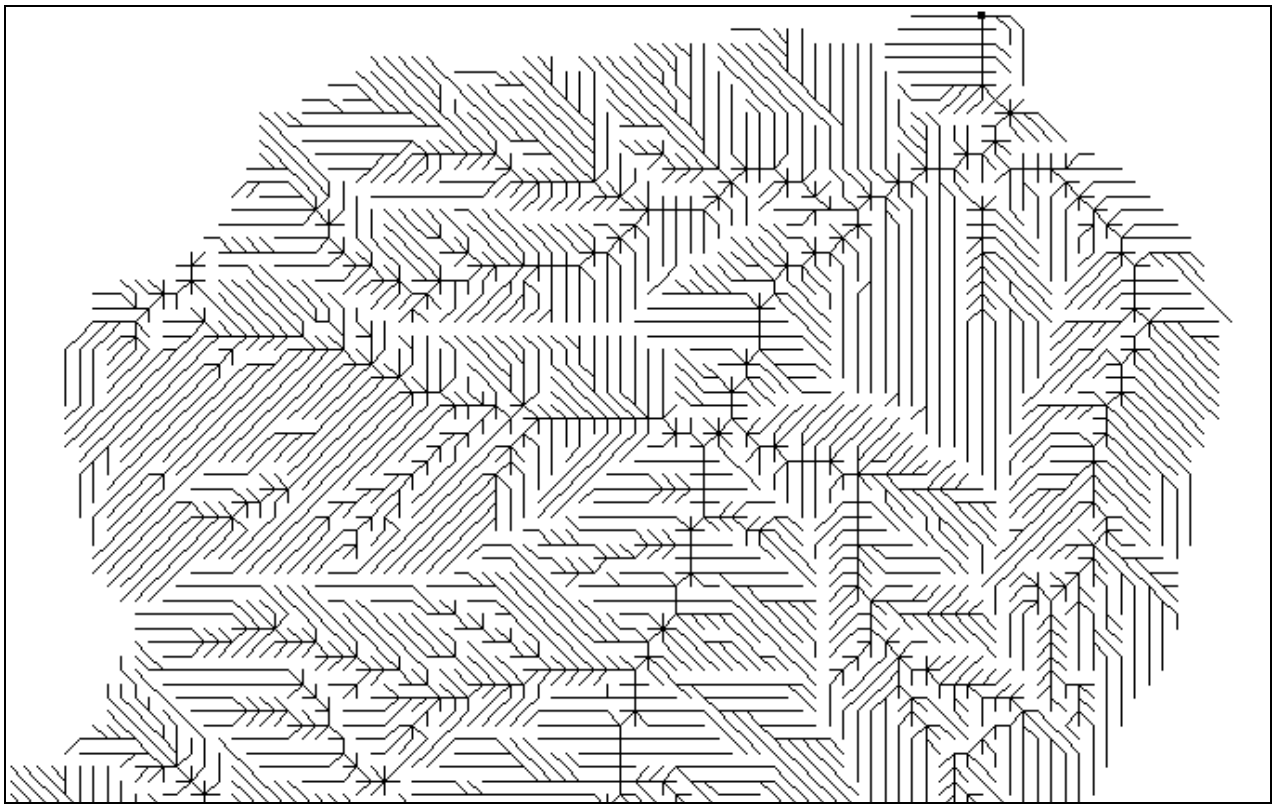

Figure 3.5: Flow Direction Map (section near outlet at Oberried) of Brugga catchment.

To get the flow path distribution of the channel network, the number of channel cells at a discretised distance from the outlet is counted. Distance is measured along the flow path as described above.

For the hillslopes distance to the nearest stream cell is determined.

3.4 Tracers

Tracer concentrations at the basin outlet are modelled within this study as part of multi-criteria validation. Tracers supply information on spatial origins of storm runoff and holding times in the system. If tracer concentrations cannot be modelled correctly, the dominating processes of runoff generation are not adequately represented in the model.

3.4.1 Silica

Silica, also called silicic acid (H_4SiO_4), is produced by chemical weathering of silicate minerals, which are found in the crystalline bedrock underlying the Brugga basin. Biogenous or other sources are insignificant. Silica concentrations in precipitation are neglectable (SCANLON ET AL. 2001). Furthermore, silica concentrations in runoff components are more stable than other solutes (HAINES AND LLOYD 1985).

This makes silica a suitable geochemical tracer to determine sources of runoff and to separate runoff into components using the 'end member mixing approach' (EMMA).

$$Q_{tot} = \sum_i Q_i \tag{3.23}$$

and

$$c(Si) = \frac{\sum_i Q_i c_i}{Q_{tot}} \tag{3.24}$$

determine the silica concentration c at the basin outlet, where Q_{tot} is total runoff, Q_i and c_i are the runoff and silica concentrations of the different components. Solving Eq. (3.23) and Eq. (3.24) gives the shares of the different components. For two runoff components Q1 and Q2 this yields

$$\frac{Q_1}{Q_{tot}} = \frac{c - c_2}{c_1 - c_2} \tag{3.25}$$

where Q_1 is the runoff of the first component and c_1 and c_2 are the concentrations in the first and second component. To separate n components, n-1 tracers have to be used.

3.4.2 Oxygen-18 and Deuterium

Oxygen-18 (^{18}O) and deuterium (^{2}H) are stable isotopes of the atoms of the water molecule. In 10^6 atmospheric water molecules are about 2000 $^{1}H_2{}^{18}O$ molecules and 320 $^{1}H^{2}H^{16}O$ molecules (MOSER AND RAUERT 1992, p. 267). $^{1}H^{2}H^{18}0$ is very rare and may therefore be neglected.
Chemically they behave just like their lighter counterparts ^{16}O and ^{1}H. This makes them ideal conservative tracers. But due to their higher mass their vapour pressure is lower than that of light water ($^{1}H_2{}^{16}O$). This leads to fractionation effects at phase changes. Heavier water molecules need more energy to evaporate and are easier frozen than light water.
The results of this fact can be subsumed as:

- Latitude and seasonal effect
  As fractionation is temperature-dependent, low surface temperatures lead to lighter precipitation. Therefore rain is depleted of heavy molecules in high latitudes and cold seasons (compared to a global annual mean).

- Continental effect
  During cloud formation, heavier isotopes condensate and precipitate easier than lighter ones. Therefore precipitation gets lighter as a cloud system moves from the coast to the inner of a continent.

- Amount effect
  Because of the same reasons as for the continental effect, the ratio of heavy to light isotopes in precipitation is higher at the beginning of an event than at the end.

- Altitude effect
  As clouds are forced to rise when encountering a mountain chain, heavier isotopes precipitate first. Therefore rain gets lighter with rising altitude.

Oxygen-18 and deuterium are natural tracers, distributed over the whole catchment by precipitation. The content of these in water probes gives information on the age of the water (if an input function with pronounced seasonal differences is available) and on the altitude of the area where it precipitated.

Due to the very small concentrations of heavy isotopes in natural waters, it is difficult to directly measure the content of heavy isotopes. Instead, samples are compared to a standard of known composition, like the Vienna Standard Mean Ocean Water (V-SMOW) issued by the International Atomic Energy Agency (IAEA). δ-values are defined as

$$\partial^{18}O = \frac{R_{sample} - R_{standard}}{R_{standard}} \cdot 1000\ ‰ \tag{3.26}$$

$$R = \frac{^{18}0}{^{16}0} \tag{3.27}$$

where ^{x}O is the content of isotopes of mass x. The δ^2H-value is defined analogously. As standard and sample are measured with the same instrument, the δ-value is more robust against miscalibrated equipment than absolute values.

Mixing may be calculated analogously to normal concentrations:

$$\partial^{18}O = \frac{\sum_i Q_i \partial_i {}^{18}O}{Q_{tot}} \tag{3.28}$$

where δ_i is the δ-value of a runoff component.

3.5 Calibration Techniques

Parameters are used to adjust a model to a special catchment. In the best case, their values can be measured directly in the field, which is one of the main goals of physics-based models. However, even parameters with physical meaning, like Darcy's k_f-value to describe saturated subsurface flow, may be hard to determine directly, as an effective

average value for each cell of e.g. 50*50 m² is needed, whereas measurements are often made at a much smaller scale (for discussion see for example BEVEN 2001b, or DURAND 2002). For conceptual models, this problem is even bigger, as simplified process descriptions may change the meaning of parameters. For example, in this study, all areas are taken to contribute the same amount of runoff (see chapter 4) regardless of their distance to the stream. This simplification leads to unnaturally long flow paths, which necessitate higher flow velocities.

So, even if parameters are named like measurable values, care has to be exercised when using measures or values of homonymous parameters from different models. Do these values mean the same thing in both cases, or are they *incommensurate* (BEVEN 2001a, p.20)?

A solution for this problem is the *inverse method*. If measured input and output data are available, the model output is fitted to the measured output by parameter adjustment. This process of finding an ideal parameter set is called calibration.

If possible, the data used for calibration should cover a wide range of hydrological conditions, as extrapolation to more extreme conditions is difficult.

3.5.1 Performance Measures

Calibration requires a measure for goodness of fit. This can be qualitative and subjective ("a good/adequate/reasonable fit"), or a statistical method. The method chosen also depends on the model purpose.

Two ways to evaluate overall goodness of fit are the coefficient of determination R^2 (Eq. 3.29) and modelling efficiency R_{eff} (Eq. 3.30, NASH AND SUTTCLIFFE 1970).

$$R^2 = \frac{(\sum (x_i - \bar{x})(y_i - \bar{y}))^2}{\sum (x_i - \bar{x})^2 \sum (y_i - \bar{y})^2} \tag{3.29}$$

$$R_{eff} = 1 - \frac{\sum (y_i - x_i)^2}{\sum (x_i - \bar{x})^2} \tag{3.30}$$

where y_i = simulated value at time i
x_i = measured value at time i
$\bar{x}$ = arithmetic mean of the x_i values
$\bar{y}$ = arithmetic mean of the y_i values

R^2 gives the fraction of variability in y that can be explained by variability in x. Values range from one for a perfect correlation to zero for no correlation.

R_{eff} values range from one for a perfect fit to -∞. A value of zero indicates, that the modelled output is not better than just using the arithmetic mean of x for all time steps, a negative value shows that the model performs worse than the mean.

While higher values of R^2 and R_{eff} signify higher correlation, there is no apparent threshold value for good or poor results. SCHLITTGEN (2001) proposes a classification (Table 3.1).

Table 3.1: Interpretation of values of R^2 (SCHLITTGEN 2001).

Coefficient of determination R^2	Interpretation
0	no correlation
0.01 –0.24	weak correlation
0.25 – 0.64	medium correlation
0.65 – 0.99	strong correlation
1	perfect correlation

In contrast to the coefficient of determination, the Nash-Sutcliffe-efficiency is sensitive to a difference between $\bar{x}$ and $\bar{y}$. Both are highly sensitive to time lags: if y models x well, but lags a few time steps behind, R^2 and R_{eff} deteriorate. Also, as overall goodness is considered, good predictions of the recession limb of the hydrograph can lead to a high goodness of fit even though peak runoff may be predicted rather badly.

Even though they are not perfect measures to evaluate simulations, both are standard methods frequently used. Other common measures of goodness are the volume difference between measured and simulated discharge, comparison of modelled and actual peak runoff and the use of logarithmic values for model efficiency and coefficient of determination. The latter two are especially useful for low-flow-studies, as high discharge values have less influence on model efficiency than in their non-logarithmic counterparts.

3.5.2 Parameter sampling

Once the criteria for successful simulation are defined, the range of possible values for each parameter has to be determined. Then, parameter sets have to be chosen and compared for their suitability. The simplest sampling strategy is 'trial and error', where values are chosen by the modeller based on his expert knowledge. This may be possible for simple models, where the effects of parameter change are easily predictable. With complex models, where many parameters interact, this is virtually impossible.

A common strategy is the Monte Carlo method, where a large number of automatically created parameter sets are compared. Some authors (e.g. MELCHING 1995) use the term Monte Carlo only for randomly created combinations while others (BOOLTING 2001) also include equidistant parameter sampling and similar strategies. As a huge number of model runs has to be made, computational requirements are high, especially for complex models.

For a single parameter, performance for different values may be represented as dotty plots (Figure 3.6 (a) and (b)). A measure of goodness is plotted against the domain of the parameter. Each dot represents one model run. Several dots with the same parameter value but differing goodness result from the variation of other parameters.

The set of possible parameter combinations plotted against a performance measure forms an n-dimensional response surface, where n is the number of parameters of the model. For two parameters, they may be visualized as in Figure 3.6 (c) and (d). If the response surface is convex as in Figure 3.6 (c), the parameters are well-defined, i.e. they have a clear optimum and performance deteriorate, if the value departs from this optimum. Figure 3.6 (d) shows a response surface with many local optima. Several combinations are equally successful in modelling the system. This is addressed as equifinality and complicates model calibration, as an optimal parameter set is hard to define. BEVEN (2001a, p.22) questions the whole concept of an optimal parameter set.

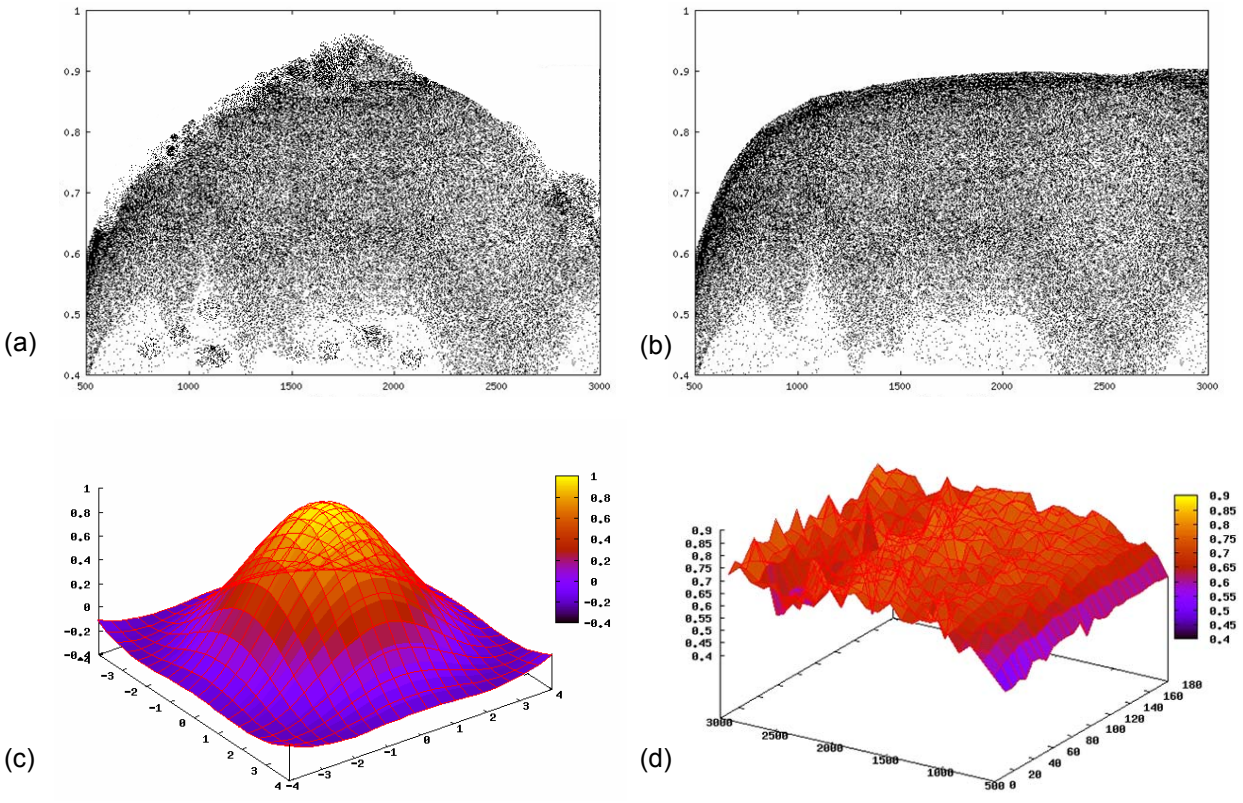

Figure 3.6: Visualizations of Monte-Carlo simulations: (a) Dotty plot for a well-defined parameter. (b) Dotty Plot for a badly defined parameter. (c) Response surface for two well-defined parameters. (d) Response surface for two badly defined parameters.

Stratified sampling denotes strategies, where parameters are taken from specified intervals within the domain of a parameter. This ensures, in contrast to random sampling strategies, that the whole parameter space is sampled with a fixed number of model runs. Random sampling has the advantage of eliminating the bias of the modeller.

Advanced algorithms for automatic parameter optimization exist. In short, these vary parameter values dependent on the performance of the previous model run. Hill climbing techniques like the Simplex method (NELDER AND MEAD 1965) aim at finding the global optimum by following the slope of the response surface to obtain better performance. Difficulties arise if the response surface has many local optima.
Genetic algorithms (e.g. FORREST 1996) use the analogy of biological evolution. A 'population' of parameter sets is randomly generated. At each iteration unsuccessful sets are sorted out. Promising sets are subject to random changes (*mutation*) and information exchange (*cross-over*).

SOROOSHIAN AND GUPTA (1995) give an overview of optimization techniques used in hydrology.

3.5.3 Multi-Criteria Calibration

The use of additional data like groundwater levels or mineralization of streamflow may help to reduce parameter uncertainty (SEIBERT 2000). Furthermore the ability of a rainfall-runoff model to predict various hydrological variables reliably shows an adequate representation of the internal processes of a catchment. This is important to predict extreme events which are not included in the calibration period.

3.6 Model Validation

Model validation is used to check the performance of the parametrization found by calibration. Some authors (e.g. ORESKES AND BELITZ 2001) argue that validation is a misleading term, since good results in validation do not imply that the model is 'valid' for all possible conditions. However, the term validation is still widely used.

To evaluate the model, predictions are compared to measured data, using the performance measures given in chapter 3.5.2. If the model yields good results, it is assumed to reach a similar accuracy in the prediction of future events.

3.7 Java

Java is a modern object-oriented programming language (GOSLING AND MCGIBBON 1996). Based on C++, Java is designed to overcome C's shortcomings, like its error-prone memory management.

Java is platform independent, meaning that a program can be run under different operating systems (like Unix or MS Windows) without the need to rewrite source code. This is achieved by the combination of a compiler and an interpreter, the 'Java Virtual Machine' (JVM). The compiler produces system-independent byte code which is translated to native code by the interpreter at runtime. Implementations of JVMs are available for all major platforms. Therefore programs may be run on all popular systems.

Object-oriented languages, in contrast to procedural ones like C, organize data structures and methods to manipulate them in objects. Objects can interact with other objects by sending messages, calling methods to perform operations. But they are unable to access data stored in another object directly. This principle is known as encapsulation.

This seems complicated at first, but avoids safety problems caused by improper manipulations. Also debugging (i.e. finding errors in programmes) is made easier, because the source code can be split in autonomous parts. Reuse of code is made easier as well.

Each object is made from a class. Classes may be seen as blueprints for objects, defining their contents and initial states. While you can create multiple objects of the same type, they are all instances of the same class.

A disadvantage of Java is that programs are generally slower than their counterparts written in C++.

3.8 Conclusions

The unit hydrograph is a well-known and frequently used routing technique. The underlying assumptions of uniform distribution of precipitation and linear catchment response are gross simplifications. Precipitation heterogeneity poses a bigger problem in mountainous catchments like the Brugga than in flat ones. Convective events are more likely to be in inhomogeneously distributed than advective ones. Whether this inhibits sound rainfall-runoff modelling will be examined in chapter 5. In spite of these problems, unit hydrograph approaches have proven to be successful in meso-scale catchments and allow parsimonious model parameterization.

The use of DEM-derived flow path distributions provides an effective way to describe catchment topography. The data required are available for many sites worldwide.

Parameter values can be set objectively via Monte-Carlo simulations. Multi-criteria calibration allows constricting possible values, to diminish the risk of equifinality and to check the correct representation of the runoff-generating processes. Silica concentrations tend to be very stable in runoff components and provide a way to check the origin of runoff.

4 GUHmod

GUHmod is a rainfall-runoff-model based on the GIUH approach using area functions. A regular grid DEM is used to define a flow path for each hill cell to the channel network, and for each channel cell to the basin outlet. Flow paths are classified according to their length and weighted by the ratio of contributing area to total area. Baseflow is held constant during the event.

Hillslope response may be split into multiple components, e.g. a fast and a slow one. Each component is then represented by its own FPD and characteristic wave celerity. They are weighted by the number of cells in their FPD.

Besides runoff, silica and isotope concentrations can be modelled. A fixed concentration of silica is assigned to each hillslope FPD and to baseflow, and water is mixed in the channel. For isotopes an input function giving the δ-values of precipitation for each time step is used. Water is routed through the basin and mixed, but no further processes (e.g. evaporation from soils) are accounted for.

As described in chapter 3.2, GUHmod assumes uniform precipitation over the catchment and neglects pre-event water and pressure transmission processes like Piston flow.

The GUHmod package consists of five main modules: the model itself, a routine for Monte Carlo simulations used for model calibration, an evaluation tool to compare modelled and measured hydro- and chemographs, a visualisation tool, and a graphical user interface (GUI) for easy use. All parts are written in Java.

4.1 Input Data

Input data needed to model runoff are

- Precipitation data
- FPDs for hillslopes
- FPD for channel network
- Wave celerity for each FPD
- Baseflow

To model silica concentrations, mineralizations for the hill FPDs and the baseflow have to be known. Modelling natural isotopes requires an isotope signature of precipitation and a constant δ-value for baseflow.

The formats required for input data are described in the appendix.

4.1.1 Precipitation Data

Rainfall data have to be supplied as effective precipitation in millimetres per time step, using the same temporal discretization as the model. If data from several rainfall gauges are available, an average effective rainfall should be calculated.

4.1.2 FPDs for Hillslopes

Catchment topography is represented using flow path distributions. Flow path length to the channel is calculated for each hill cell as described in chapter 3.3. Lengths are grouped into equidistant classes. FPDs give the number of cells in each class.

Hillslopes may be subdivided into areas of similar runoff generation. Each type is represented by a single FPD and assigned a constant wave celerity and silica mineralization.

However, only the source cells are regarded. The type of the cells through which the water passes on its path to the channel is not accounted for. The error made by this assumption depends on the catchment characteristics.

Spatial discretization of the FPDs (class size) is variable, but cell size is hard coded to 50m (variable `cellSize`[1] in `Model.java`). Therefore recompilation is necessary, if a different grid resolution is used.

Distances have to be given in metres.

4.1.3 FPD for the Channel Network

The channel network is represented by a single FPD, giving the distances of channel cells to the basin outlet. As wave celerity is higher than in the hillslopes, class size may be bigger. Again, metres are used as units. Due to the higher flow velocities a larger class size may be used than for the hillslope FPDs.

4.1.4 Wave celerities

Wave celerities are the calibration factors of GUHmod, as FPDs are given by catchment topography and dispersion is calculated as a fixed function of flow path length. Celerities have to be given in metres per time step.

---

[1] Names printed in the font "`Simsun`" refer to methods or variables in the source code of the computer programme or to other software.

4.1.5 Baseflow

Baseflow is held constant during the event (see chapter 5.2.2). It is added to the storm runoff after convolution of catchment response and used for silica modelling. Baseflow has to be given in cubic metres per second.

4.1.6 Silica concentrations

Concentrations of dissolved silica have to be given for all hill FPDs and for baseflow. Unit is milligram per litre. These concentrations are held constant during the event.

4.1.7 Isotope signatures

An input function for precipitation has to be given as a table of δ-values (see chapter 3.4.2) for each time step. Note that δ-values are negative, as precipitation is depleted in heavy isotopes compared to the standard ocean water. Baseflow is assigned a constant δ-value. If no input function for precipitation is available, a constant value ('bulk mean') may be assigned for precipitation as well. Then the isotope signature of the runoff will only reflect the ratio of event water to baseflow.

4.2 Runoff calculation

The central part of GUHmod is the method `convolution` in the modelling module. After the input data have been loaded into memory, runoff and solute load are modelled.
Figure 4.1 shows the schematic structure for two hill FPDs. In a first step, the responses of the hill FPD to precipitation are determined, using the wave velocities v_{H1} and v_{H2}. The sum of the runoff produced by the hills is used as input to the channel network. A uniform runoff contribution to each channel cell is assumed. Flow is routed through the channel using the velocity v_C. At last, baseflow is added to the channel response and discharge at the outlet is written to file.

To determine the response of hillslopes and channel network, the unit hydrograph is calculated, using the weights derived from the FPDs and Eq. 3.18 as response function. The mean residence time t_0 used in Eq. 3.18 is determined by

$$t_0 = \frac{x}{v} \tag{4.1}$$

where x is flow path length in meters and v is the wave celerity in meters per timestep.

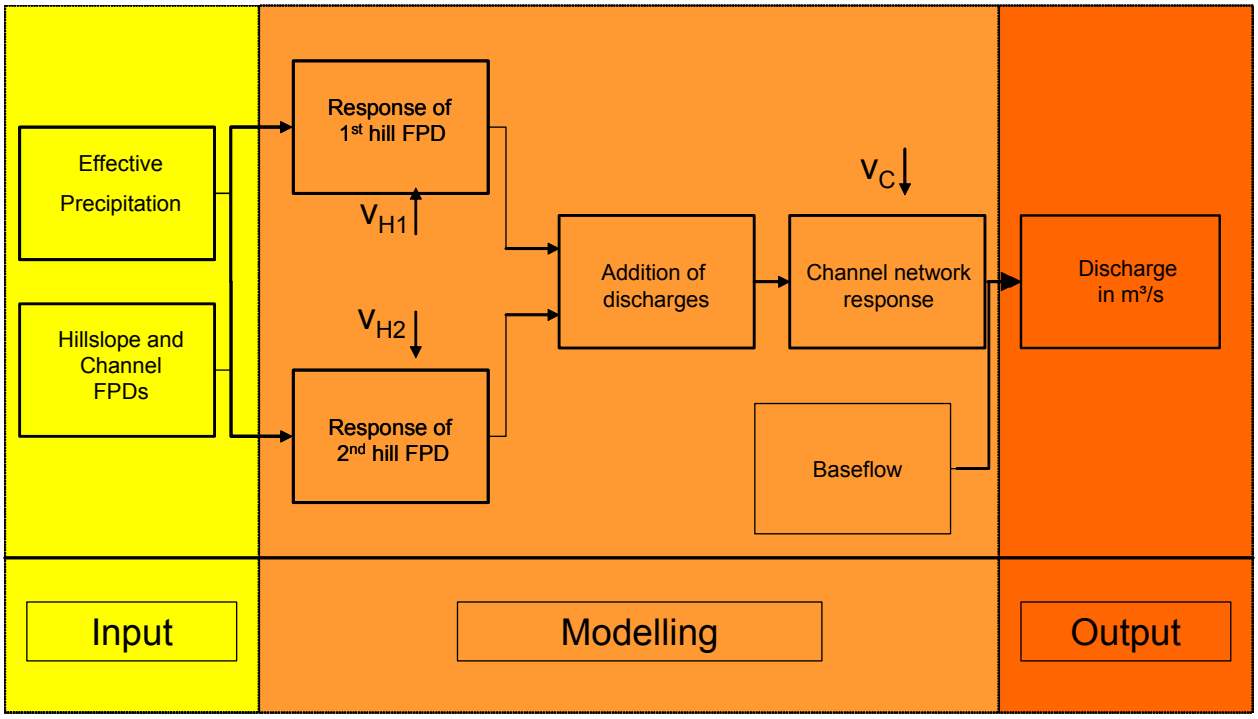

Figure 4.1: Model structure for runoff simulation (for two hill FPDs).

Peclet numbers for hill slope response are calculated by

$$Pe_{Hillslope}(x) = \frac{x}{0.83\,(\log_{10}\,x)^{2.141}} \qquad (4.2)$$

where $Pe_{Hillslope}(x)$ is the dimensionless Peclet number (XU AND ECKSTEIN 1995). Figure 4.2 shows a plot of Eq. 4.2.

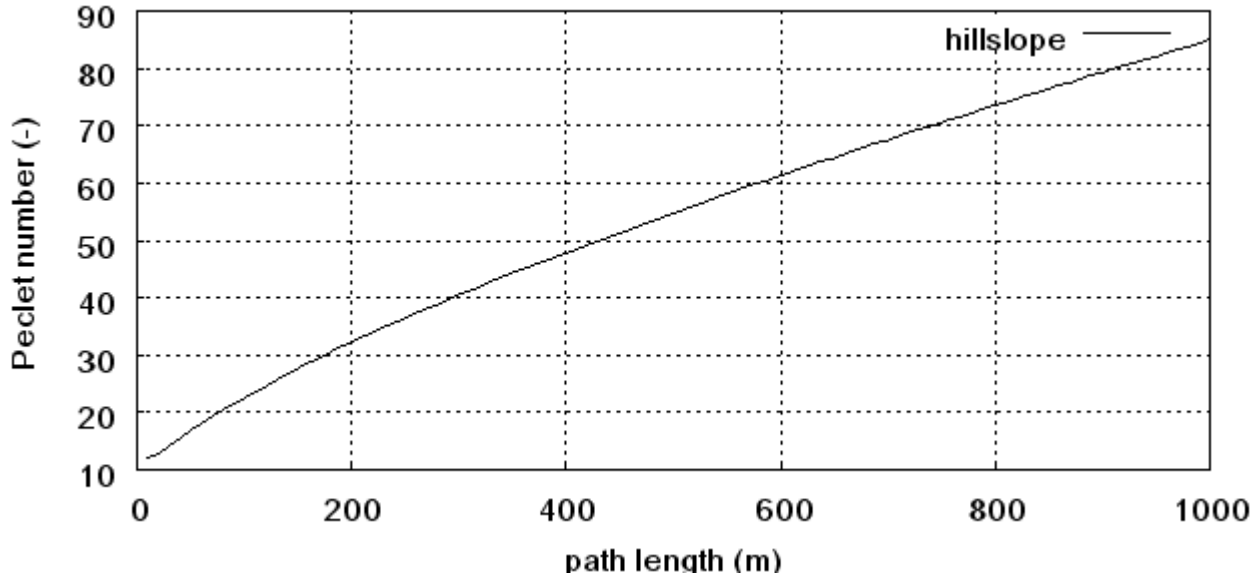

Figure 4.2: Peclet number versus path length for calculation of hillslope response.

As the convolution integral (Eq. 3.2) cannot be solved analytically, it has to be converted into a sum:

$$q_{Hillslope}(t) = z\sum_{i=0}^{m-1}\sum_{j=0}^{n-1} a_{i,j}\sum_{\tau=1}^{t} P_{eff}(t-\tau)h(\tau) \tag{4.3}$$

q(t)	volume of hillslope response at time t (m^3)
t	time as number of timesteps (-)
P_{eff}	effective precipitation (mm)
h(τ)	response function at time τ
m	number of hill FPDs
n	number of classes in a hill FPD
$a_{i,j}$	weight of class j in hill FPD i
z	conversion factor (cell area in m^2)

Technically this is achieved by four nested loops. Figure 4.3 shows a structure chart of the implemented algorithm. The integer variables `t`, `c`, and `i` are used as counting variables for the loops, `time_max` is the total number of modelling steps, `q` and `temp` are floating point variables to temporarily store runoff data (not temperature), and P_{eff} and τ are used as defined above.

Note that channel network routing is not described explicitly. In general, it is analogous to the calculation of hill response, except for the missing loop for several FPDs. Also relative class weights w_i are used, with

$$w_i = \frac{n_i}{N} \tag{4.4}$$

where n_i is the number of cells in class i and N is the total number of cells in the FPD, and

$$\sum_{i=1}^{m} w_i = 1 \tag{4.5}$$

where m is the number of classes in the channel FPD. In the hillslope convolution, the number of cells in each class are used and multiplied with the cell size to transfer water volume from millimetres to cubic metres.

Network response is then calculated as

$$q_{Network}(t) = \sum_i w_i \sum_{\tau=1}^{t} q_{Hillslope}(t-\tau+1)\cdot h(\tau) \tag{4.6}$$

where $q_{Network}$ is the runoff volume routed to the outlet at time t in litres.

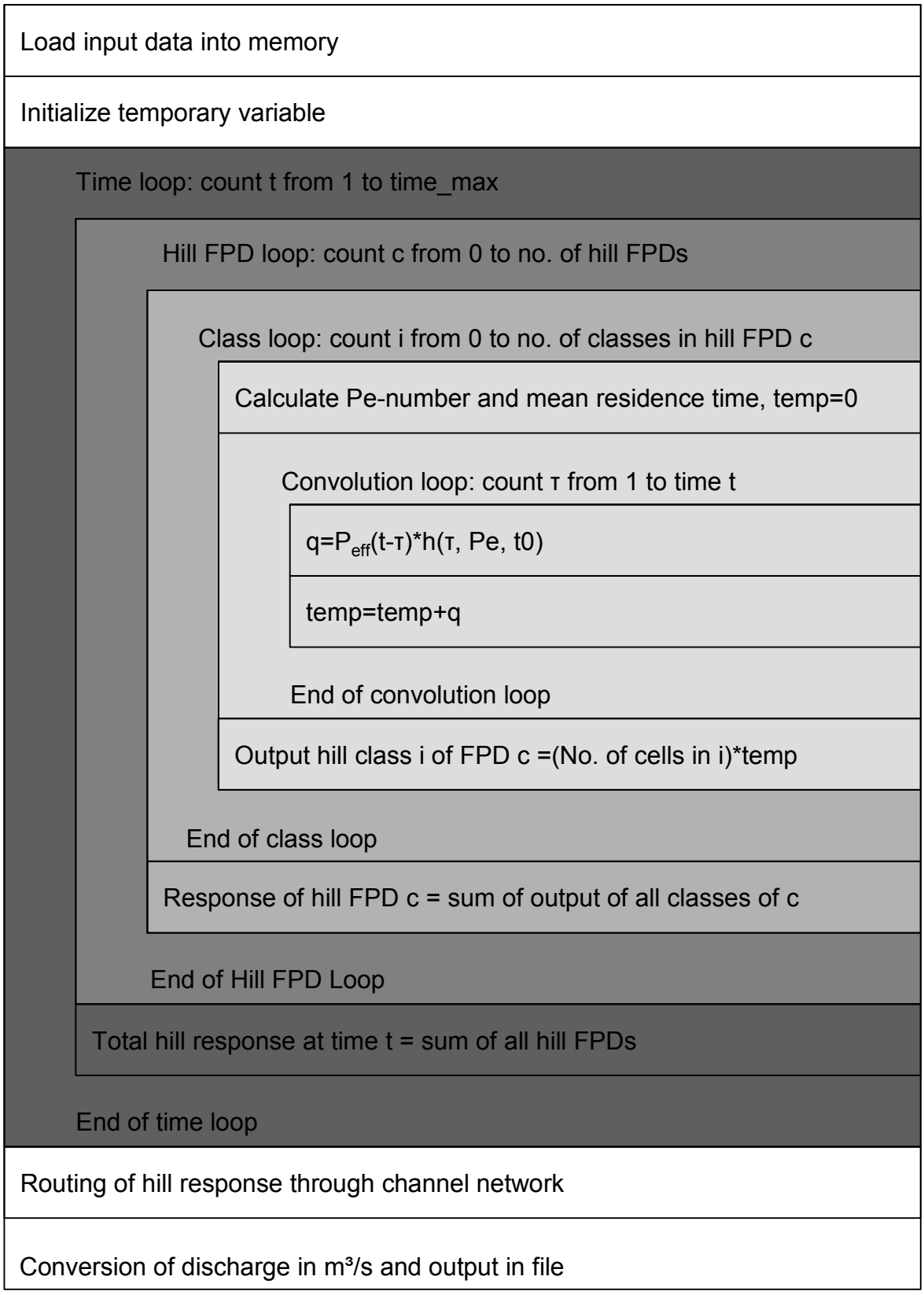

Figure 4.3: Structure chart (Nassi-Schneidermann-Diagram) of runoff modelling (see text for details).

The response function is the same as for the hillslopes, but Pe-numbers are calculated by

$$Pe_{Network} = 4.45\, x^{0.6} \tag{4.7}$$

where x is flow distance in meters. This equation is derived by regression analysis from tracer experiments in the Brugga (ARMBRUSTER 1997, p. 36) and is plotted in Figure 4.4.

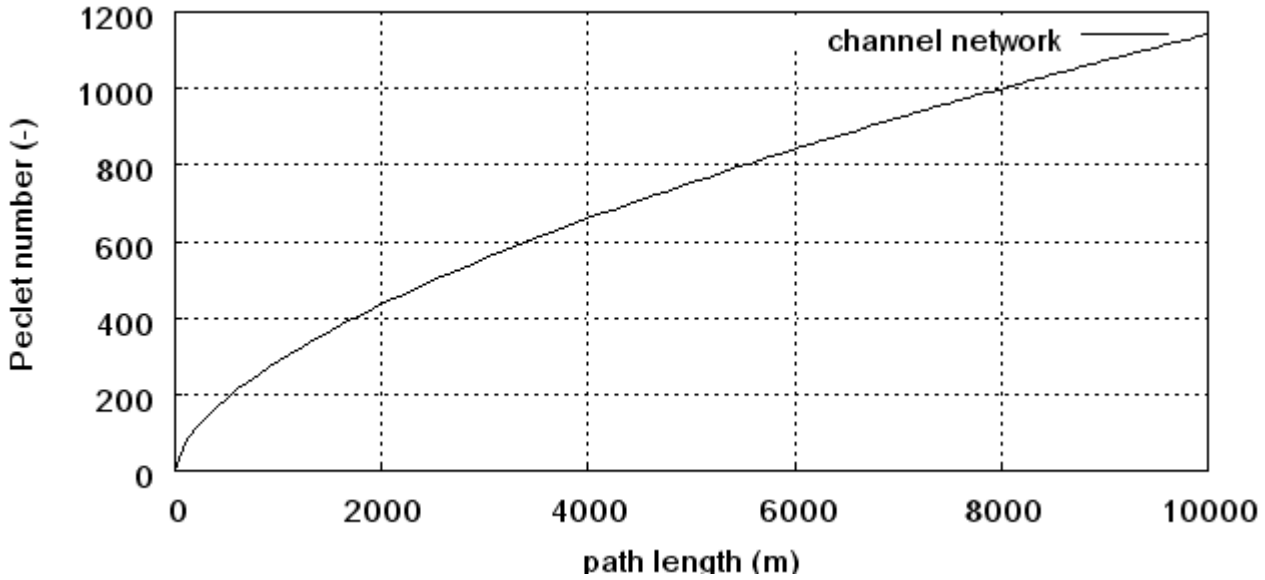

Figure 4.4: Peclet number versus path length for channel network response.

Runoff is calculated as

$$Q(t) = \frac{q_{Network}(t)}{1000\Delta t} + Q_{Baseflow}(t) \tag{4.8}$$

where Δt is the length of a timestep in seconds and QBaseflow(t) is the baseflow (m^3/s). Q(t) is given in cubic metres per second.

4.3 Solute Modelling

Silica and natural isotope modelling is build into the model as an option. Silica mineralization is assumed to happen during runoff generation in the hillslopes as a consequence of contact to the bedrock.

Silica concentrations of the hillslope response are calculated by

$$c_{Si}(t) = \frac{z\sum_{i=0}^{m-1} c_i \sum_{j=0}^{n-1} a_{i,j} \sum_{\tau=1}^{t} N(t-\tau)h(\tau)}{q_{Network}(t)} \tag{4.9}$$

where c_i is the mineralization of runoff generated in hill FPD i in (mg/l). In a second step, the solute load of baseflow is added and silica concentration of total runoff is calculated.

This is implemented by a combined use of loads and concentrations.

For each time step the runoff q_i generated in the hill FPD i is multiplied with the corresponding mineralization c_i of the FPD to get the solute load. These are added and divided by total runoff to get the silica concentration:

$$c_{Hillslopes}(t) = \frac{\sum_{i}^{m} c_i q_i(t)}{\sum q_i(t)} \tag{4.10}$$

This results in a mineralization of total hillslope response for each time step. During the channel routing, solute load is calculated as

$$c_{Outlet}(t) = \frac{(w_i \sum_{\tau=1}^{t} q_{Hillslope}(t-\tau+1) c_{Hillslope}(t-\tau+1) h(\tau)) + Q_{Baseflow}(t) c_{Baseflow}}{q_{Network}(t) + (Q_{Baseflow} \cdot \Delta t \cdot 1000)} \tag{4.11}$$

where $c_{Baseflow}$ is the constant silica concentration of baseflow (mg/l).

Deuterium and oxygen-18 are taken to be independent of flow paths. Isotope signature of precipitation changes during the course of the event but remains unchanged during routing. Therefore Eq. (4.9) changes to

$$\delta(t) = \frac{z \sum_{i=0}^{m-1} \sum_{j=0}^{n-1} a_{i,j} \sum_{\tau=1}^{t} n(t-\tau+1) \delta_P(t-\tau+1) h(\tau)}{q_{Network}(t)} \tag{4.12}$$

where $\delta_P(t)$ is the δ-value of precipitation at time t. The other equations remain unchanged, except that concentrations c(t) are exchanged for the corresponding δ-values.

Note that loads, i.e. the product of runoff volume and solute concentration, have no physical meaning in the case of isotopes, because no amount of substance or number of atoms is calculated. Nevertheless, these “virtual loads” can be used to calculate δ-values, since mixture equations (3.24) and (3.29) are of the same form.

4.4 Model Output

Runoff and, if modelled, solute data for each time step are reported a file. If runoff data used for evaluation have a coarser temporal resolution than precipitation input, the output may be aggregated. This is done by writing only every n^{th} value to file. No mean values are

calculated. Standard output format is in hours (every 6th value). The source code of the method convolution has to be changed and recompiled to set temporal aggregation.

4.5 Evaluation Module

To determine the model's performance, an evaluation tool is provided. Model output can be compared to measured hydro- and chemographs. For each file containing the measured data, the start row, the column containing the data and the number of data points for evaluation have to be specified. If a value of zero is assigned to the number of data points, measured and simulated data are compared until the shorter data series ends.

GUHmod provides the following measures of goodness:

- Coefficient of determination
- Nash-Sutcliffe model efficiency
- Comparison of modelled and measured peak flow
- Comparison of modelled and measured time to peak (time lag)
- Volume error

4.6 Monte Carlo Module

For calibration studies, a parameter sampling tool has been developed. Random sampling and stratified sampling are provided in the classes McRandom.java and McStratified.java. The Monte Carlo module repeatedly chooses parameters, starts the model and evaluates model performance. The name of the output file, the parameter values and the goodness of fit of all runs are written to a common file.

For random sampling, the range for each parameter and the number of simulation runs has to be provided. Parameter values are generated assuming a uniform distribution of values, i.e. each value has the same probability of being chosen.

Stratified sampling needs a range and a step size for each parameter. Starting at the lower boundary, the parameters are increased by the step size to obtain a regular mesh of samples. No random values are used.

In both cases, output files are assigned a name or prefix, a start number and a file suffix. The number is incremented for each model run to obtain differing file names. For example if a hundred simulations are made, prefix is set to "runoff", start number is zero and prefix is "dat", the output files are named "runoff0000.dat", "runoff0001.dat" to "runoff0100.dat".

4.7 Visualization Module

To conveniently display hydro- and chemographs and dotty plots from Monte Carlo simulations, the freeware graphics tool Gnuplot is integrated. After specifying the type of plot to make, input data, diagram title and the labels of the axes, a script is automatically generated, Gnuplot is called and the diagram is written to file.
One or two data series can be displayed as hydrographs. If additional data shall be displayed (e.g. rainfall data), the user can edit the script and start Gnuplot manually.

4.8 Graphical User Interface

The GUI provides easy access to the modules of GUHmod. It consists of three tabbed panes and can be controlled by mouse and by keyboard. The first pane (Figure 4.5), called Input, provides fields to set the number of hillslope FPDs, input files and mineralizations. Silica and isotope modelling can be toggled on and off by check boxes.

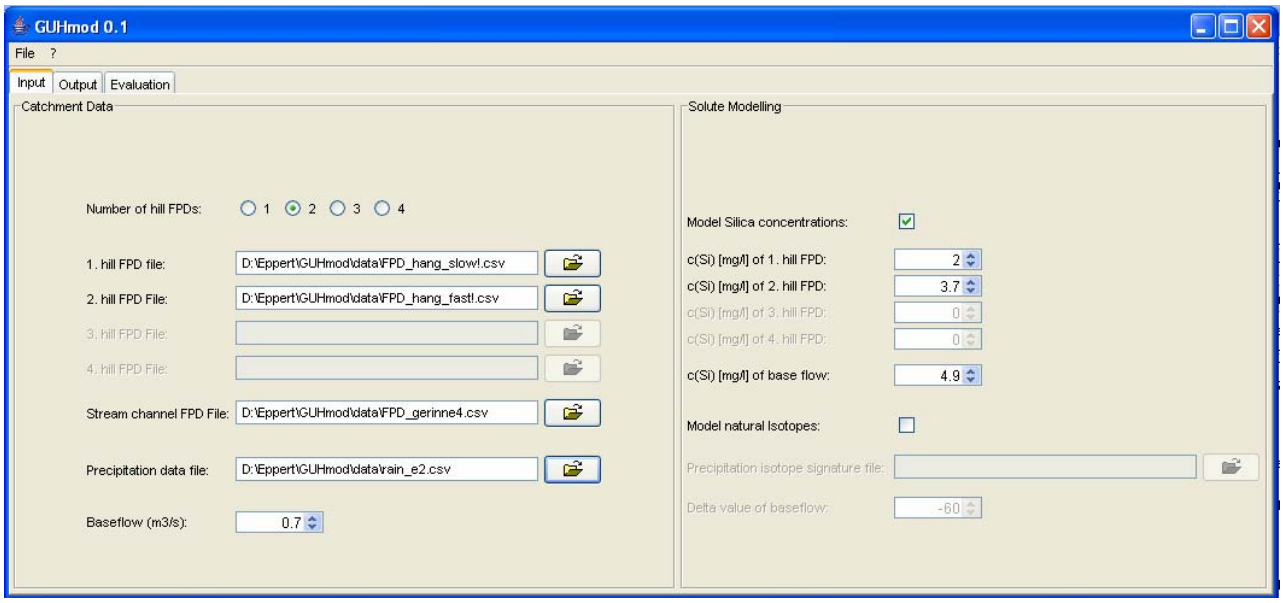

Figure 4.5: GUHmod user interface, INPUT pane.

After setting the input data, the user can proceed to the Output pane (Figure 4.6) by clicking its label in the upper left side of the screen. The user may choose between single model runs or Monte Carlo simulations with stratified and random sampling. For the former, parameter values have to be set. The latter two require ranges of parameter values and the number of simulations or the step sizes. Clicking one of the two buttons in the lower right section starts the model. Output data to control model state are written to the standard output stream (DOS prompt on MS-Windows systems, Bash or another shell on Unix systems).

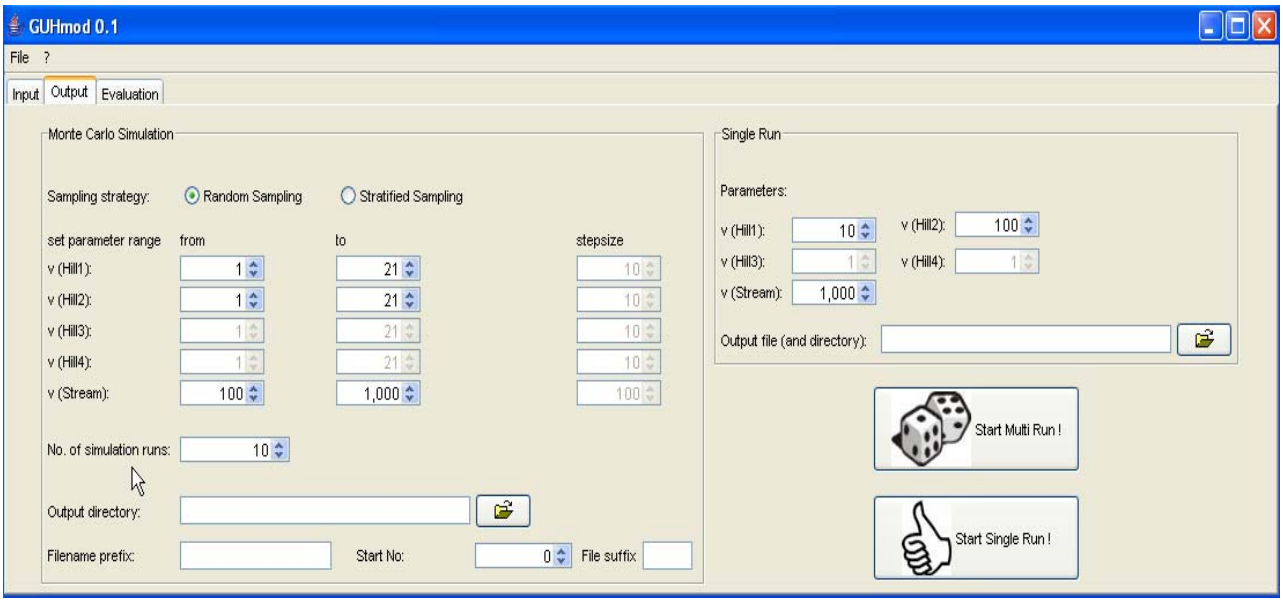

Figure 4.6: GUHmod user interface, Output pane.

Evaluation of model outputs can be activated in the third pane. Therefore the files containing the measured data have to be set and the evaluation measures have to be chosen.

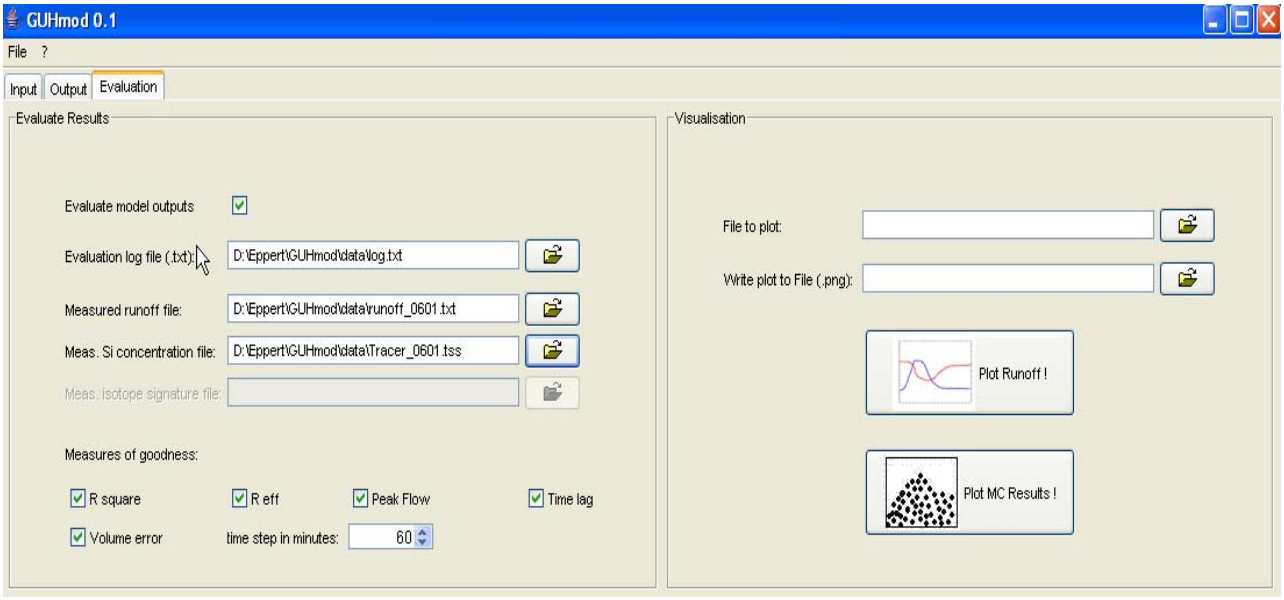

Figure 4.7: GUHmod user interface, Evaluation pane.

Also this pane gives access to the visualization module. After setting input and output file, the type of plot (hydrograph or dotty plot) has to be chosen. Then an extra dialog asks the user for title, labels and so forth.

A manual page is provided with the programme.

4.9 Conclusions

GUHmod is a modelling package based on the GIUH approach. Catchment structure is described using flow path distributions. To represent areas with differing dominant runoff generation processes, several hill FPDs may be used, each with a characteristic wave celerity and silica concentration. Hill responses are summed and routed through the channel network. Geogenic tracers and natural isotopes can be modelled.

Alongside with the model come modules for Monte Carlo simulations, with stratified or random sampling strategy, and for evaluation, providing five measures of goodness.

The visualization routine is based on the freeware programme Gnuplot. Hydro- and chemographs and dotty plots can be generated conveniently. A graphical user interface provides an integrated environment with easy access to these features.

5 Model application

To test its performance, GUHmod is applied to the Brugga catchment and to a subcatchment, the St. Wilhelmer Talbach. Four events are used for calibration and four for validation. Two methods to calculate effective precipitation are compared. Validation parameter sets are determined for each type of precipitation for either catchment to check the scale dependency of parameters. Another parameter set is determined regarding both runoff and silica concentration prediction.

5.1 Previous studies

The Brugga catchment was a study site for the project "Runoff generation and catchment modelling" funded by the German Research Foundation (Deutsche Forschungsgesellschaft, DFG). During this project, several studies were conducted. In a first step tracer experiments were carried out to determine source areas and amounts of runoff and to date the age of different water components (UHLENBROOK ET AL. 2002). UHLENBROOK (1999) integrated the results into the conceptual semi-distributed model TAC (Tracer aided catchment model). Regions with the same governing runoff generation processes were mapped and are modelled as hydrotopes. Each hydrotope is assigned a characteristic silica concentration and silica concentrations at the outlet are used to check for a correct contribution of each hydrotope.

ROSER (2001) developed a fully distributed version called TAC^d (Tracer aided catchment model, distributed). OTT (2002) applied it to the Dreisam catchment and changed the evaporation routine. SIEBER (2003) made parameter and sensitivity analyses with TAC^d.

DIDSZUN (2004) conducted field studies in the Brugga catchment to examine the scale dependency of runoff generation.

ARMBRUSTER (1997) wrote an event-based model based on the GIUH approach and applied it to the St. Wilhelmer Talbach. In contrast to this study, no calibration was performed but wave celerities were determined by tracer experiments. Saturated and unsaturated areas were modelled separately.

This study is based on the approaches of ARMBRUSTER (1997) and UHLENBROOK (1999). Event data are taken from the theses of SIEBER (2003) and DIDSZUN (2004).

5.2 Data Preprocessing

Data preprocessing deals with editing available information to make them useable by a model. For GUHmod, this includes converting the DEM of the catchment to flow path

distributions, calculating effective precipitation for the events and converting runoff data to a readable format.

5.2.1 Building Flow Path Distributions

A raster-DEM with a cell size of 50 x 50 m² for the Brugga catchment is taken from SIEBER (2003). The channel network was digitized from topographical maps (TK 25 and 50), converted to raster data and edited manually. Calculating the channel network from the DEM failed, as the height of the canopy layer rather than ground surface is represented by the DEM. For this study, unconnected links were deleted from the channel network (Figure 5.1), because it is impossible to model stream links which run dry with this approach.

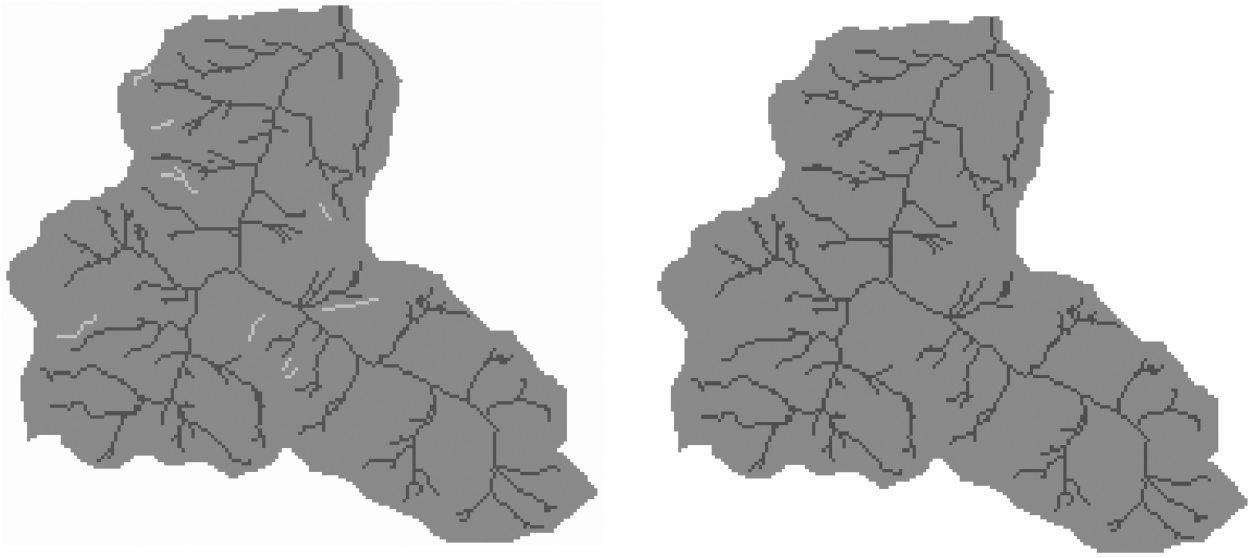

Figure 5.1: Brugga channel network. (a) Old version. (b) New version.

Hillslope response is divided into a fast and a slow component, henceforth called *hill fast* and *hill slow*. This is done on basis of the delineation of dominant runoff generation processes developed for the TAC^d model (Figure 5.2). Delayed interflow, strongly delayed interflow and deep seepage in valley sediments are aggregated to slow hillslope response. Fast hillslope response combines saturation overland flow, fast interflow and fast lateral interflow.

The flat areas on hilltops (unit type 4) are considered to not contribute any runoff on the event-scale and are therefore excluded. The other components are aggregated into two classes, leading to a distribution as in Figure 5.3.

The resulting FPDs are shown in Figure 5.4.

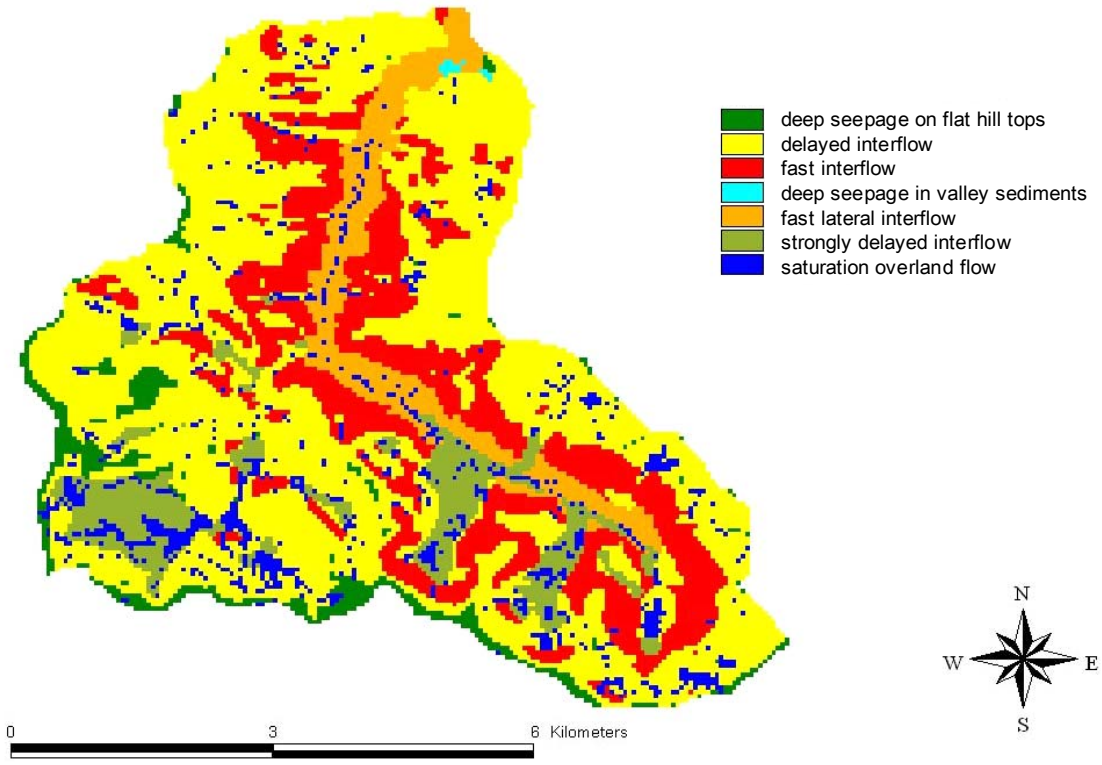

Figure 5.2: Spatial delineation of units with the same dominant runoff generation processes (*UHLENBROOK ET AL. *2004).

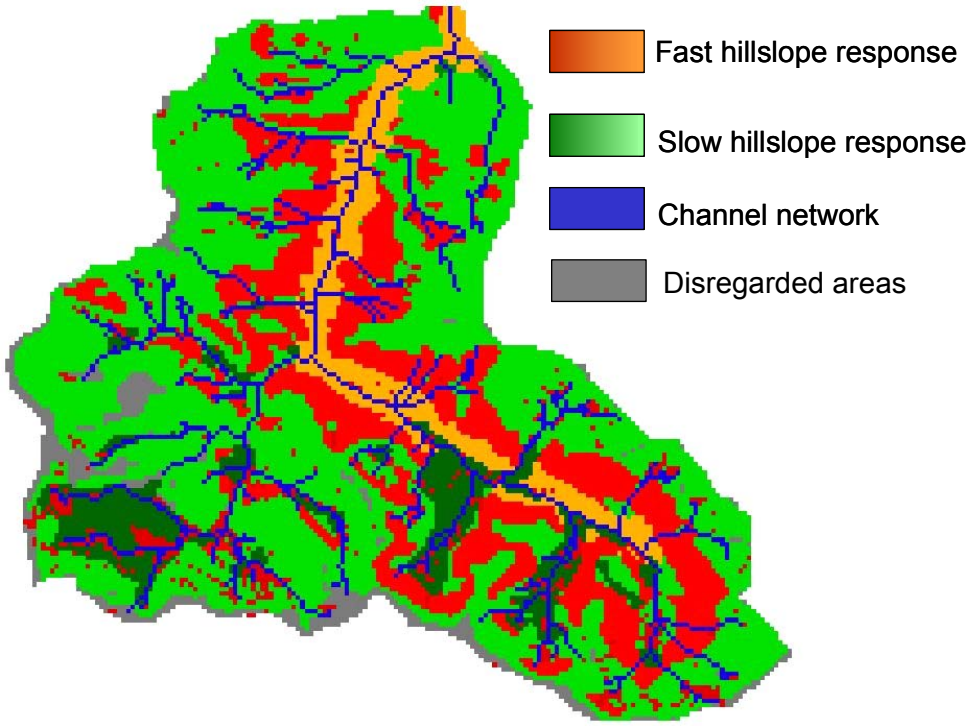

Figure 5.3: Deliniation of fast (red) and slow (green) responding hill cells.

Table 5.1 gives an overview on the number of cells in each FPD. Note that channel network cells are also regarded as hill cells, because maximal stream width in the Brugga catchment is six meters (ROSER 2001, p. 63), whereas the raster cells have a size of 50 x 50 meters. For these cells, a distance to the channel of 1/3 of cell size (16.67 m) is assumed.

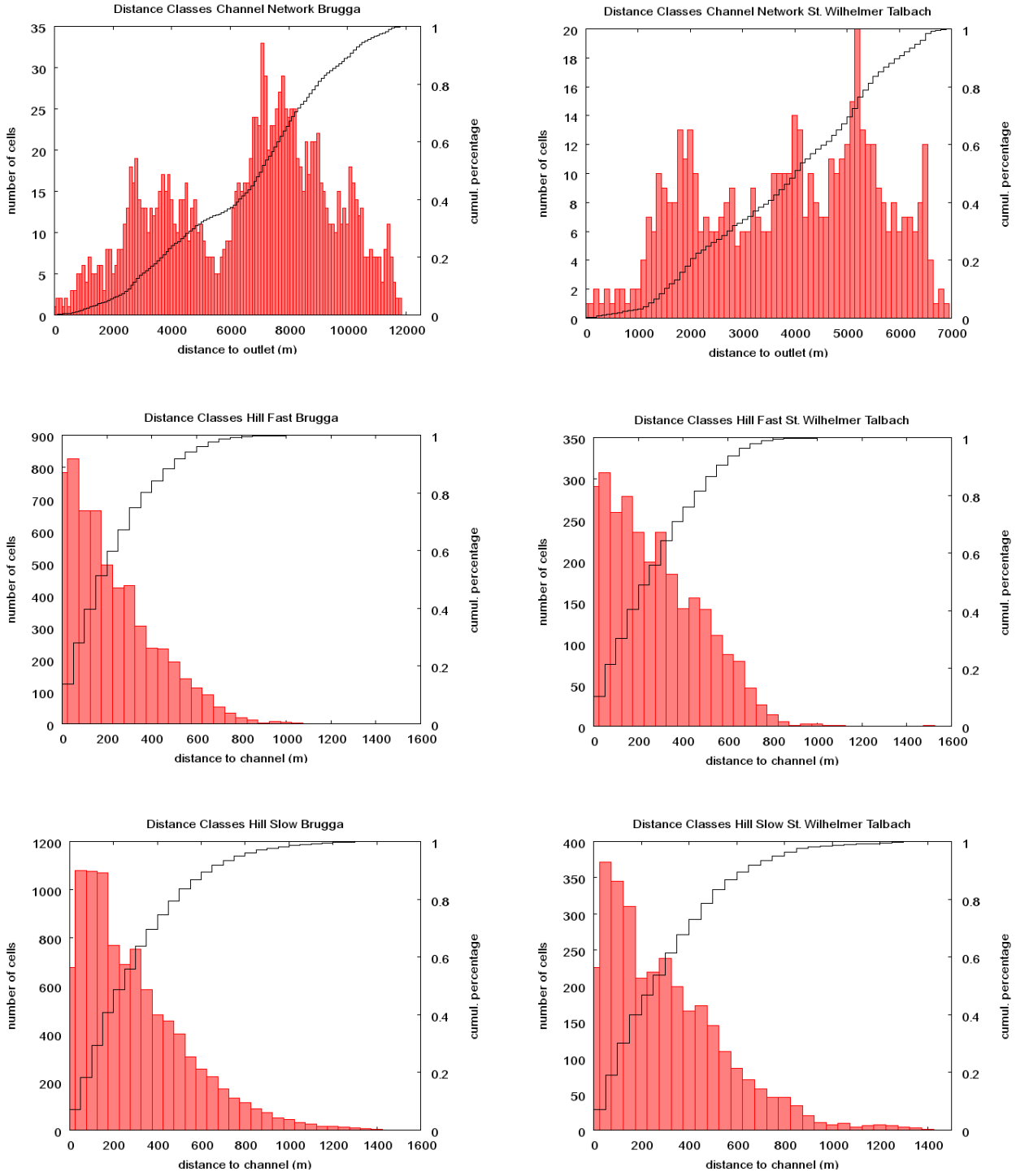

Figure 5.4: Flow path distributions for the Brugga and the St. Wilhelmer Talbach.

The fast responding hill cells make up 37% of the Brugga catchment and 47% of the St. Wilhelmer Talbach catchment. Slow responding hills contribute 63% and 53%

respectively. Ten percent of all cells in the Brugga catchment and nine percent in the Talbach catchment are stream channel cells.

Table 5.1: Number of cells for the FPDs of the Brugga and St. Wilhelmer Talbach catchment.

	Brugga	St. Wilhelmer Talbach
Channel network	1471	517
Hill fast	5733	2808
Hill slow	9606	3126
Total no. of cells	15339	5934

The hill FPDs have a class size of 50m, the channel network of 100m, due to the higher wave velocities in the streams.

5.2.2 Calculation of Effective Precipitation

As the events are all *hindcast*, i.e. precipitation and runoff data are available and modelling is ex post, effective rainfall volume can be set equal to storm runoff volume. To determine storm runoff volume, a hydrograph separation has to be made.

Although tracer data are available for the events, a graphical method is chosen, as this considers response time rather than residence time or source areas. Three simple alternatives are shown in Figure 5.5. The first (Figure 5.5 (a)) assumes a linear rise of baseflow and is probably the most common. But the increase in baseflow has to be induced by event precipitation, therefore a storm runoff volume will be smaller than the volume of effective precipitation.

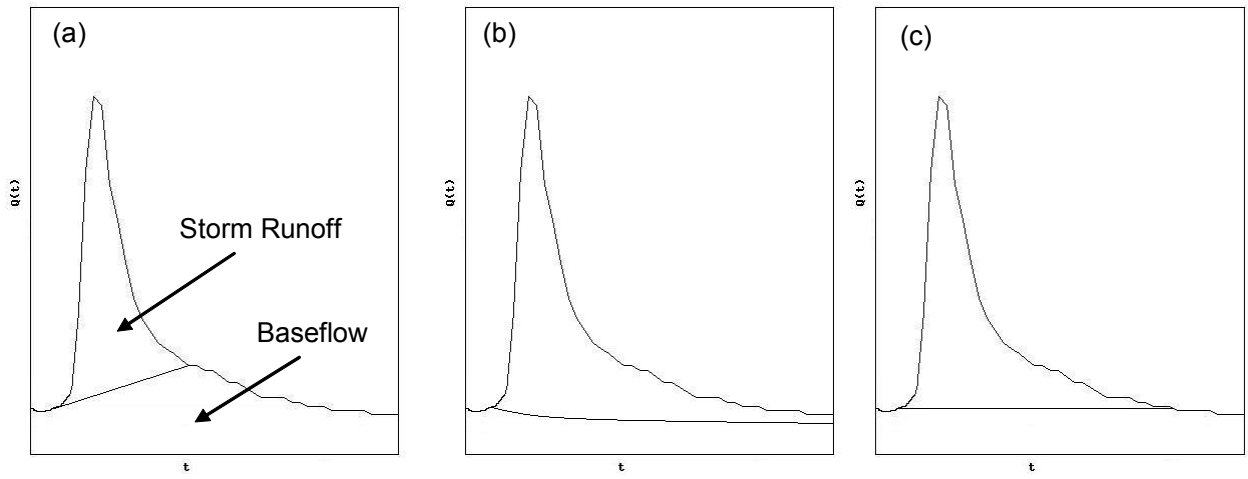

Figure 5.5: Graphical methods of hydrograph separation.

The second method (Figure 5.5 (b)) assumes an exponential recession of baseflow. This is the most realistic estimation of how discharge would have developed without rainfall. But

this method may lead to a very long tailing (BEVEN 2001a, p.32). Assuming constant baseflow (Figure 5.5 (c)) leads to very similar results for the event time scale and is easier to implement into the computer programme. Therefore, it is the method of choice in this study.

Two approaches to determine effective precipitation are considered, as shown in Figure 5.6. The red boxes show total precipitation and the green boxes show effective precipitation for several time steps.

In Figure 5.6 (a), a constant runoff coefficient for the whole event is determined by dividing storm runoff volume by precipitation volume. Precipitation for all time steps is multiplied with the runoff coefficient.

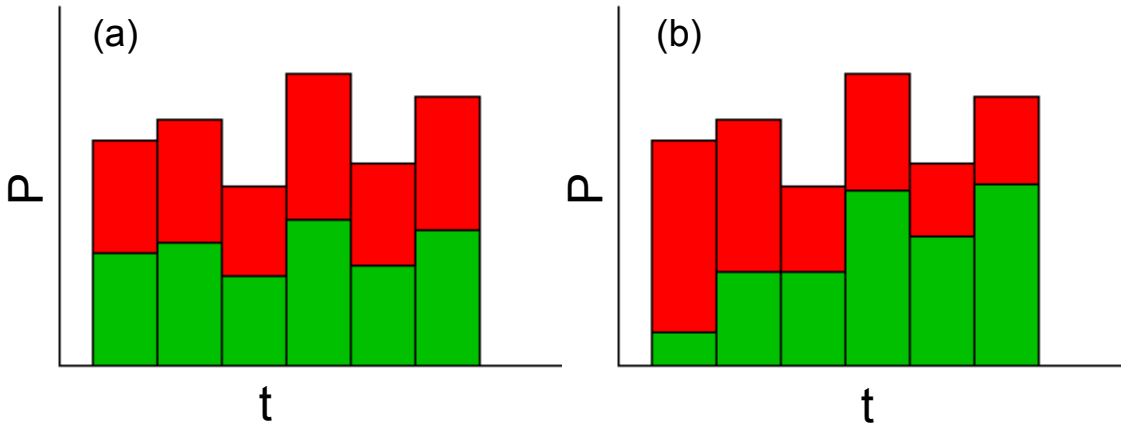

Figure 5.6: Scheme for determination of effective precipitation. (a) Constant runoff coefficient. (b) Exponential decrease of losses.

The second approach (Figure 5.6 (b)) is an exponential decrease of losses. The runoff coefficient is very small for the first few time steps and rises during the event. This is done to reflect initial losses and the saturation process of soils. The total volume of effective precipitation is the same as with a constant runoff coefficient, but it reaches the catchment at a later time.

5.3 Parameter sensitivity of response function

The characteristics of the inverse Gauss function (Eq. 3.18) are tested for various parameters. The mean residence time has much more influence on the shape of the response function than the Peclet number (Figure 5.7). ARMBRUSTER (1997, p. 47) found that the use of an increase of Peclet number with flow path length in contrast to a constant Peclet number for all lengths does not result in a significant difference in hydrograph shape.

Note that for residence times smaller than one the response function is not well defined, i.e. its integral yields less than one (Figure 5.7 (c)). This results in volume losses. They occur in hill cells close to the channel network and channel cells close to the outlet if wave celerity is so high that more than one cell is crossed in one time step. As few channel cells are close to the outlet, the effect is neglectable for the network. However, to minimize the error, temporal resolution should be high. Therefore all events are processed in ten minute time steps, even if only hourly precipitation data are available. Coarser spatial discretization for the channel network than for hillslope response also reduces the error, as fewer classes are affected.

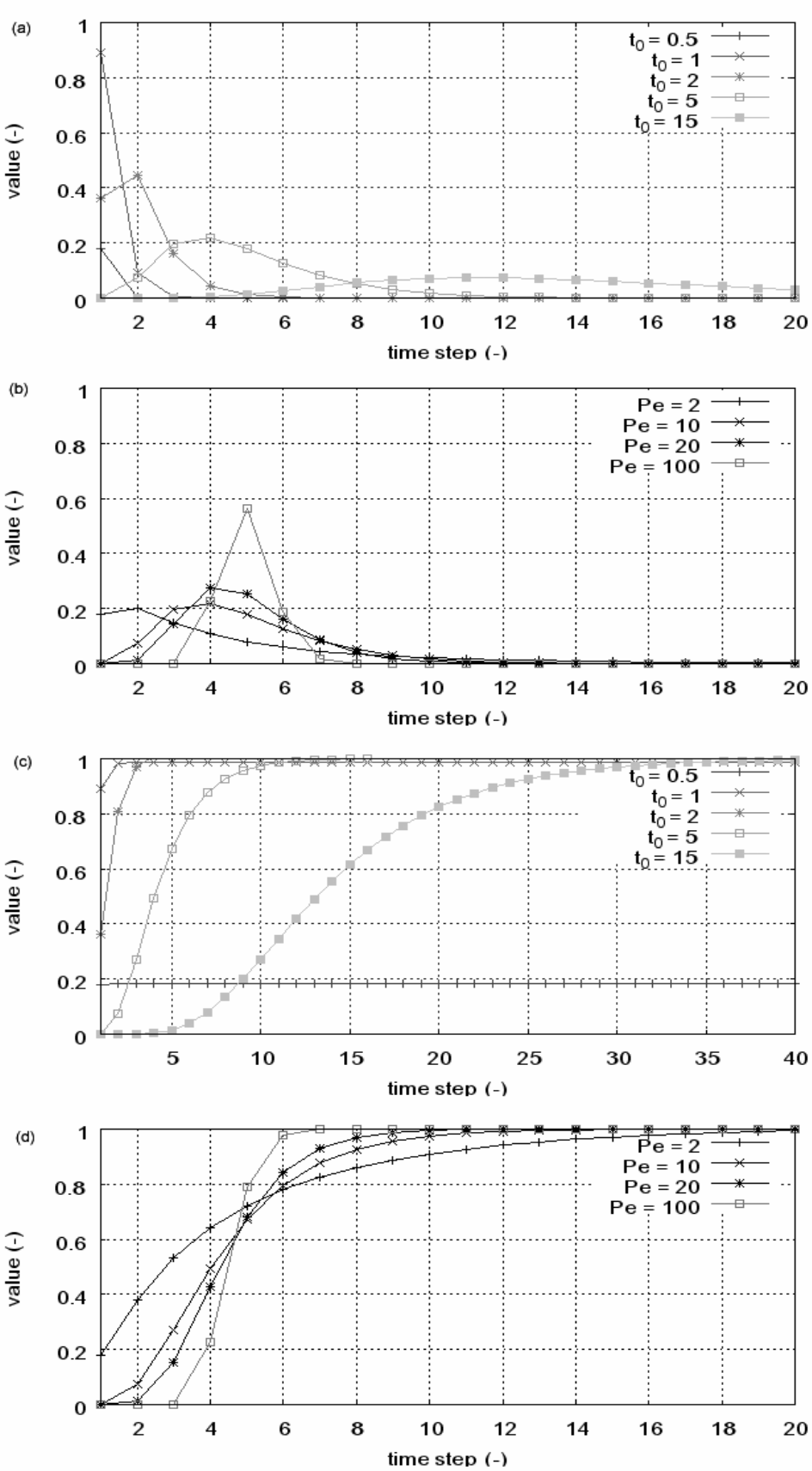

Figure 5.7: Sensitivity of inverse Gauss function to parameter variation. (a) Variation of mean residence time t_0, Pe=10. (b) Variation of Peclet number Pe, t_0=5. (c) Cumulated response for variation of t0. (d) Cumulated response for variation of Pe.

5.4 Model calibration

Four events are used for model calibration (Table 5.2). Runoff of Brugga and St. Wilhelmer Talbach, and silica concentrations at the Brugga outlet in Oberried are modelled.

Table 5.2: Overview of events used for calibration.

Name	Date (DD/MM/YY)	Precip. Dura-tion(h)	Precipitation Volume (m^3)	Storm Runoff Volume Brugga (m^3)	Runoff Coefficient (%)	Peak Discharge Brugga (m^3/s)
CE1	23/08/98	10	1,586,142	106,271	6.7	4.0
CE2	24/08/98	28	2,234,743	257,848	11.5	8.0
CE3	02/06/01	36	2,525,239	434,836	17.2	4.8
CE4	14/12/00	11	813,603	64,080	7.4	3.3

For each event runoff and solute load at Oberried (Brugga) and runoff at St. Wilhelm are modelled, considering two ways to determine effective precipitation (see chapter 5.2.2) with 4,500 Monte Carlo runs each. The used parameter ranges are given in Table 5.3. Runs in which the celerity of the fast hillslope component (v_{hf}) is slower than the celerity of the slow hillslope component v_{hs} are disregarded, so that the valid runs amount to about 4,300. Parameter sets are determined using random sampling and values are taken to be uniformly distributed over their whole range. The same parameter sets are used for Brugga and St. Wilhelmer Talbach. Silica concentrations are held constant for all events to reduce the number of calibration parameters.

Table 5.3: Parameter ranges for Monte Carlo Simulations.

Parameter name	Lower Boundary	Upper Boundary
Wave celerity fast hillslopes vhf (m/10 min)	1	210
Wave celerity slow hillslopes vhs (m/10 min)	1	21
Wave celerity channel network vc (m/10 min)	600	3600
Silica concentration fast hill slopes (mg/l)	2.0	
Silica concentration slow hillslopes (mg/l)	3.7	
Silica concentration channel network (mg/l)	4.9	

5.4.1 Calibration Event 1, 23/08/98

This event (CE1) is a summer event with low antecedent soil moisture. Both streams show single-peak discharge (Figure 5.8). The runoff coefficient is low. The data for this event are taken from SIEBER (2003, p. 64).

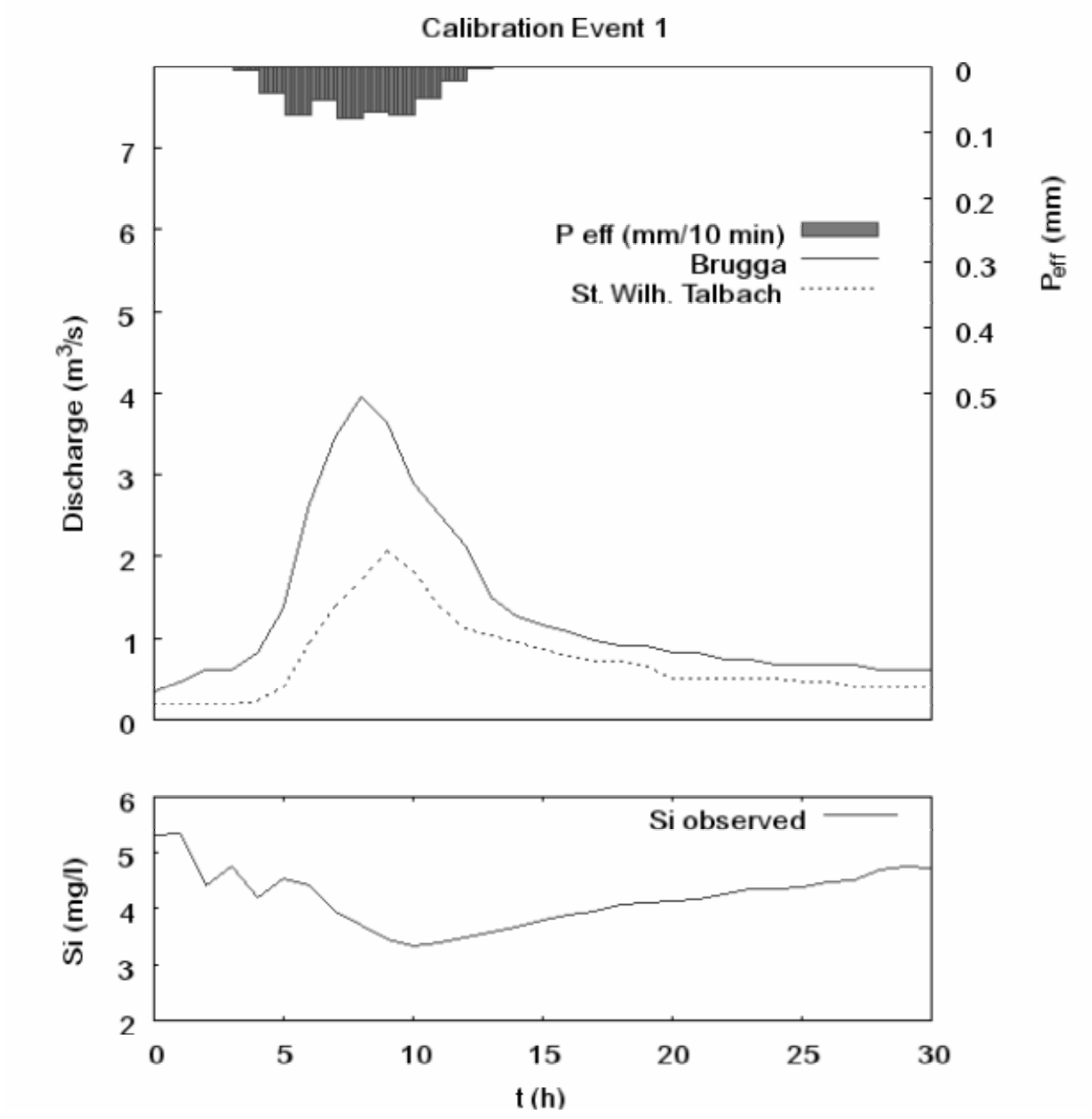

Figure 5.8: Observed discharge and regional precipitation (upper) and silica concentrations (lower) for calibration event 1.

Precipitation data from seven gauging stations are used. Three of them provide hourly data, four others measure daily sums. The latter are disaggregated to hourly data. A combination of an inverse distance method (80%) and an elevation gradient method

(20%) is used for regionalization (SIEBER 2003, p. 53, called *Ereignis 1*). Hourly discharge and silica concentration data are available for the Brugga at Oberried. For the St. Wilhelmer Talbach, only discharge data were provided.

For this study, precipitation data is disaggregated to ten minute values by dividing hourly sums by six.

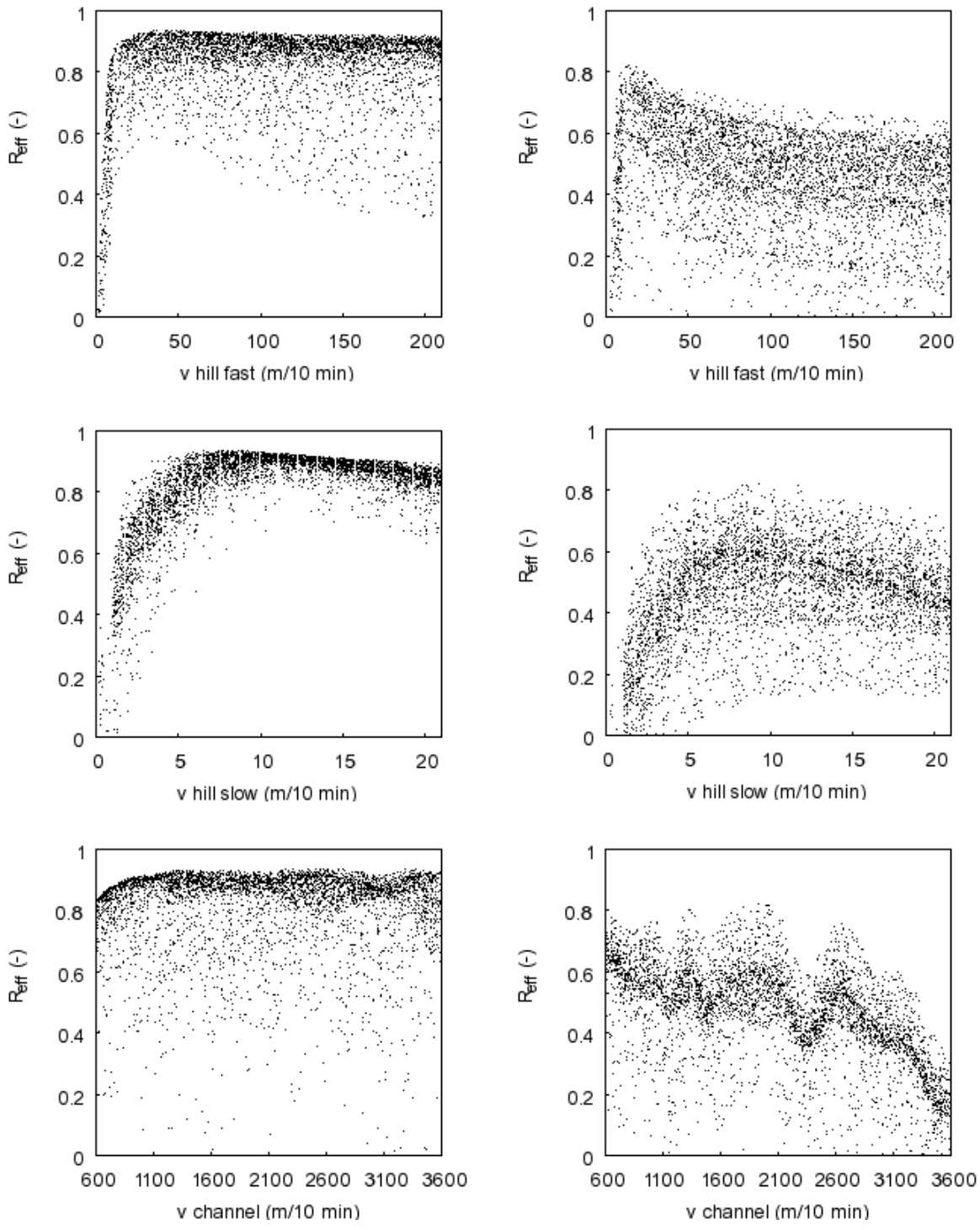

Figure 5.9: Dotty Plots of Monte Carlo simulations for CE1 with constant runoff coefficient for Brugga (left) and St. Wilhelmer Talbach (right), n_R = 4197.

Figure 5.9 shows the Nash-Sutcliffe model efficiency plotted against the parameter values. Effective precipitation is calculated using a constant runoff value. Brugga and St. Wilhelmer Talbach are modelled with 4197 runs each.

Very good results around 0.9 are found for the Brugga. The fast hillslope velocity vhf yields excellent results over a range from 10 to 210 m/10 min, but poor results for values smaller than 10 m/10 min. The channel velocity vc yields good and poor results over its whole range of values. Slow hill velocity vhs is the best-defined parameter, yielding highest R_{eff}-values around 8 m/10 min, poor goodness for lower velocities and nearly as well values for higher velocities. It stands out that all runs with vhs > 8 m/10 min yield efficiencies of 0.6 or better.

Modelling the St. Wilhelmer Talbach shows a different picture (Figure 5.9, right side). Maximum model efficiency is around 0.8. Fast and slow hillslope velocities both have a peak around 10 m/10 min. Goodness of fit plotted against channel velocity seems to oscillate, yielding its optima in distances of approximately 600 m/10 min.

Figure 5.10 shows the goodness of fit for calculating effective precipitation with exponential losses. Virtually no difference to Figure 5.9 can be seen, although values vary slightly as can be seen in the data files.

The only small difference between the two methods to determine effective precipitation may be explained with the low rainfall intensities at the beginning and the end of precipitation. Therefore the differences in runoff coefficient for the first and last few time steps do not amount to a considerable difference in effective precipitation.

Figure 5.11 shows the results of solute modelling. The best runs yield an efficiency about 0.6 for constant and 0.7 for exponential precipitation losses. The latter method seems to prefer low values for all three parameters, while the former reaches best results for values of vhs around 10 m/10 min.

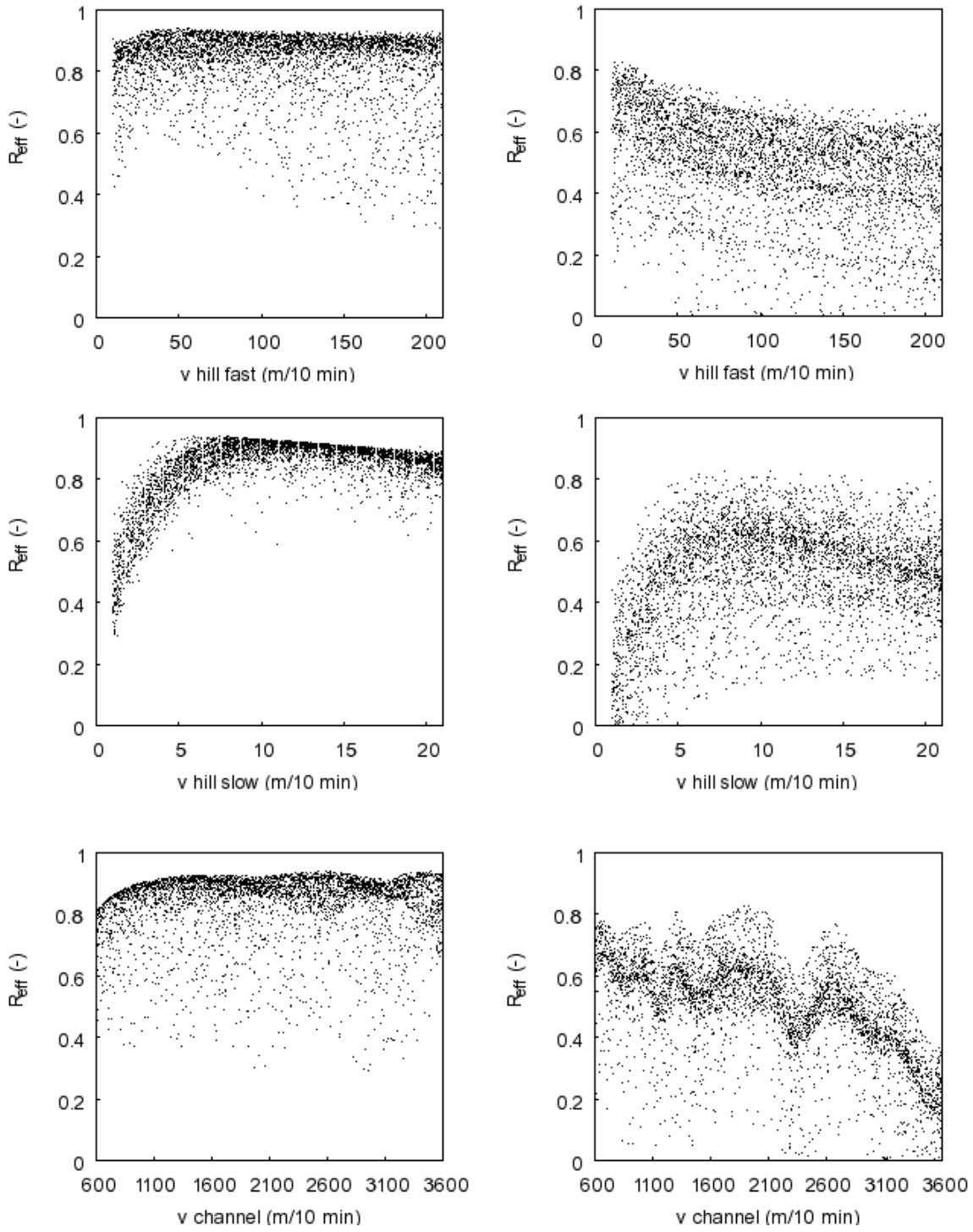

Figure 5.10: Dotty Plots of runoff simulations for CE1 with exponential precipitation losses for Brugga (left) and St. Wilhelmer Talbach (right), n_R = 4212.

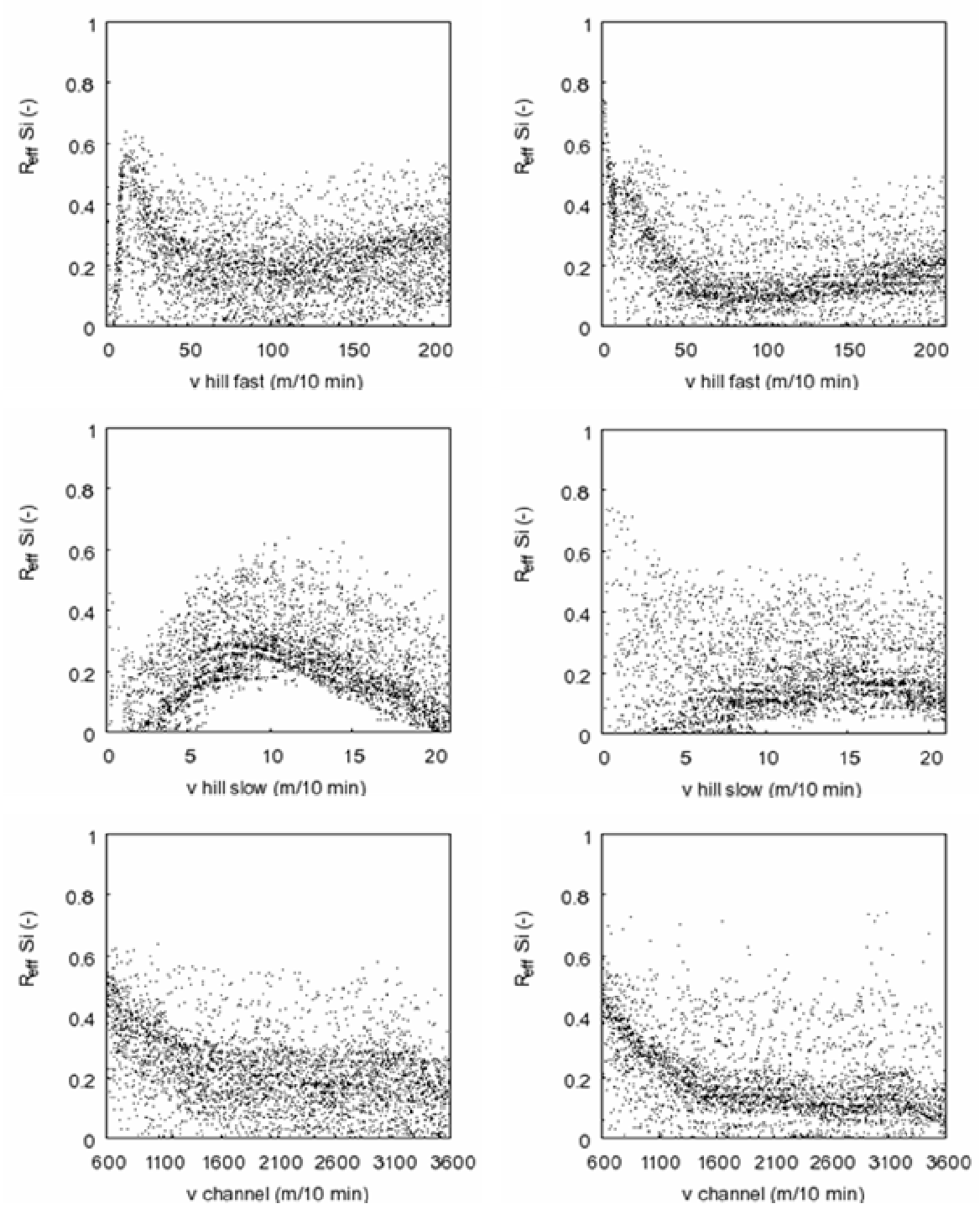

Figure 5.11: Dotty Plots of silica concentration modelling for CE1 at the Brugga outlet with constant runoff coefficient (left) and exponential precipitation losses (right).

5.4.2 Calibration Event 2, 24/08/98

This event (CE2) takes place directly after calibration event 1. Soil moisture content is therefore high and the runoff coefficient is nearly twice as high as in CE1 (Table 5.2). Again, it is a single-peak event.

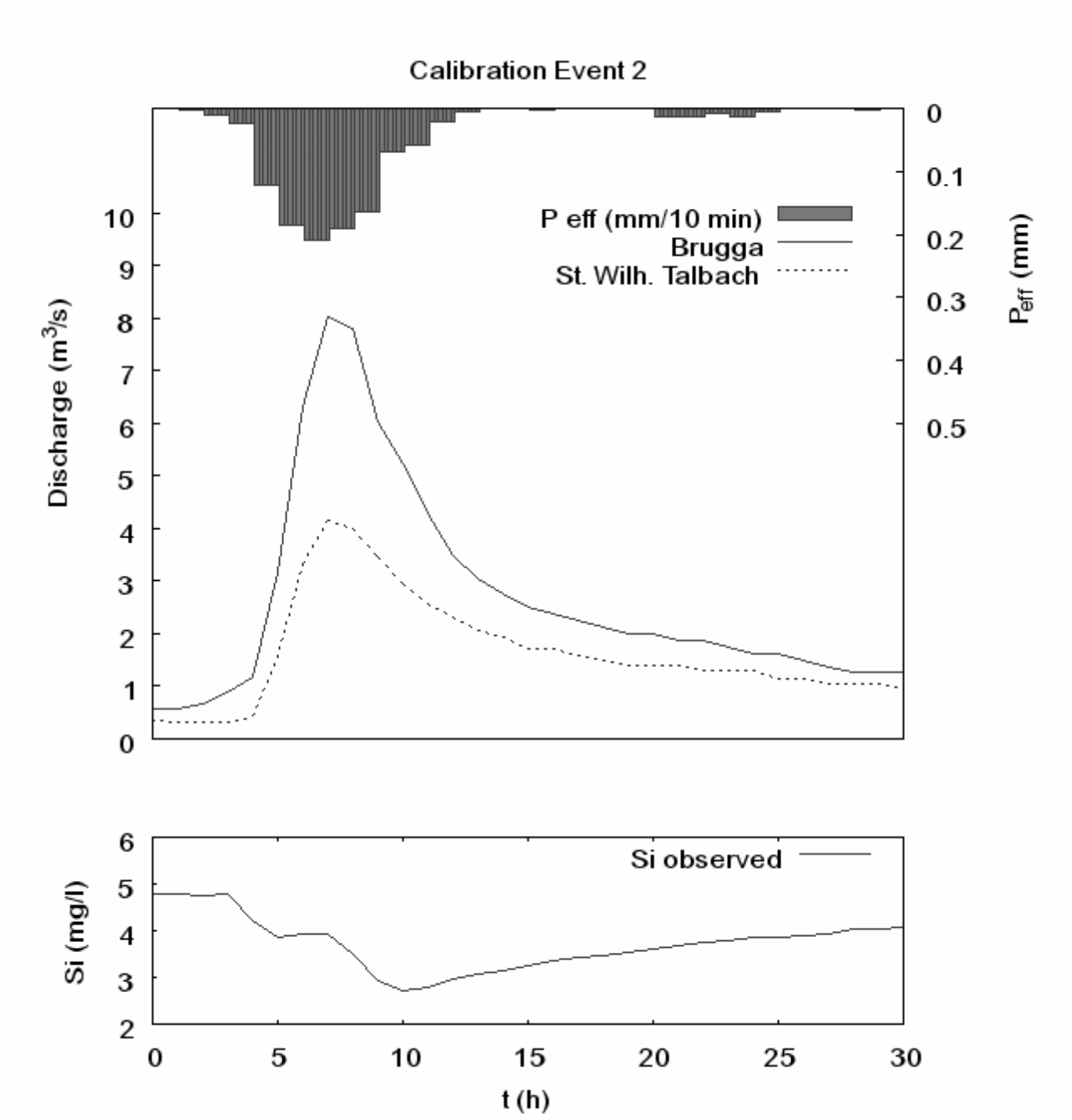

Figure 5.12: Observed discharge and regional precipitation (upper) and silica concentrations (lower) for calibration event 2.

Data are taken from SIEBER (2003, p. 64, called *Ereignis 2*) and were processed as described for the previous event.

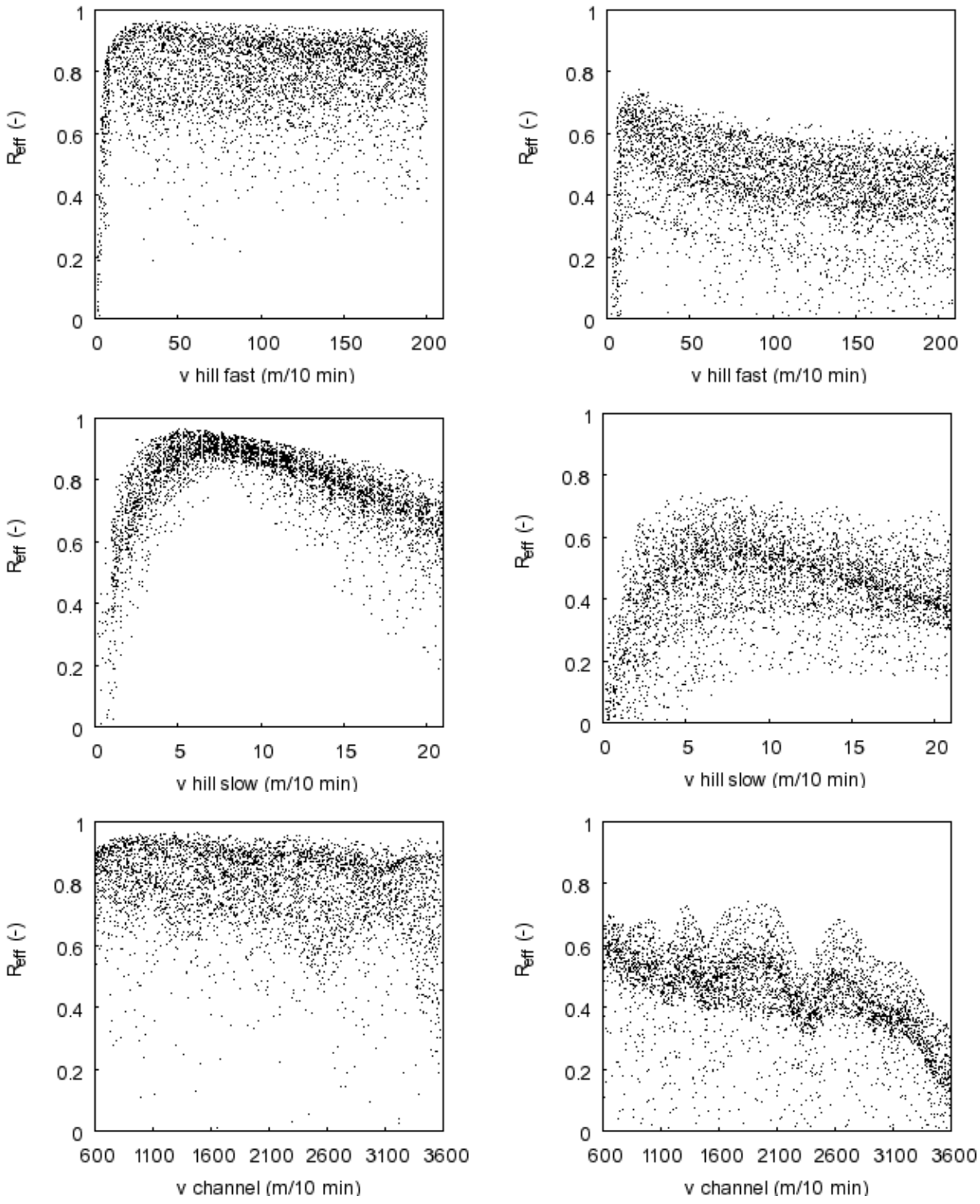

Figure 5.13 Dotty Plots of Monte Carlo simulations for CE2 with constant runoff coefficient for Brugga (left) and St. Wilhelmer Talbach (right), n_R = 4290.

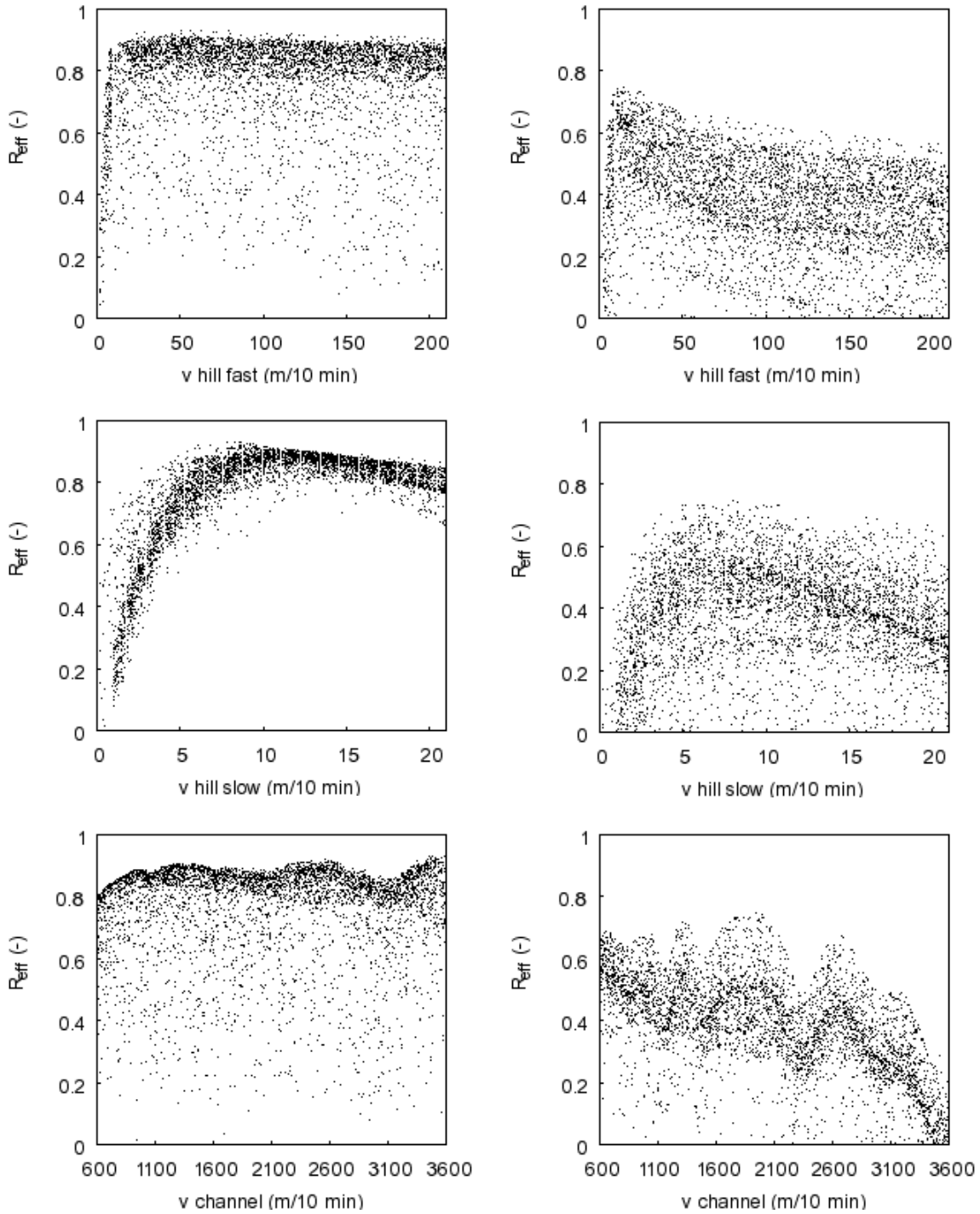

Figure 5.14: Dotty Plots of runoff simulations for CE2 with exponential precipitation losses for Brugga (left) and St. Wilhelmer Talbach (right), n_R = 4310.

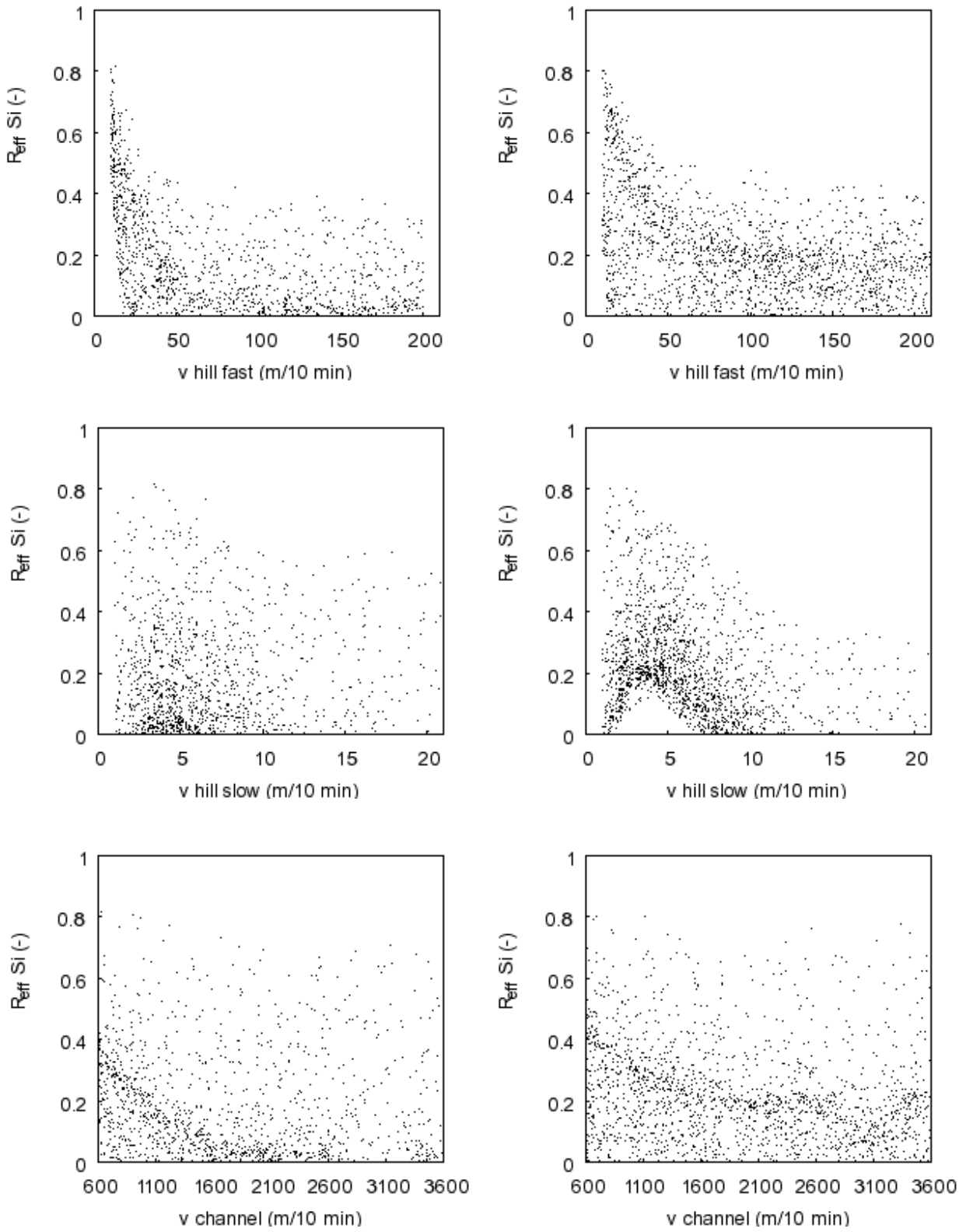

Figure 5.15: Dotty Plots of silica concentration modelling for CE2 at the Brugga outlet with constant runoff coefficient (left) and exponential precipitation losses (right).

5.4.3 Calibration Event 3, 02/06/01

Calibration Event 3 (CE3) is a convective summer hail storm. It is a complex multi-peak event (Figure 5.16). Due to a wet spring soil, moisture content and runoff coefficient are high. As it is a convective event, spatial distribution of precipitation is inhomogeneous and the second and third runoff peak of the Brugga are not well-defined in the St. Wilhelmer Talbach.

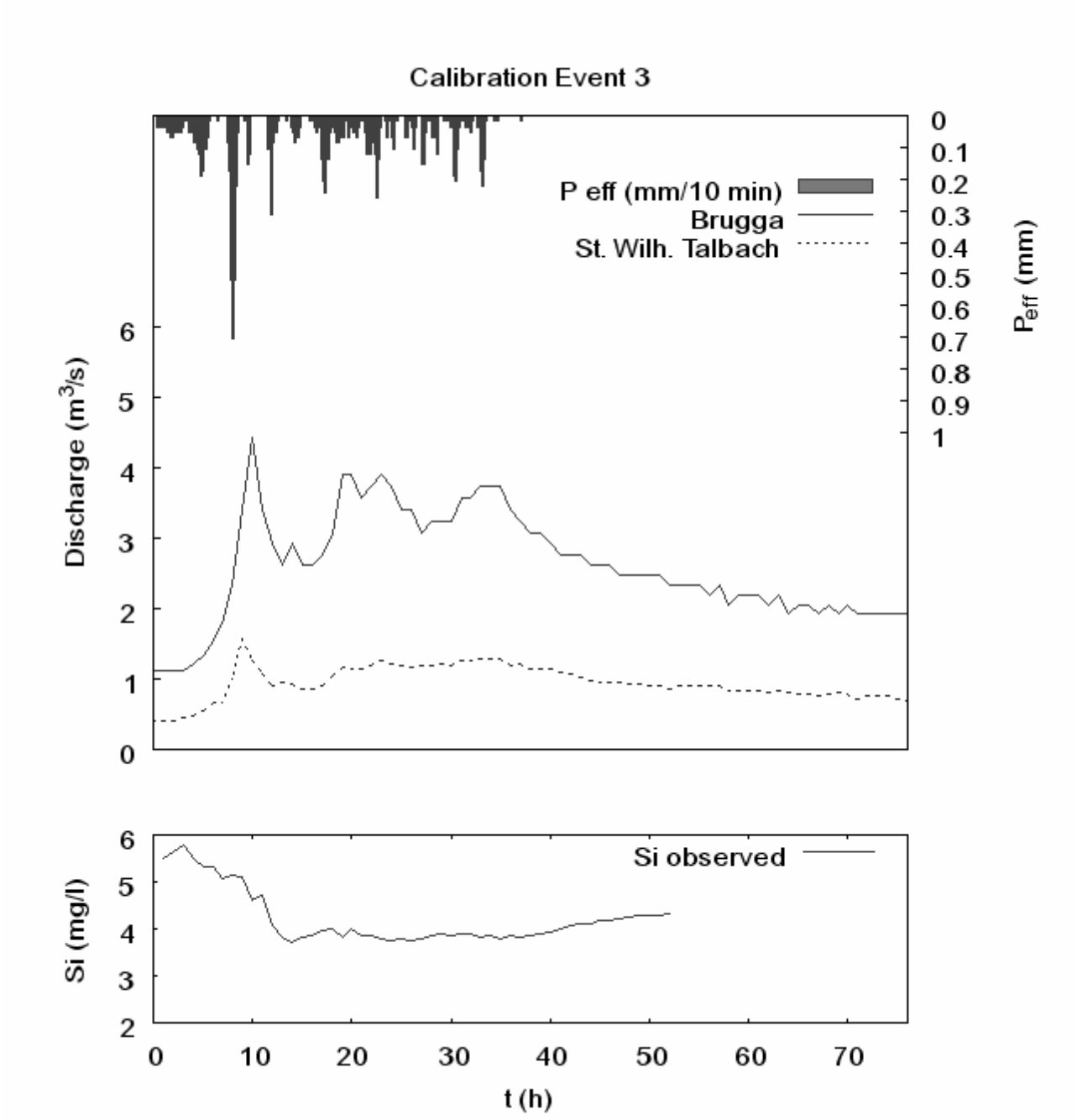

Figure 5.16: Observed discharge and regional precipitation (upper) and silica concentrations (lower) for calibration event 3.

The data are taken from Didszun (2004, p. 112, called *BRU-3*). Precipitation data are taken from the gauging station St. Wilhelm. Ten-minute runoff data for gauging station St. Wilhelm are provided for this event.

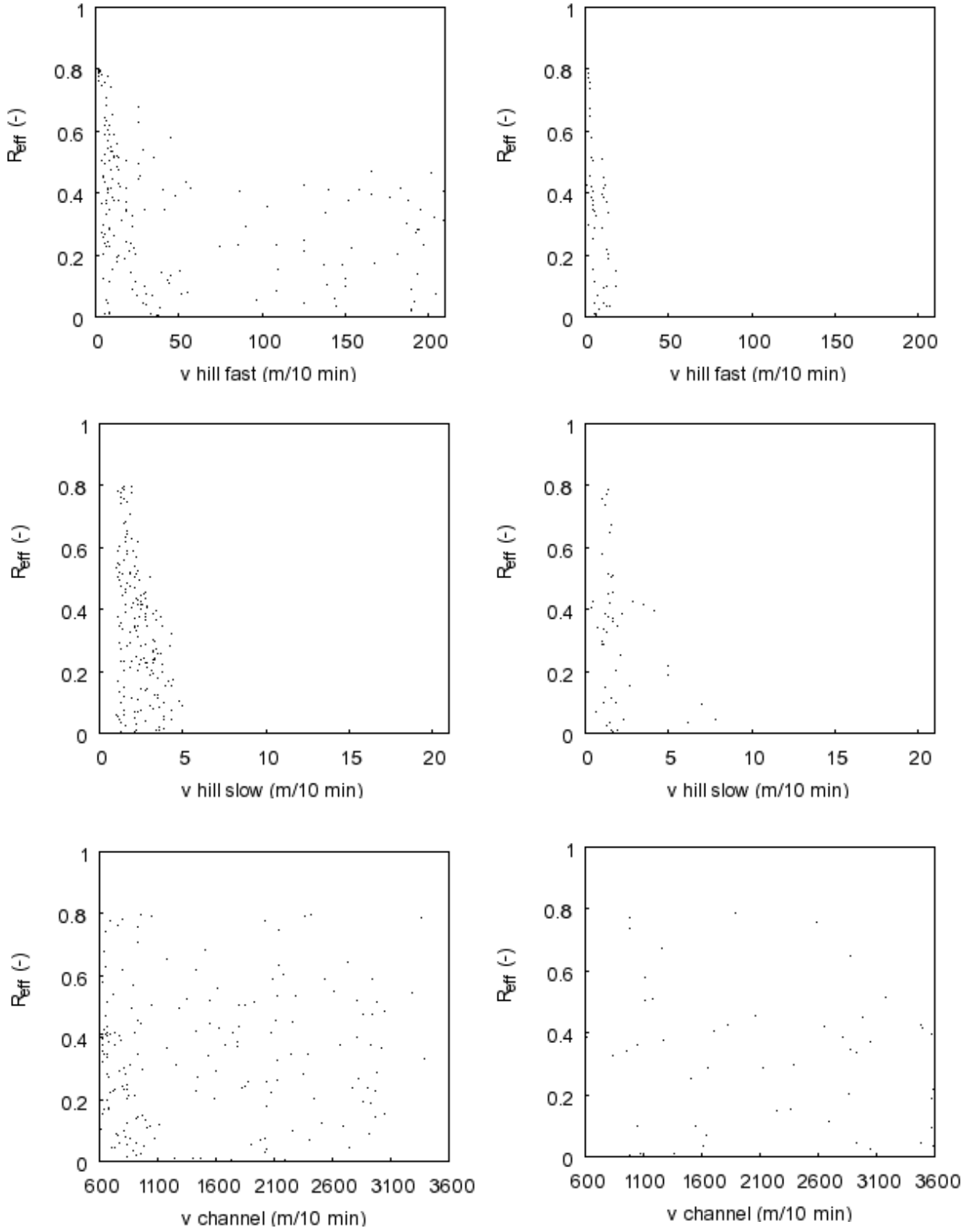

Figure 5.17: Dotty Plots of Monte Carlo simulations for CE3 with constant runoff coefficient for Brugga (left) and St. Wilhelmer Talbach (right), n_R = 4113.

Figure 5.17 and Figure 5.18 show the modelling results for the two patterns of effective precipitation. Only a few runs yield positive R_{eff}-values up to 0.8 for the Brugga and 0.45 for the Talbach. These are generally achieved with very small values for vhf and vhs.

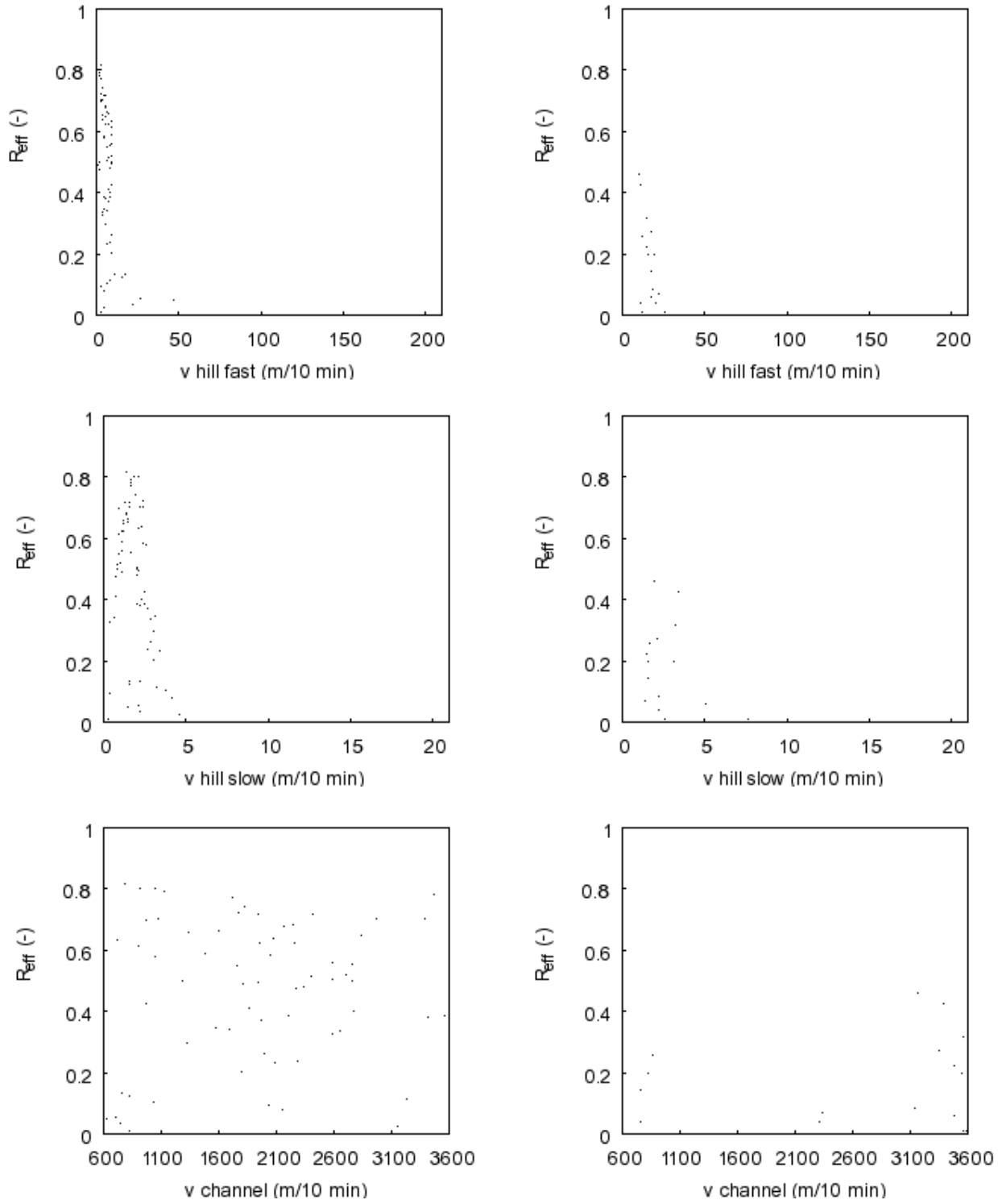

Figure 5.18: Dotty Plots of runoff simulations for CE3 with exponential precipitation losses for Brugga (left) and St. Wilhelmer Talbach (right), n_R = 4112.

This applies to Brugga and Talbach. Over the whole range of values of channel wave celerity vc good modelling results are achieved for the Brugga. The Talbach modelled with the exponential pattern of effective precipitation yields best results for high values of vc.

Solute modelling was not successful. No parameter set obtained positive R_{eff}-values regarding silica concentrations. Therefore, these results are not displayed.

5.4.4 Calibration Event 4, 14/12/00

This event (CE4) is an advective single-peak event. Although preceding soil moisture is similar to Calibration Event 3, the runoff coefficient is substantially smaller (7.4% versus 17.2%). Snow melt did not contribute to runoff.
Data are taken from DIDZSUN (2004, p. 112, event is called *BRU-2*).

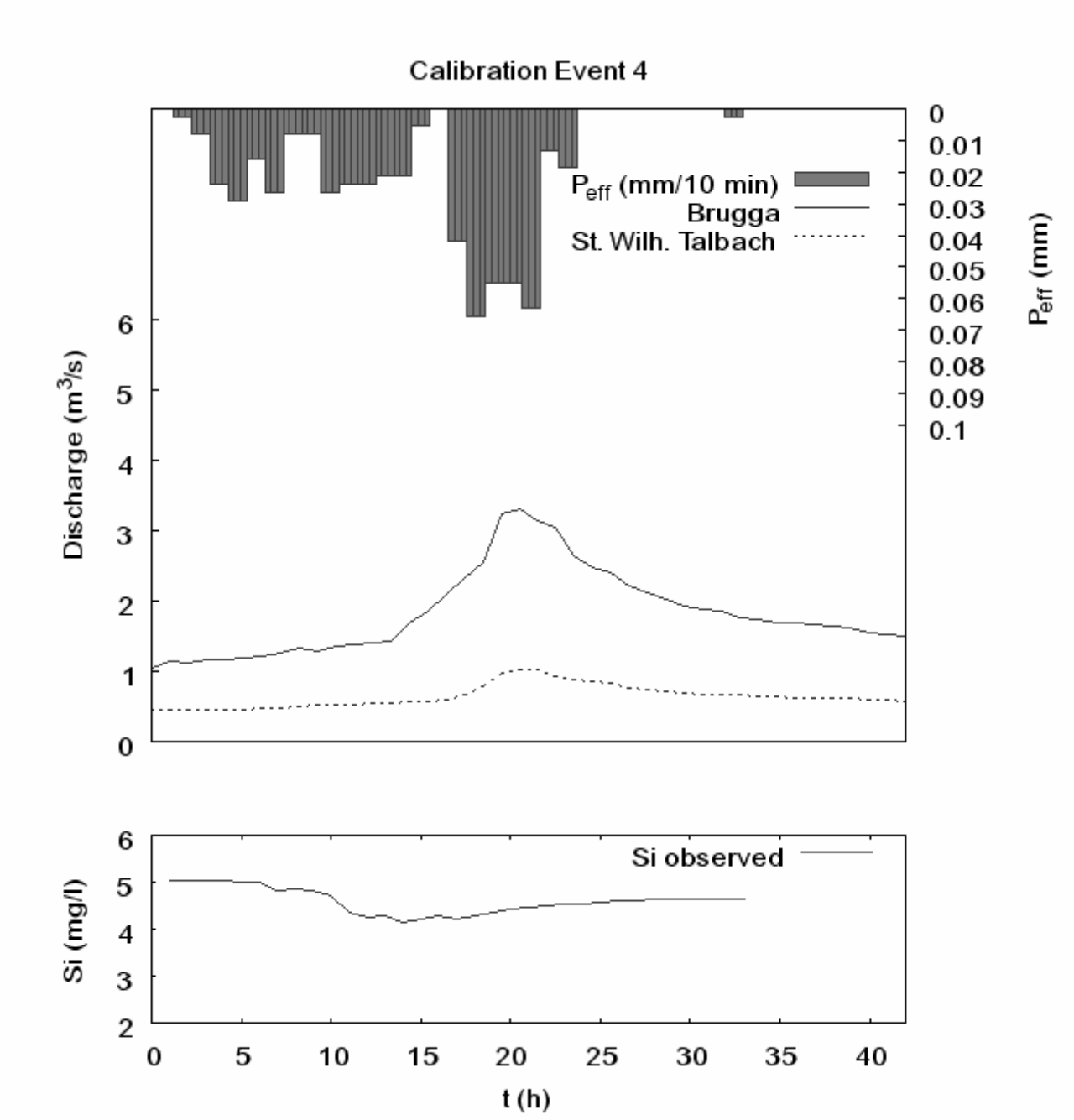

Figure 5.19: Observed discharge and regional precipitation (upper) and silica concentrations (lower) for calibration event 4.

Figure 5.20 and Figure 5.21 show the modelling results for this event. Both effective rainfall patterns yield model efficiencies up to 0.8 for the Brugga and slightly higher ones for the St. Wilhelmer Talbach. For both catchments, low values for vhc yield the best results. Performance deteriorates only slightly for the Brugga, but clearly for its subcatchment.

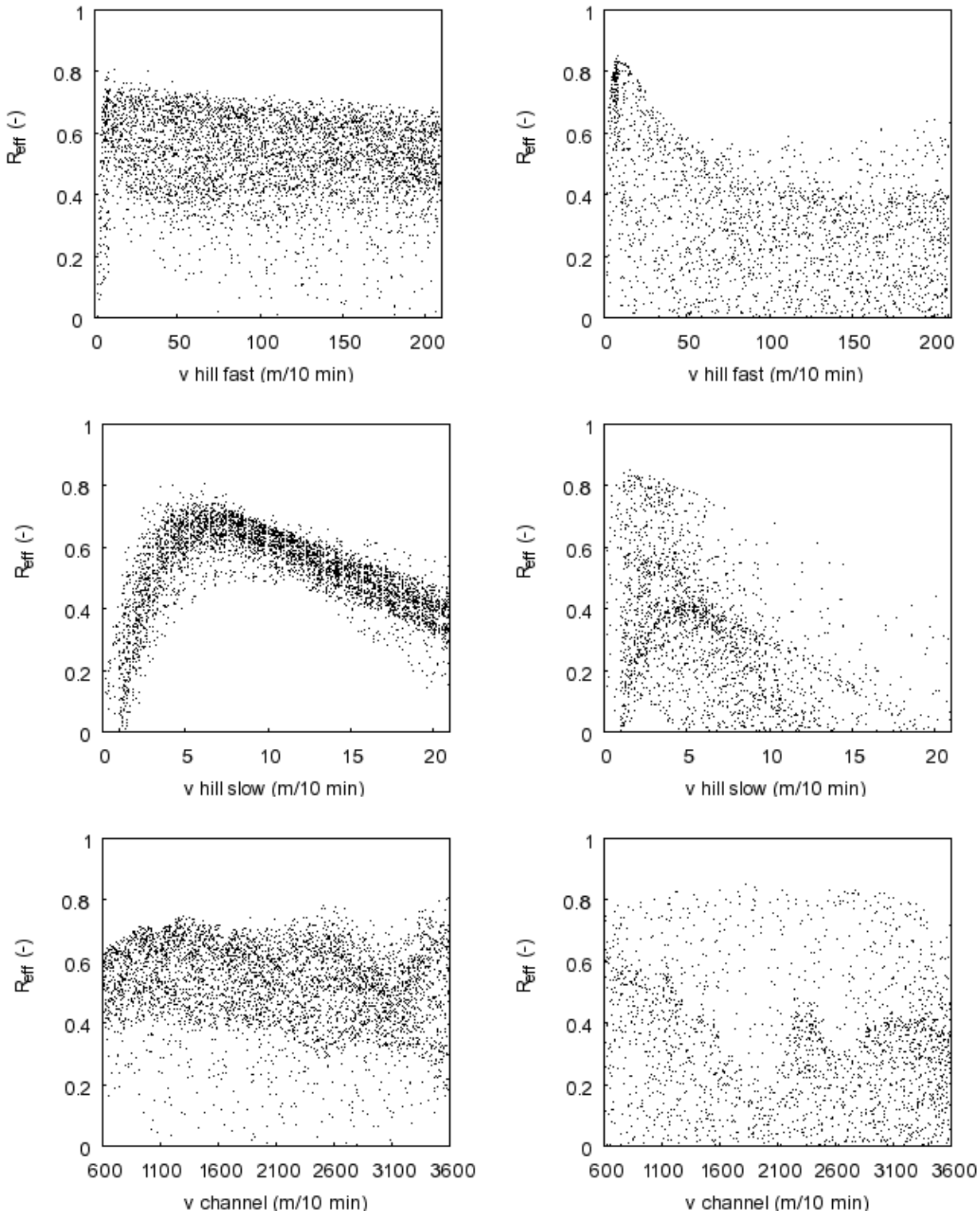

Figure 5.20: Dotty Plots of Monte Carlo simulations for CE4 with constant runoff coefficient for Brugga (left) and St. Wilhelmer Talbach (right), n_R = 4197.

The slow hillslope celerity vhs shows a well-defined peak at 6 m/10 min for the Brugga and about 2 m/10 min for the Talbach, but some higher celerities also succeed in the case of exponential losses (Figure 5.21, middle). For channel velocity vc, values at the upper boundary are most successful for the Brugga. For the Talbach, this parameter seems not well-defined.

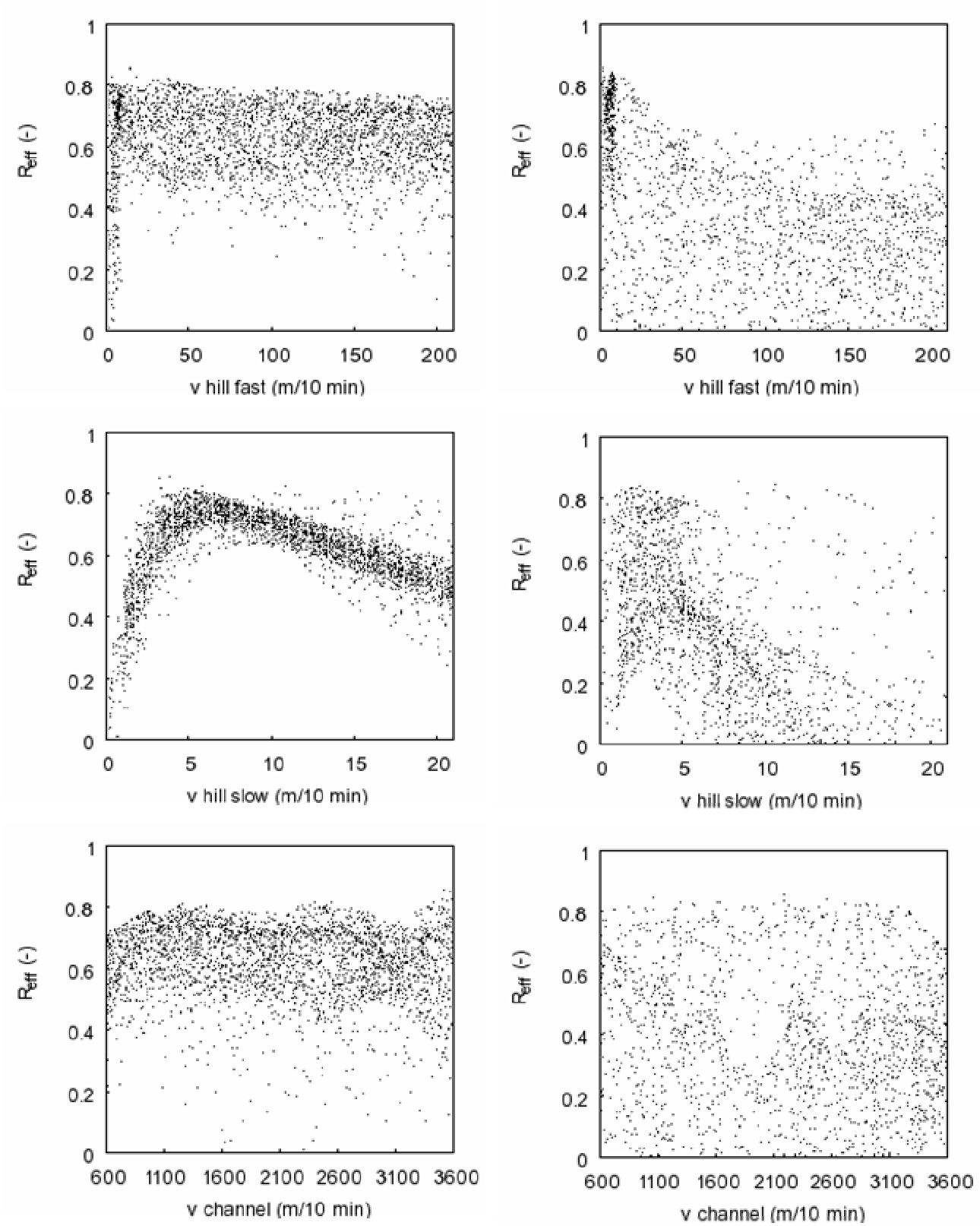

Figure 5.21: Dotty Plots of Monte Carlo simulations for CE4 with exponential losses for Brugga (left) and St. Wilhelmer Talbach (right), n_R = 2858.

Figure 5.22 displays the results of silica load modelling. Positive model efficiency can be achieved only with very small hillslope celerities, whereas the channel wave celerity is not sensitive.

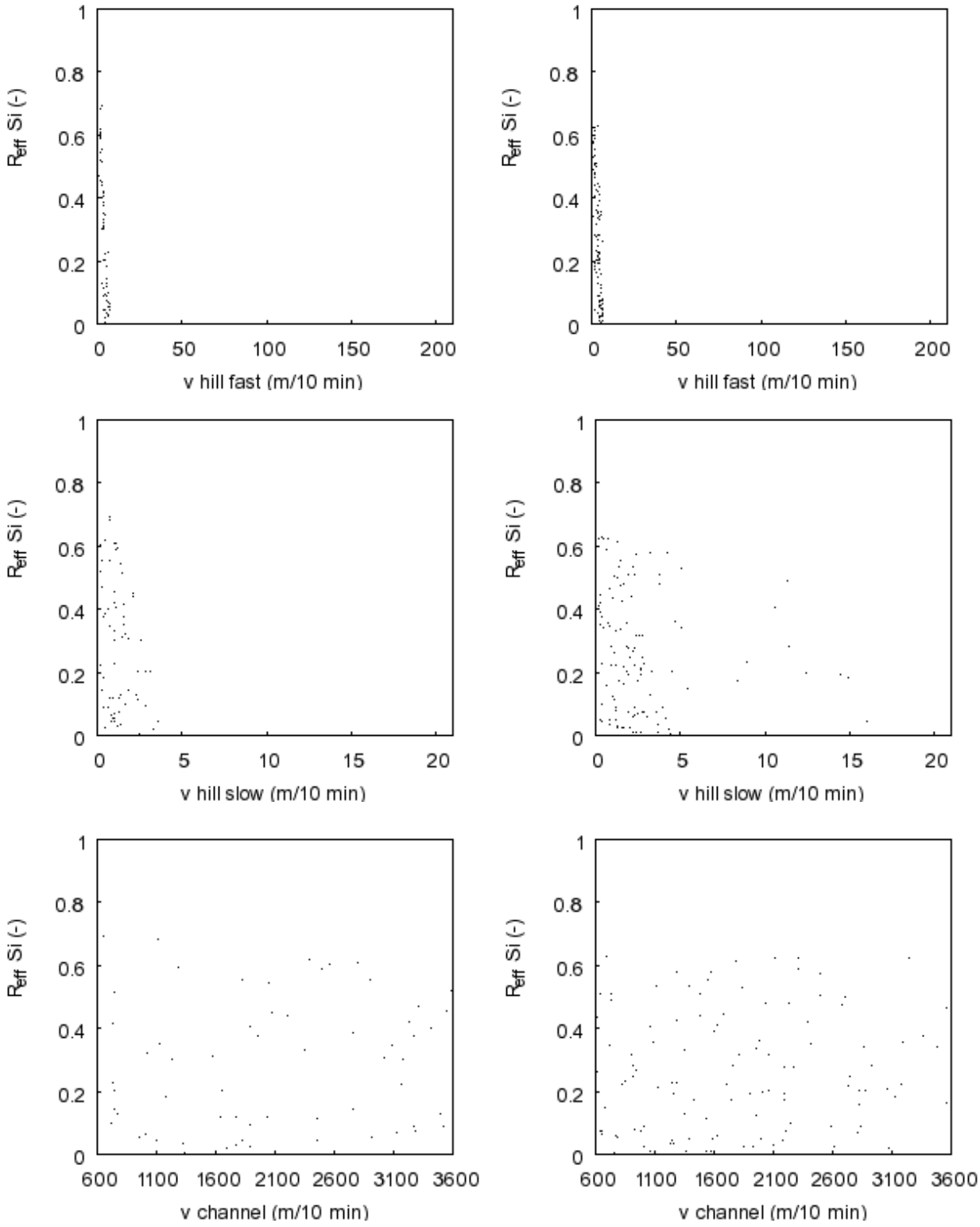

Figure 5.22: Dotty Plots of silica concentration modelling for CE4 at the Brugga outlet with constant runoff coefficient (left) and exponential precipitation losses (right).

5.4.5 Choice of validation parameter sets

As each event is modelled for two patterns of effective precipitation and for two catchments, many successful simulation runs were made with differing parameter sets. To determine a representative set of parameters for all events, the 50 runs for each event with highest Nash-Sutcliffe model efficiency are compared to each other. As parameter values have been chosen randomly, they do not coincide for the events. Therefore values close to successful parameter sets are taken.

This is only possible for continuous response surfaces. CE2 has been sampled around a point of (vhs=5 m/10 min; vhf=30 m/10 min; vc=1926 m/10 min). Parameter values are varied in steps of 1 m/10 min (Figure 2.1). The surface is continuous in a sense that small changes in parameter values result in small changes of model efficiency. Channel celerity was changed within a range from 1920 to 1932 m/10 min but proved completely insensitive. However the small indention at (vhs=8 m/10 min; vhf=31 m/10 min) cannot be explained, but efficiency loss is small.

Figure 5.24 and Figure 5.25 show the results for the Brugga catchment. For constant runoff value, the parameter sets of each event are clustered, with CE1 preferring the highest values for vhs around 9 m/10 min, CE2 and CE4 around 6 m/10 min and CE3 the lowest between 1 and 3 m/10 min. For vhf, the values of all four events are between 1 and 100 m/10 min, with four outliers. Three of for events overlap around the parameter set given in Table 5.4. For exponential losses, the celerities have bigger ranges, especially vhf. CE3 values are clustered around two centres, the very small celerities as for the other pattern of effective precipitation and amongst the values for CE1 and CE2. This time, vhf-values for EC4 are below those of the other events.

The channel wave celerities cover a wide range from 1200 to 3600 m/10 min, where CE1 and CE2 yield the highest celerities and CE4 the lowest for exponential losses and from 1000 to 3500 m/10 min for constant runoff coefficient, this time yielding the highest celerities for CE4.

The St. Wilhelmer Talbach (Figure 5.26 and Figure 5.27) is most successfully modelled with very slow velocities for CE3 and CE4 (constant runoff coefficient), whereas values for CE1 and CE2 show a wider range of successful values. Again wave celerities are higher for the exponential rainfall pattern.

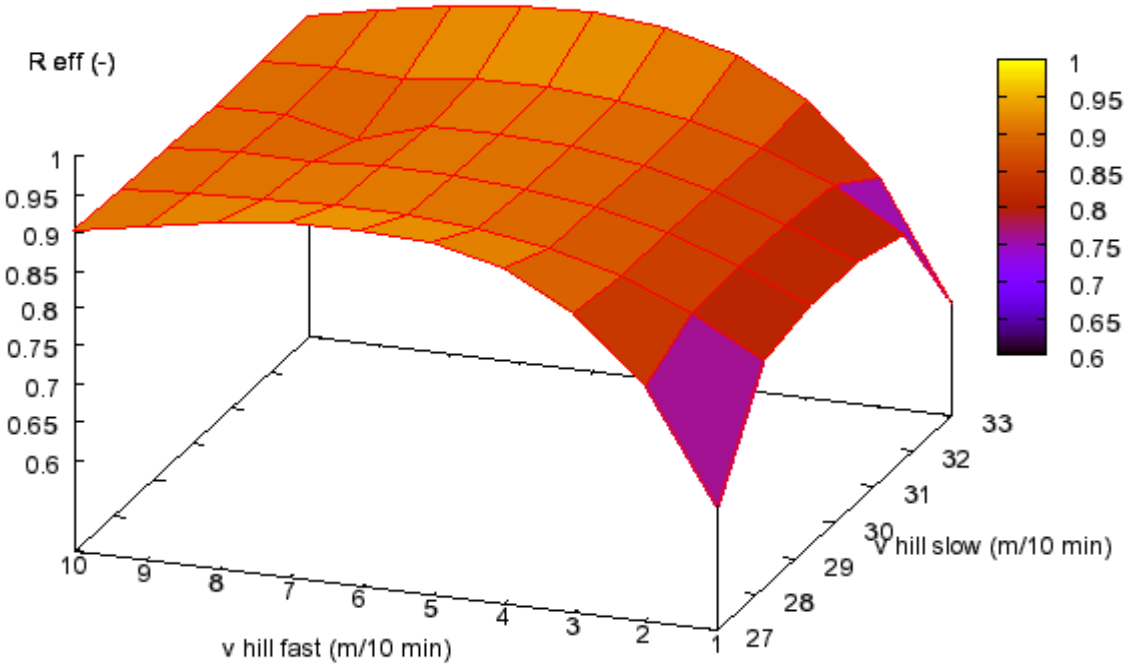

Figure 5.23: Part of response surface of CE2, stratified sampling.

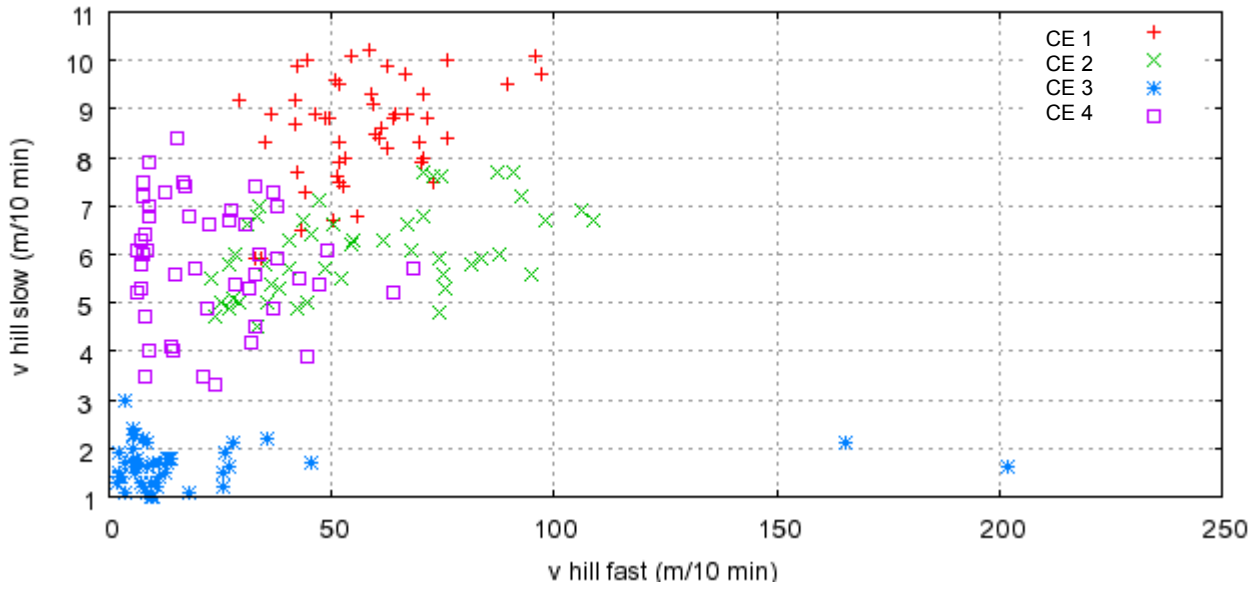

Figure 5.24: 50 most successful parameter sets (regarding runoff model efficiency for Brugga) for constant runoff value.

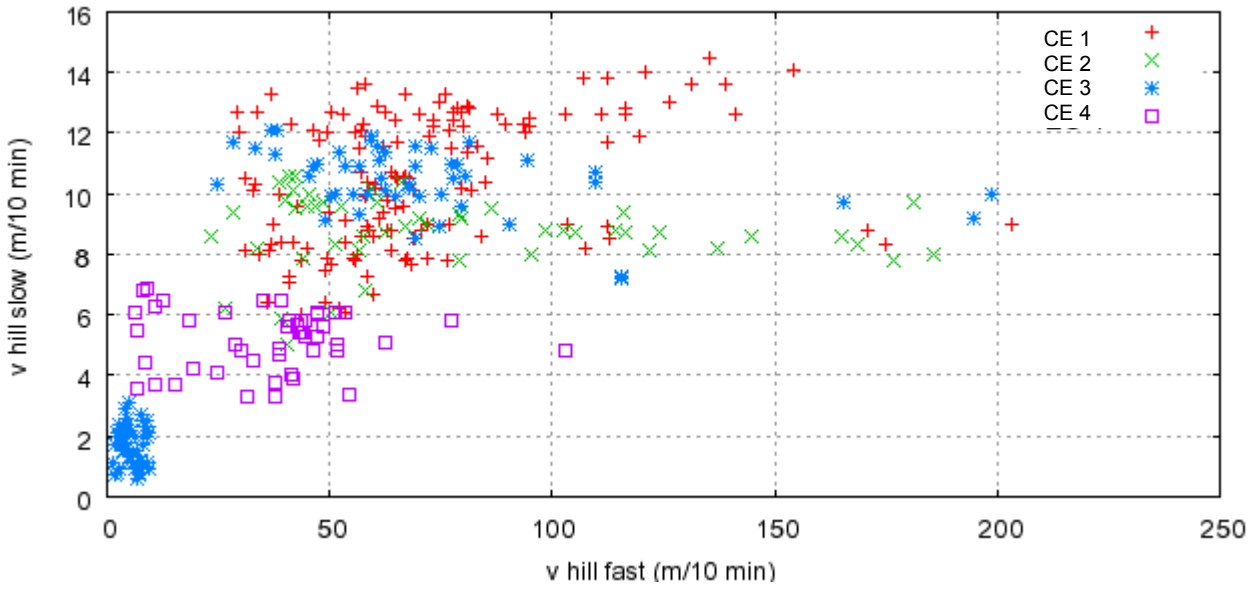

Figure 5.25: 50 most successful parameter sets (regarding runoff model efficiency of Brugga) for exponential decrease of losses.

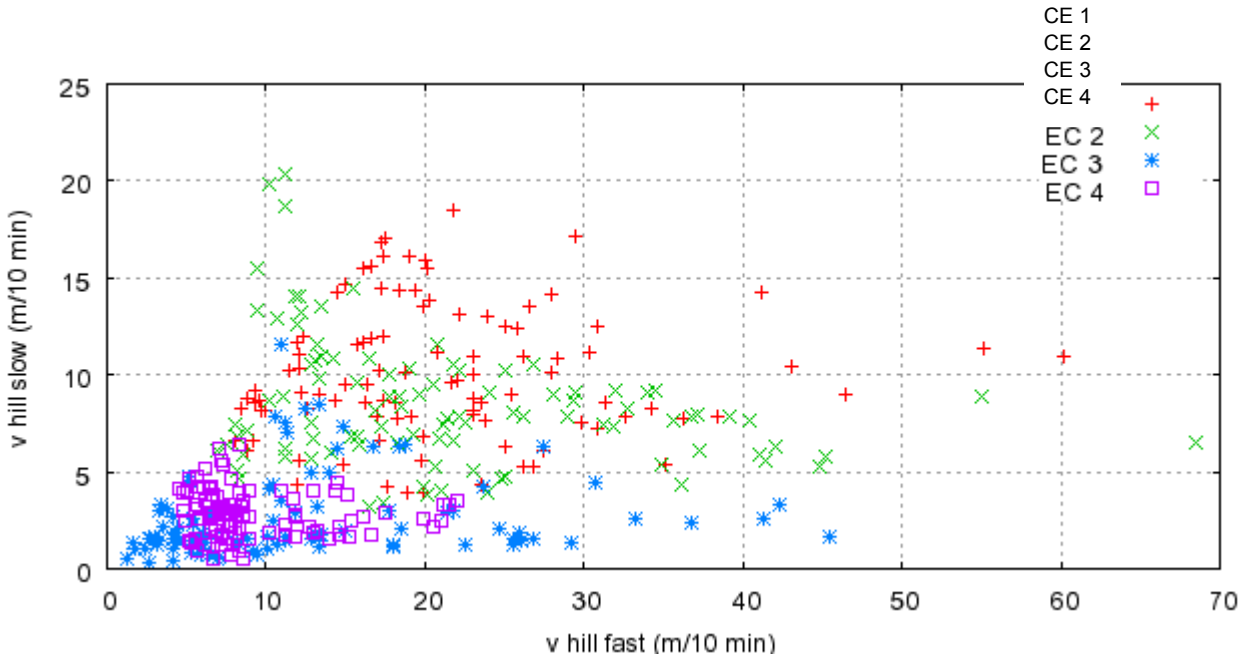

Figure 5.26: 50 most successful parameter sets (regarding runoff model efficiency of St. Wilhelmer Talbach) for constant runoff value.

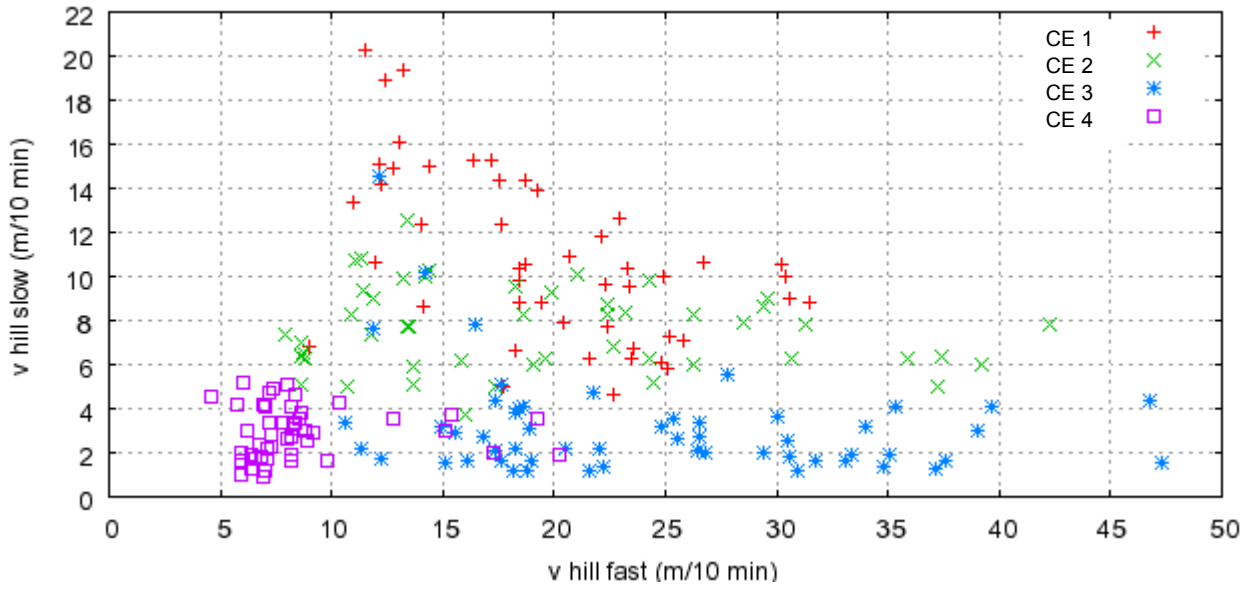

Figure 5.27: 50 most successful parameter sets (regarding runoff model efficiency of St. Wilhelmer Talbach) for exponential decrease of losses.

Table 5.4: Parameter values used for model validation.

Taken from	Name	v hill fast (m/10 min)	V hill slow (m/10 min)	v channel (m/10 min)
Brugga const	P1	40	6	2000
Brugga exp	P2	50	6	2400
St. Wilhelmer Talbach const	P3	12	5	2000
St Wilh. Talbach exp	P4	17	6	2000
Brugga silica modelling	P5	12	8	1500

Table 5.4 shows the parameter sets used for validation. The derivation of parameter set 5 (P5) is described in the next chapter. Table 5.5 shows the model efficiencies of the five parameter sets applied to the calibration events. For all events except CE3 a strong correlation is achieved with all parameter sets (considering R^2 and the classification in Table 3.1).

Table 5.5: Performance of calibration events for validation parameter sets.

Catchment	Parameter Set	Effective Precip. Pattern	Runoff R_{eff} (-) / R^2 (-)			
			CE1	CE2	CE3	CE4
Brugga	P1	const	0.89 / 0.94	0.95 / 0.96	-1.2 / 0.33	0.67 / 0.84
		exp	0.89 / 0.93	0.95 / 0.96	-1.3 /0.33	0.67 / 0.85
	P2	const	0.92 / 0.94	0.94 / 0.95	-1.7 / 0.23	0.69 / 0.83
		exp	0.92 / 0.94	0.94 / 0.95	-1.7 / 0.29	0.70 / 0.84
	P3	const	0.76 / 0.80	0.89 / 0.91	-0.5 / 0.49	0.66 / 0.83
		exp	0.74 / 0.78	0.89 / 0.91	-0.7 / 0.48	0.66 / 0.84
	P4	const	0.84 / 0.87	0.93 / 0.94	-0.9 / 0.42	0.67 / 0.84
		exp	0.83 / 0.85	0.93 / 0.94	-0.9 / 0.42	0.68 / 0.85
	P5	const.	0.81/0.81	0.88 / 0.91	-1.5 / 0.41	0.67 / 0.81
		exp.	0.88 / 0.91	0.88 / 0.91	-1.5 / 0.41	0.67 / 0.82
St. Wilhelmer Talbach	P1	const	0.73/0.83	0.69/0.86	-5.6/0.17	-0.11/0.72
		exp	0.75/0.85	0.69/0.87	-5.6/0.18	-0.11/0.73
	P2	const	0.47/.079	0.47/0.83	-3.1/0.14	0.49/0.70
		exp	0.10/0.57	0.48/0.84	-3.1/0.14	0.49/0.70
	P3	const	0.77/0.92	0.73/0.92	-3.9/0.33	0.37/0.81
		exp	0.77/0.91	0.73/0.92	-3.9/0.33	0.37/0.82
	P4	const	0.81/0.92	0.75/0.92	-4.7/0.27	0.11/0.82
		exp	0.82/0.92	0.75/0.92	-4.7/0.28	0.11/0.79
	P5	const	0.67/0.91	0.62/0.91	-2.8/0.29	0.47/0.79
		exp	0.67/ 0.91	0.62/0.91	-2.8/0.29	0.48/0.80

Figure 5.28 and Figure 5.29 show the hydrographs modelled with the calibration parameters for effective precipitation determined by constant runoff. For the events CE1, CE2 and CE4 the time of peak flow is modelled well, but peak runoff is always underestimated. The rising limb is modelled to fast, as well as with exponential decrease of losses. A fixed amount of initial loss could solve this problem, but then the modelled peak would lag the measured one.

For CE3 the models overestimate the rising limb, the first peak and the plateau. Afterwards the modelled runoff recedes to fast. Here, an increase of baseflow during the event would yield better results.

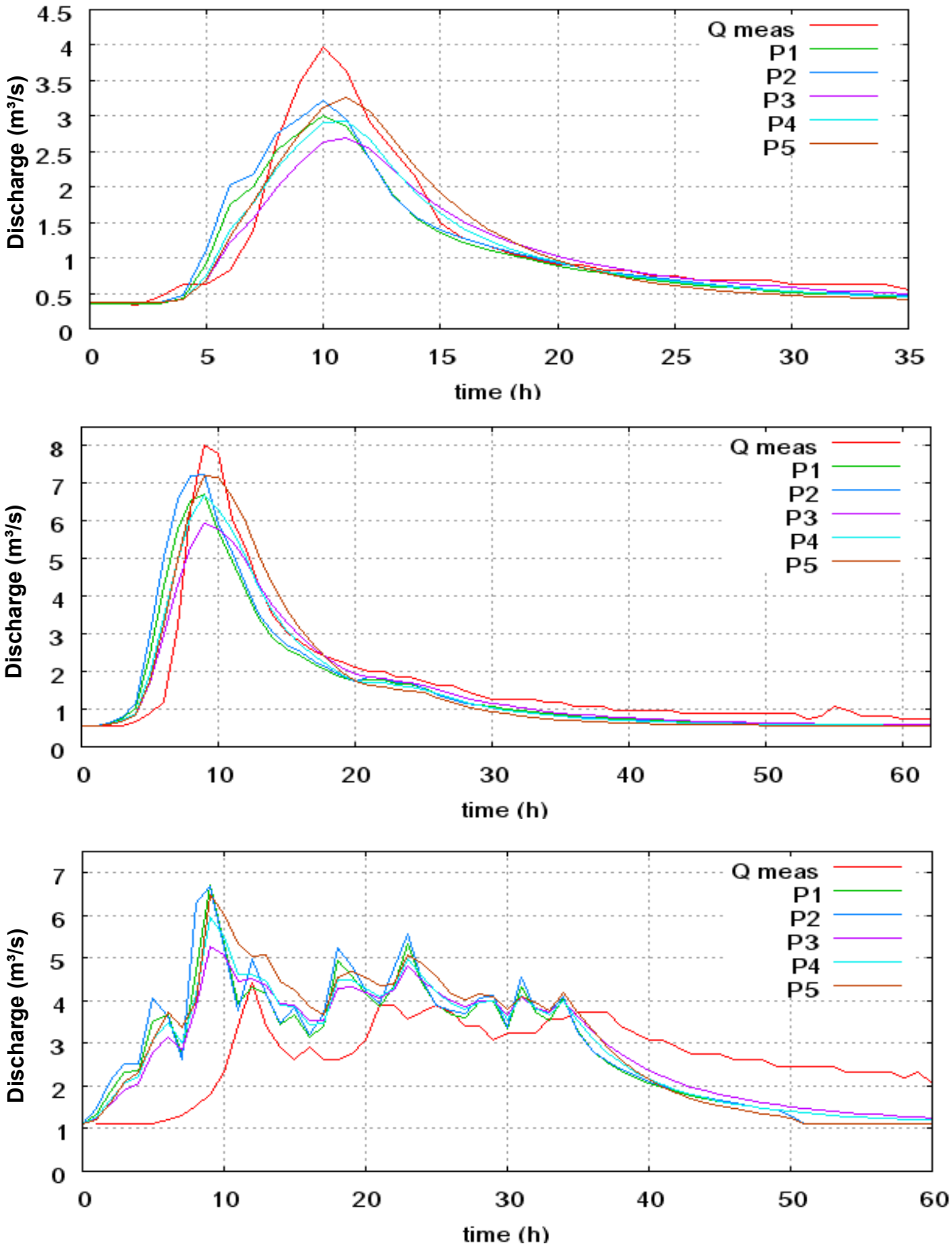

Figure 5.28: Measured and modeled runoff for CE1 (top), CE2 (middle) and CE3 (bottom).

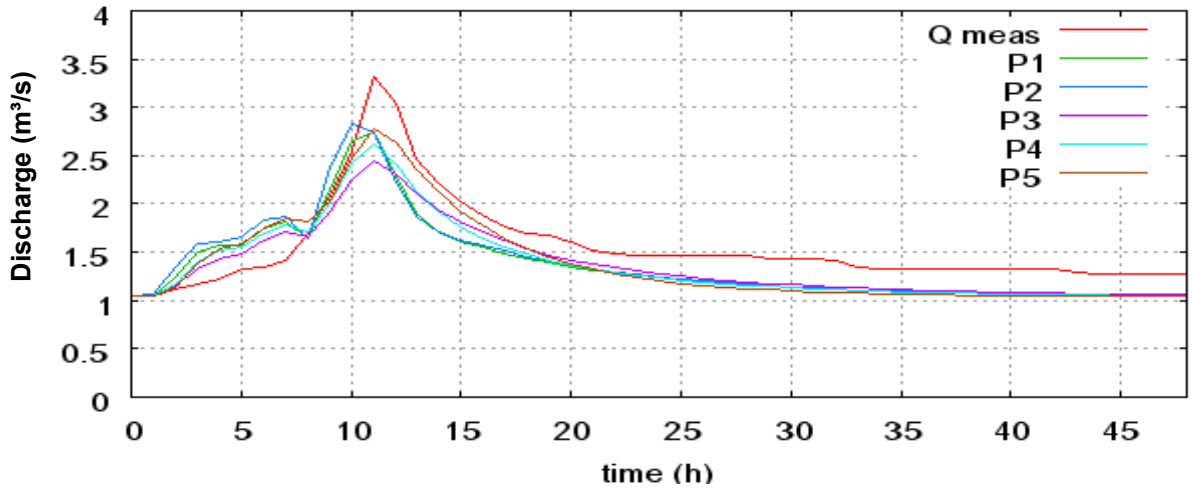

Figure 5.29: Measured and modeled runoff for CE4.

5.4.6 Parameter sets derived from Silica modelling

To check the use of multi-criteria validation, parameter sets with good results for both runoff and solute modelling are regarded. Therefore the combined model efficiency R_C is defined by

$$R_C = R_{eff}(runoff) \cdot R_{eff}(solute) \qquad \text{(Eq. 5.1)}$$

where R_{eff}(runoff) and R_{eff}(solute) are the Nash-Sutcliffe model efficiencies for runoff and solute modelling.

The event CE3 is left out, as no successful prediction of silica was possible. RC ranges from 0.62 to 0.39 for CE1 and CE2 and from 0.31 to 0.05 for CE4 for the sets displayed in Figure 5.30 and Figure 5.31.

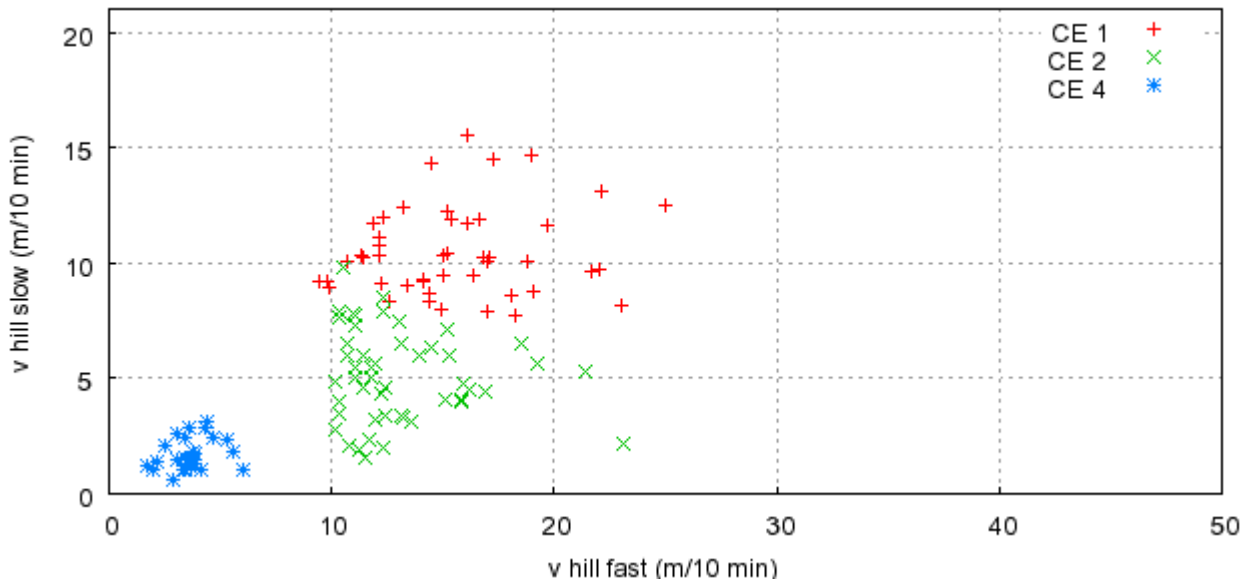

Figure 5.30: Parameter sets successful in modelling runoff and silica concentrations (Brugga) for constant runoff coefficient.

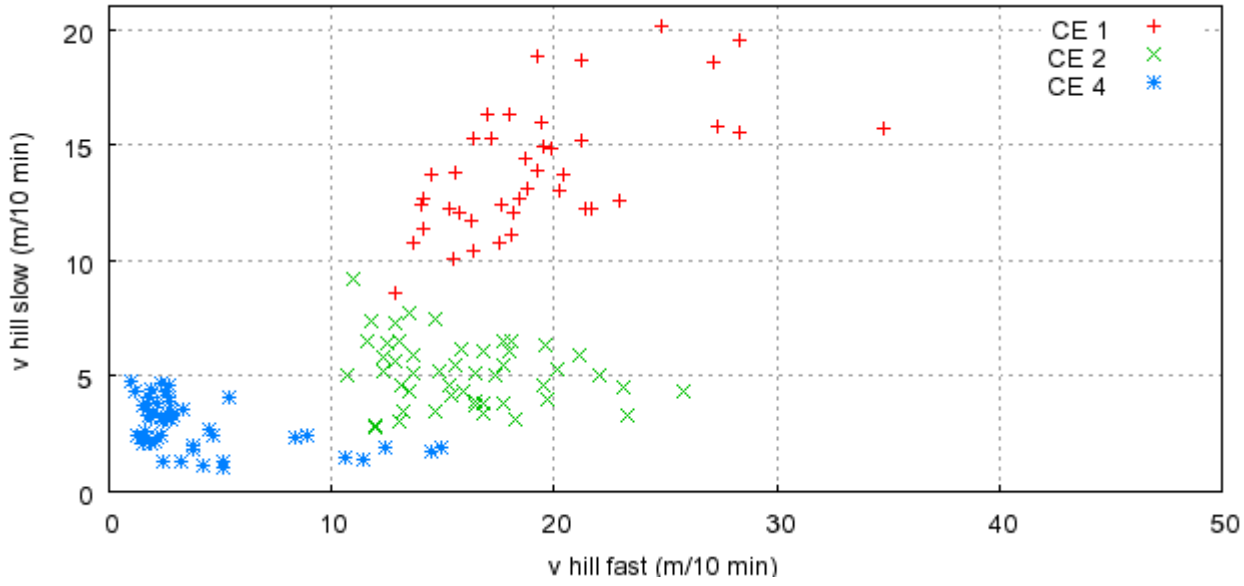

Figure 5.31: Parameter sets successful in modelling runoff and silica concentrations for exponential losses.

The parameter sets are clustered for each event and merely CE1 and CE2 overlap slightly at (vhf=12 m/10 min; vhs=8 m/10 min) in Figure 5.30. Figure 5.31 looks similar but the clusters do not overlap. In both cases, CE4 only shows values of vhs smaller than 5 m/10 min. As CE4 also has the lowest R_C values, it is disregarded and validation parameter set P5 is set to (vhf=12m/10 min; vhs=8 m/10 min; vc=1500 m/10 min).

5.4.7 Comparison of different measures of goodness

Several measures of goodness have been calculated to evaluate model output, but have not yet been discussed. The two measures for overall goodness of fit, the Nash-Sutcliffe model efficiency R_{eff} and the coefficient of determination R^2 (Eq.) are consistent in a way that higher values of one are correlated to higher values of the other, but values of R^2 are generally higher than those of R_{eff} (see Table 5.5 and Table 5.7). Therefore R_{eff} seems to be the stricter measure. But as R_{eff} may also take negative values, it is understandable that values for R^2 are higher, especially for bad simulations.

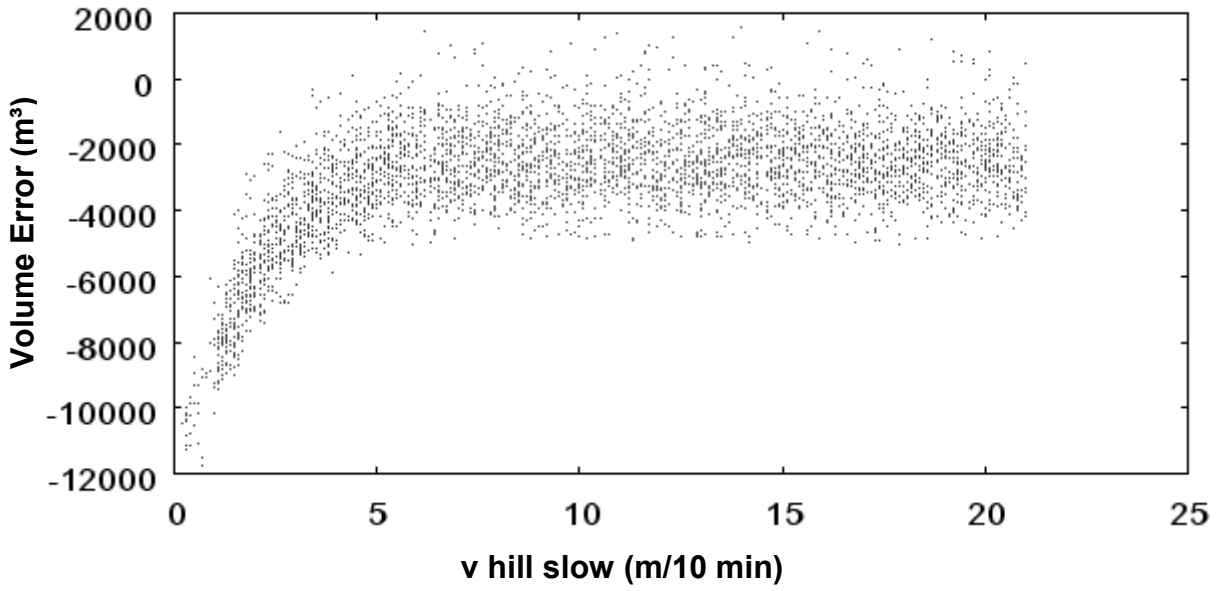

Figure 5.32: Volume error against slow hillslope celerity vhs for CE1.

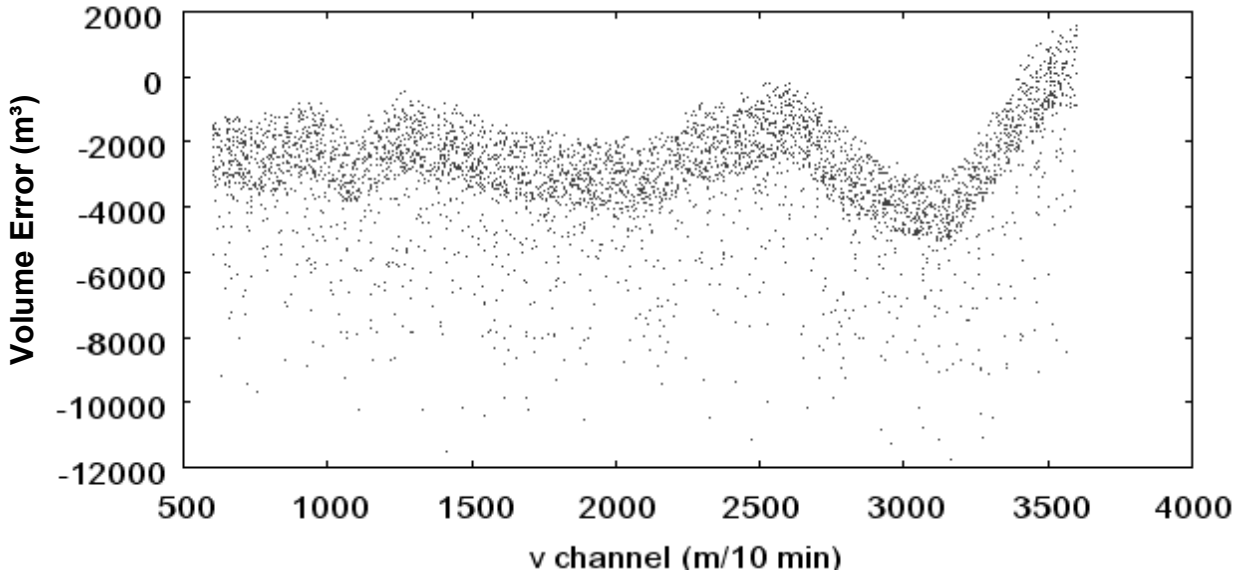

Figure 5.33: Volume error against channel celerity for CE1.

The volume error (Figure 5.32 Figure 5.33) compares measured with modelled runoff volume. Negative values indicate that the model reproduces less water than actually measured. Most runs yield a negative volume error between -1 and -5000 m³. The error is enlarged by very small hill flow celerities (plotting volume error against fast hillslope celerity looks very similar to Figure 5.32). Positive values occur for very high channel celerities. This may have several reasons:

- Not all water has yet entered the stream at the end of the time steps regarded in evaluation
- Response function is not well-defined for $t_0 < 1$ (see Chapter 5.3)
- Numerical inaccuracies

The first reason is true in any case, as the response function runs out asymptotically towards zero. Therefore it takes infinitive time to return all water. This is worsened if celerities are small (Figure 5.32).

The second reason counteracts the first as it is worsened by high flow celerities but does not seem to have a big influence, as higher celerities yield smaller volume errors.
The third reason is unavoidable when doing floating point arithmetic with computers, but seems to add up to have surprising big influence on the model results. It is taken to be responsible for the positive values of volume error for high channel celerities (Figure 5.33).

As said, most of the runs yield volume errors up to -5000 m³. The storm runoff for CE1 amounts to 106,000 m³ plus 53,000 m³ from baseflow, which means that the relative error in the vast majority of runs is equal or smaller than three percent. This is also true for the other events.

The time lag (measured time of peak runoff minus modelled time of peak runoff) of the successful runs regarded for determining the parameter sets is equal to zero or -1 for all runs in all events except for CE3, where values lie between two and -2, -12 and -13 or -23 and -24. This will be due to the three peaks, if one of the later peaks is modelled to be higher than the first (Figure 5.16).

Simulated peak discharge and time to peak are more important for engineering tasks like the dimensioning of structures and are not in the scope of this study, although they contribute significantly to overall goodness of fit.

5.4.8 Conclusions from model calibration

The events CE1 and CE2 could be modelled very successfully with model efficiencies higher than 0.9 and CE4 successfully with efficiencies slightly higher than 0.8. Parameter

sets of these three events overlap, but some loss in efficiency has to be accepted. But CE3 could only be modelled acceptably with an R_{eff} of up to 0.7 in the Brugga catchment for very slow celerities, which lead to decrease of goodness of fit for the other events. This changes for the St. Wilhelmer Talbach, where higher celerities for the fast hillslope component are successful, which hints at a very heterogeneous precipitation distribution. As CE3 was a summer hailstorm, high heterogeneity is very likely. Also the runoff coefficient 0f 17.2% is quite high, which suggests that the gauging station only recorded part of the precipitation.

Equifinality poses a problem. The range of parameter values that lead to similarly good modelling results is wide. The visual method to determine validation parameter sets from the plots (Figure 5.24 to Figure 5.27, Figure 5.30 and Figure 5.31) leads to arbitrary results. A more objective method would have been to use a stratified sampling strategy and seek the parameter set which yields the highest sum of model efficiencies for all events. However, a subjective method simplifies the use of soft data (SEIBERT AND MCDONNELL 2002), like physically meaningful parameter values.

For CE1 and CE2 precipitation data were calculated from seven stations were regionalized to the Brugga catchment. This proves to be more successful than using data from only one station as in CE4.

Three events are single-peaked, but CE3 is multi-peaked. Therefore it will also be more difficult to model, but as good fits are possible, precipitation representation seems to play a larger role.

The celerity of slow hillslope response vhs is the most sensitive parameter, followed by its fast counterpart vhf. This is in line with the higher amount of cells producing slow runoff (63%). Channel velocity proves quite insensitive. Since the Brugga catchment is rather small, channel network routing is not that important.

The comparison between effective precipitation calculated with a constant runoff coefficient and with an exponential decrease of losses shows higher wave celerities for the latter. The reason for this is that the majority of water precipitates later and has to arrive the outlet in less time. A significant advantage of using one method cannot be spotted.

The number of simulation runs, originally 4,500 and around 4,200 if parameter sets where vhf is smaller than vhs, seems to be sufficient, as the whole parameter range is sampled densely. It might be reduced for further studies with similar parameter ranges.

5.5 Influence of channel network

The channel wave celerity vc is not well-defined and good results can be achieved over its whole co-domain. This can be observed frequently for parameters of other models as well

(BEVEN 2001a, p.234). To examine the influence of the channel network, Figure 5.34 shows the hillslope response and the catchment response after channel routing for the Brugga at Oberried. Due to dispersion in the channel network, the final hydrograph is much smoother than hillslope response alone and runoff peaks are postponed for two hours. This seems to be a sensible mean travelling time regarding the size of the Brugga catchment.

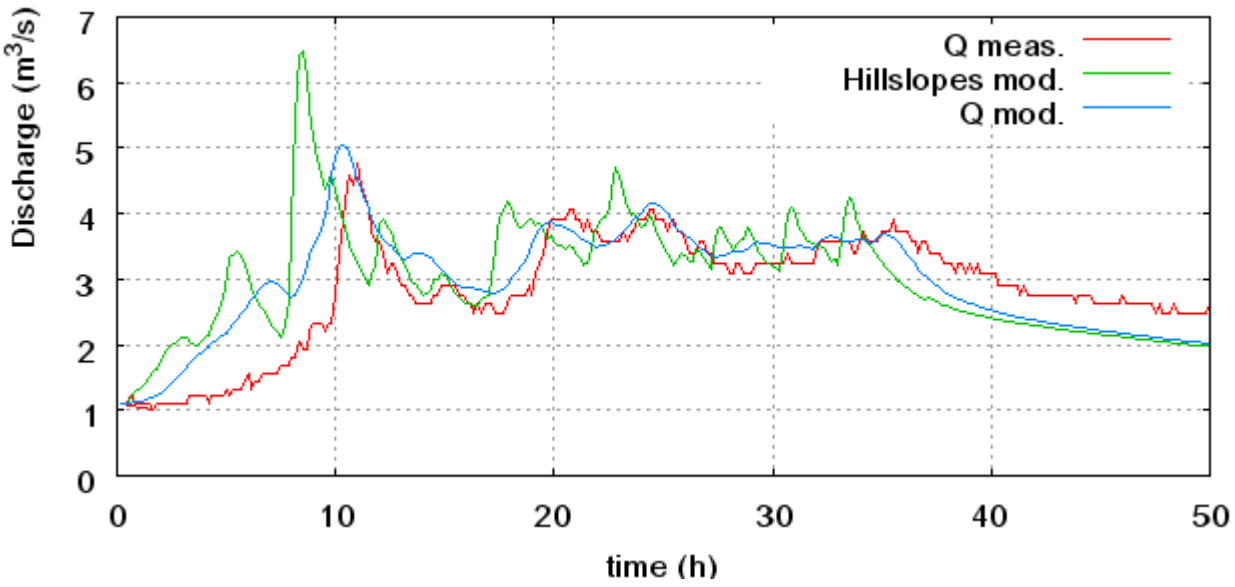

Figure 5.34: Comparison of hillslope response to catchment response for CE3.

Channel routing significantly alters hydrograph shape and should not be dismissed.

5.6 Isotope Modelling

The isotope modelling tool of GUHmod is tested for CE4. The result is shown in Figure 5.16. Runoff is modelled well with a R_{eff} of 0.80, although the peak is slightly underestimated (vhf=32 m/10 min; vhs=4 m/10 min; vc=3572 m/10 min). Below, the measured and modelled deuterium signature of discharge at gauging station Oberried and the deuterium content of precipitation water (input function) are shown.

The amount effect is clearly seen in precipitation. At the beginning of the event, isotope signature has a delta value of -30‰ which decreases to -80‰ at the end. Runoff starts with a delta value of -65‰ which goes down to -70‰ during the event. An influence of the heavier precipitation is seen in the modelled delta values which rise to -50‰, but not in the measured data.

The small influence of heavy precipitation on discharge signature can be explained by the contribution of pre-event to storm runoff. Due to pressure wave effects, lighter water is pressed into the stream by the event-water. Pre-event water was found to contribute 80% of runoff from saturated areas during floods (WENNINGER ET AL. 2003).

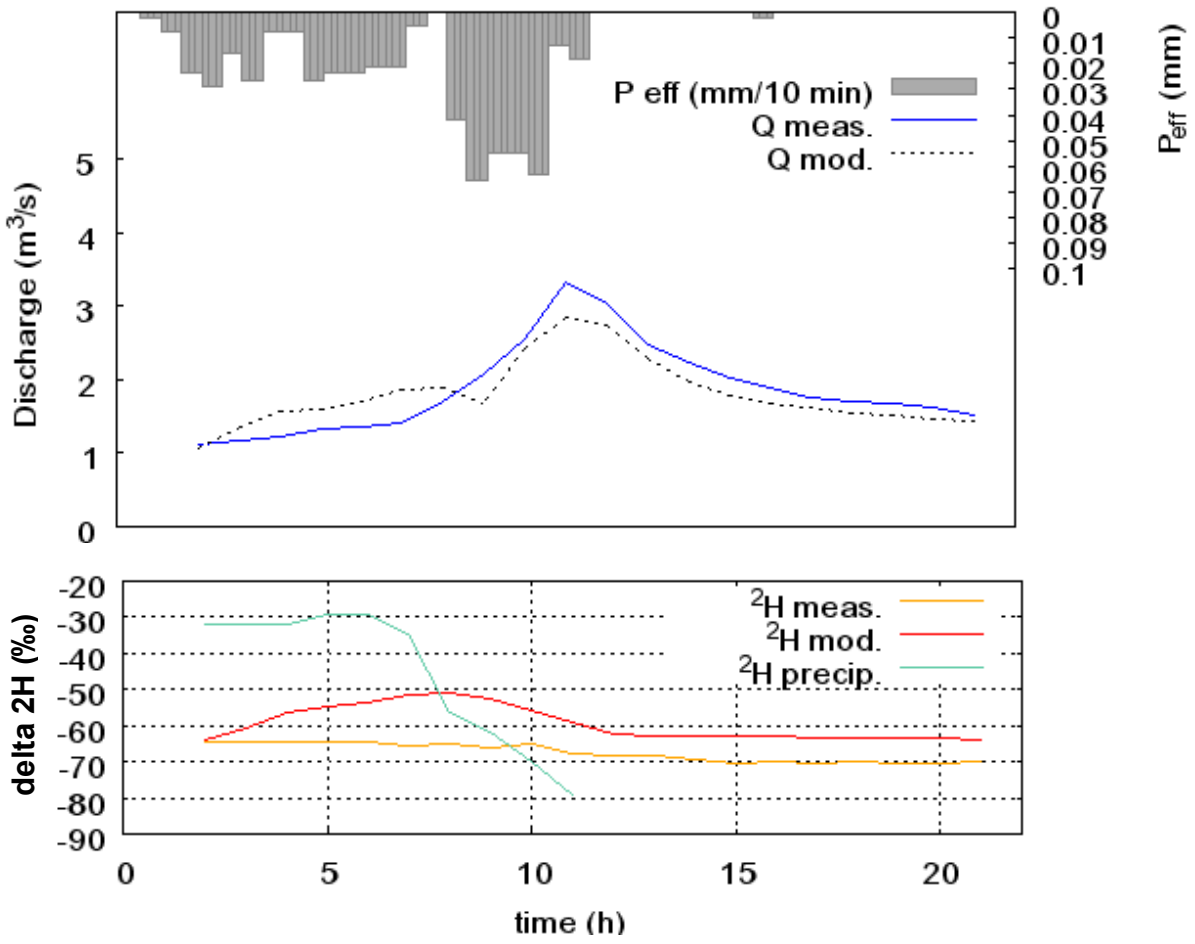

Figure 5.35: Measured runoff, modelled runoff and effective precipitation for CE4 (above). Measured and modelled deuterium (below).

As pre-event water is not considered in the concept of GIUH, the modelled runoff looks plausible but does not represent the data. This problem persists with other parameter sets as well.

5.7 Model Validation

Four events are used four model evaluation (Table 5.6). Validation events one, two and three (VE1, VE2, VE3) are taken from DIDSZUN (2004). Precipitation at the climate station St. Wilhelm is used. For VE1 no runoff data for the Talbach are available. Validation event four (VE4) is taken from SIEBER (2003, p. 64, called Ereignis 5). Precipitation is regionalized as described for CE1 (chapter 5.4.1).

The first event VE1 (DIDSZUN 2004, p.56) happened in September 2001. Pre-event discharge was high and precipitation led to a peak discharge six times the annual mean runoff. VE2 (DIDSZUN 2004, p.115, called DS-1) has a high pre-event soil moisture. Most of the precipitation occurred within three hours. VE3 (DIDSZUN 2004, p.115, called DS-2) was a thunderstorm preceded by a long drought. VE4 is an extreme event with a peak runoff of 22.5 m³/h, where snow melting contributed a lot of runoff as can be seen by the very high

runoff coefficient of 80%. This kind of event is not suited for the GIUH-approach but was taken in to test model behaviour for extreme conditions.

Table 5.6: Events used for validation.

Name	Date	Precip. Duration (h)	Precipitation Volume (m^3)	Storm Runoff Vol. Brugga (m^3)	Runoff Coeff. (%)	Peak Discharge Brugga (m^3/s)	Baseflow Brugga (m^3/s)
VE1	14/09/01	27	1,853,633	238,415	12.8	8.94	2.61
VE2	23/05/02	16	686,957	41,083	6.0	2.47	0.76
VE3	01/07/03	15	552,636	16,927	3.0	2.33	0.69
VE4	19/02/99	72	6,884,923	4,913,380	80.6	22.5	0.82

Figure 5.36 shows the measured and modelled discharge of VE1 for effective precipitation with exponential losses (Figure 5.37 to Figure 5.42 also display model runs with exponential patterns of effective precipitation).

The shape of the modelled hydrograph is reproduced by all parameter sets. Both runoff peaks are underestimated and the modelled hydrographs rise too fast. The falling limb is modelled well. The parameter sets with highest celerities, P1 and P2, react the fastest.

The same applies to VE2 and VE3 (Figure 5.37 to Figure 5.40). The model reacts faster than the real catchments and peak discharge is generally underestimated, but P1 overestimates peak discharge for VE2 in the Talbach catchment.

Validation event four (Figure 5.41 and Figure 5.42) is modelled very badly. Peak discharge is overestimated by two times for the Brugga and by three times for the Talbach. The first modelled peak appears 23 hours before the measured one. The measured hydrograph is much smoother than the modelled ones.

This can be explained by snow-melt. Precipitation is temporally stored in the snow cover and warms the snow, especially by releasing latent heat while freezing. This tends to equalize temperatures along a vertical profile at 0°C. The snow cover can hold up to 8 vol-% of water against gravity. Melting water occurs when the snow cover is saturated (*ripe*) and further energy is conveyed (WARD AND ROBINSON 2000, p. 58).
Thus, the buffering in the snow cover explains the big time lag and smoothed measured hydrograph.

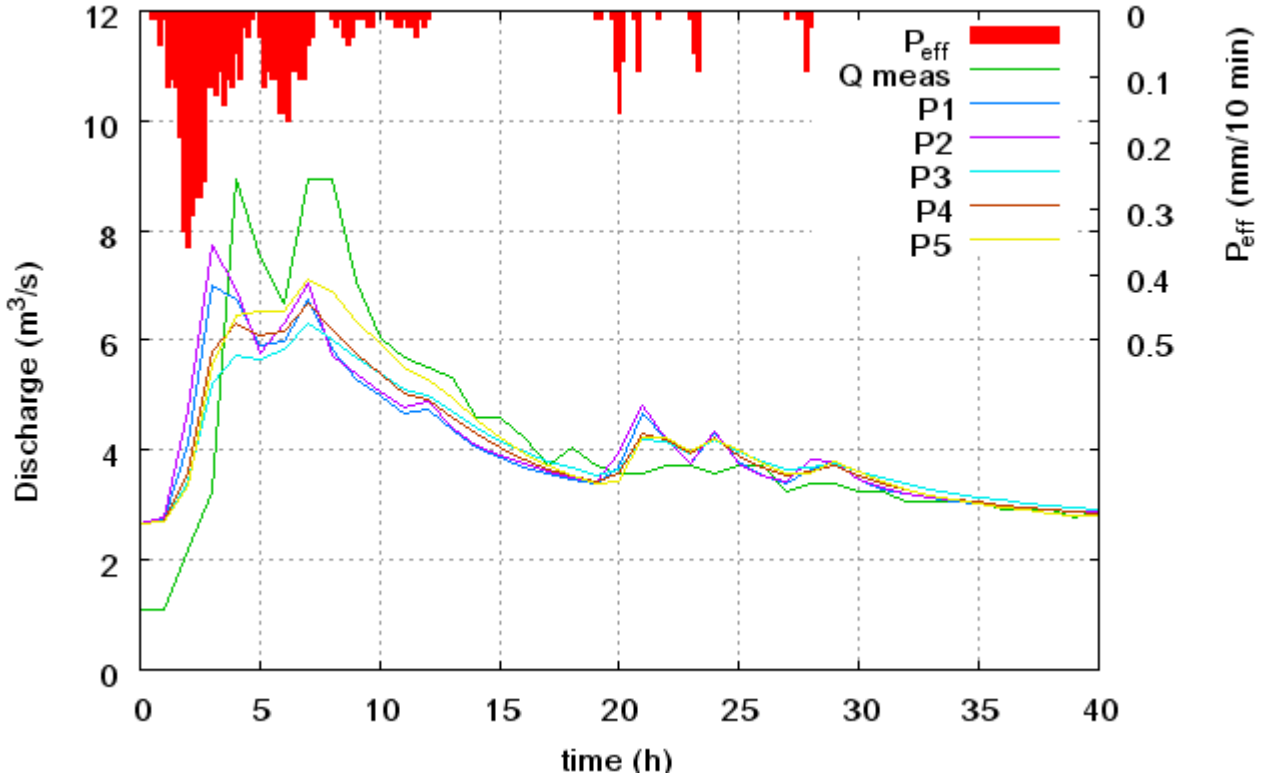

Figure 5.36: Effective precipitation, modelled and measured runoff of St. Wilhelmer Talbach for VE1.

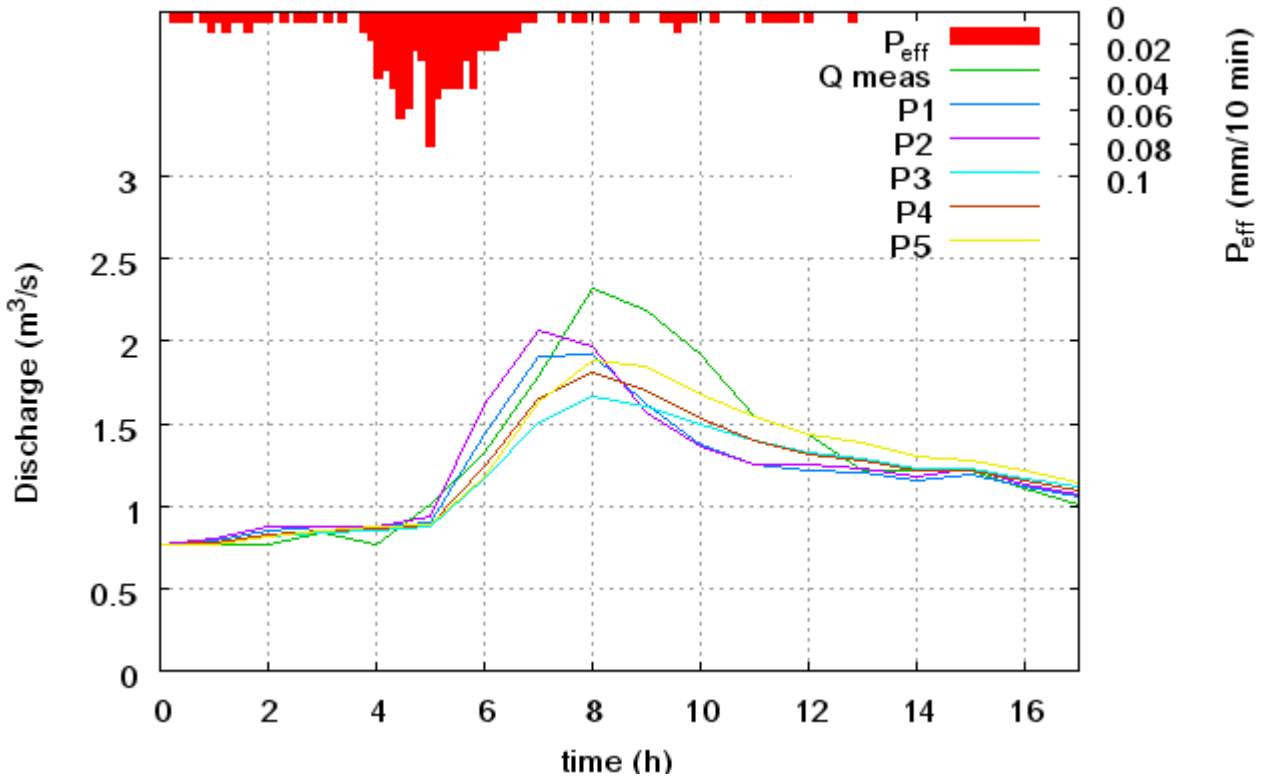

Figure 5.37: Effective precipitation, modelled and measured runoff of Brugga for VE2.

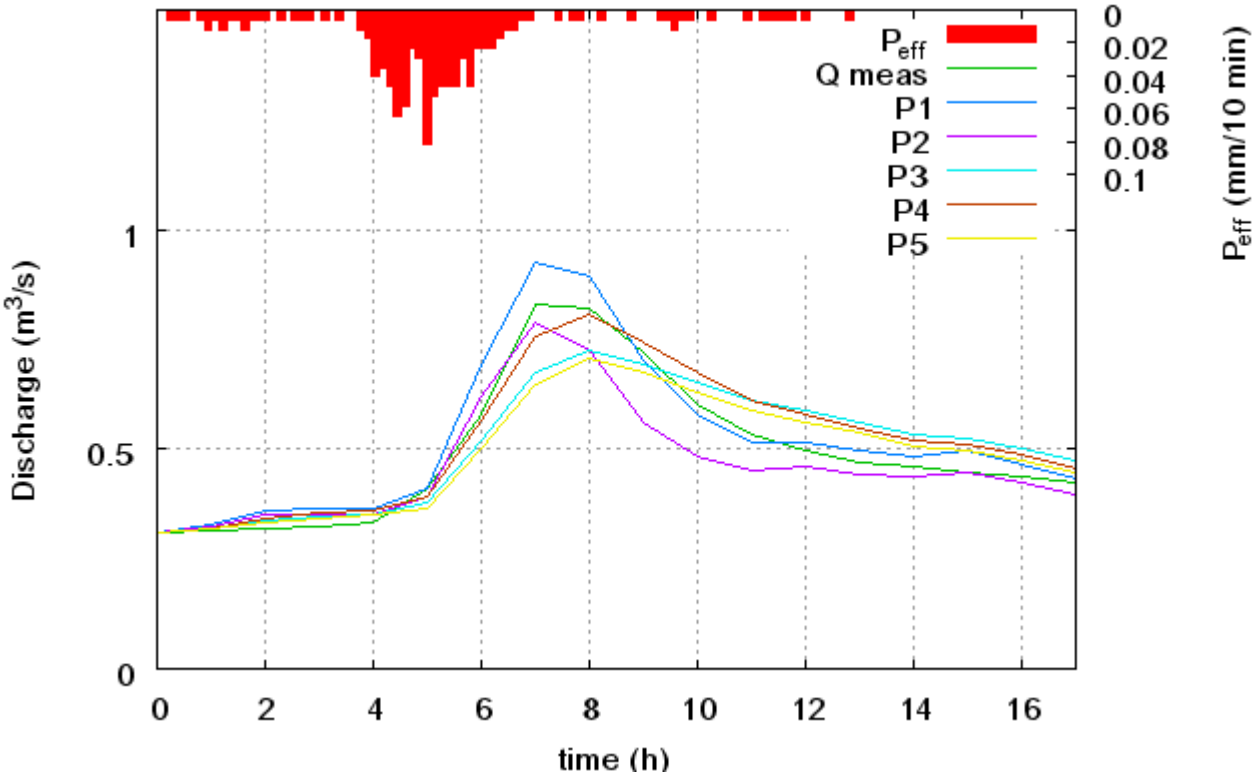

Figure 5.38:Effective precipitation, modelled and measured runoff of St. Wilhelmer Talbach for VE2.

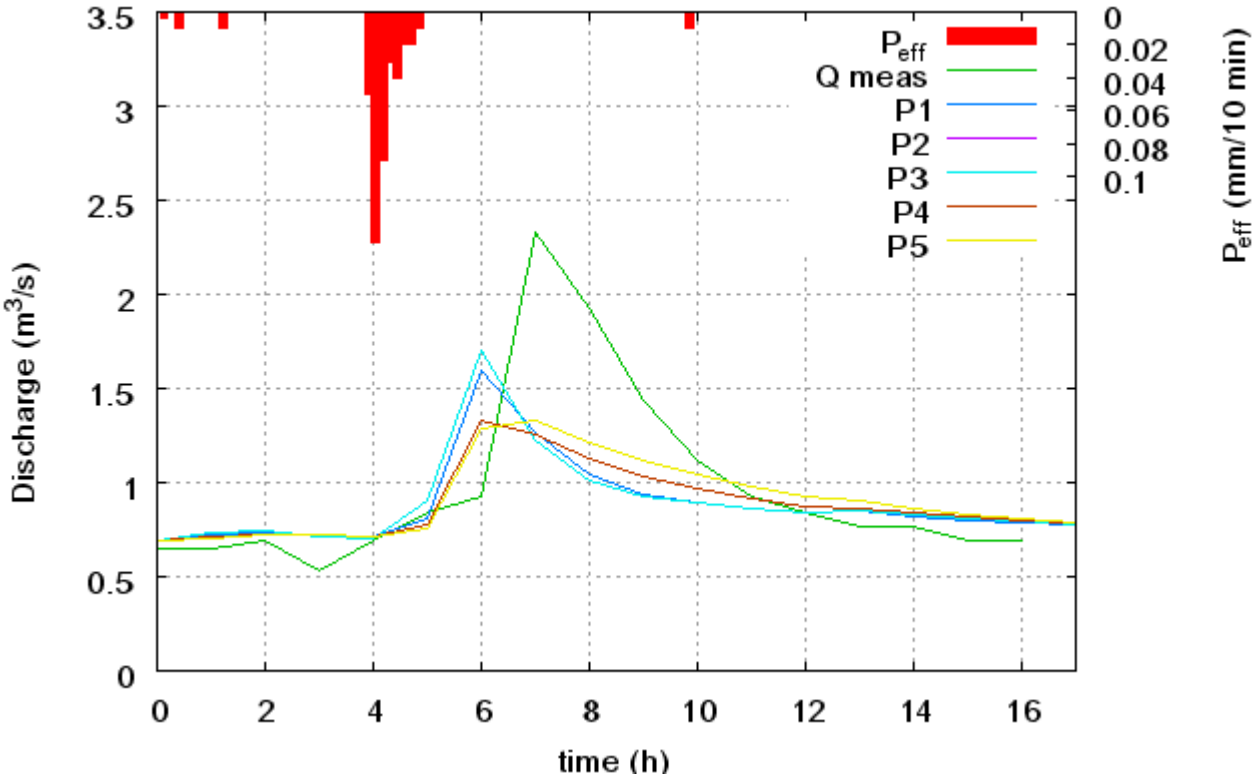

Figure 5.39: Effective precipitation, modelled and measured runoff of Brugga for VE3.

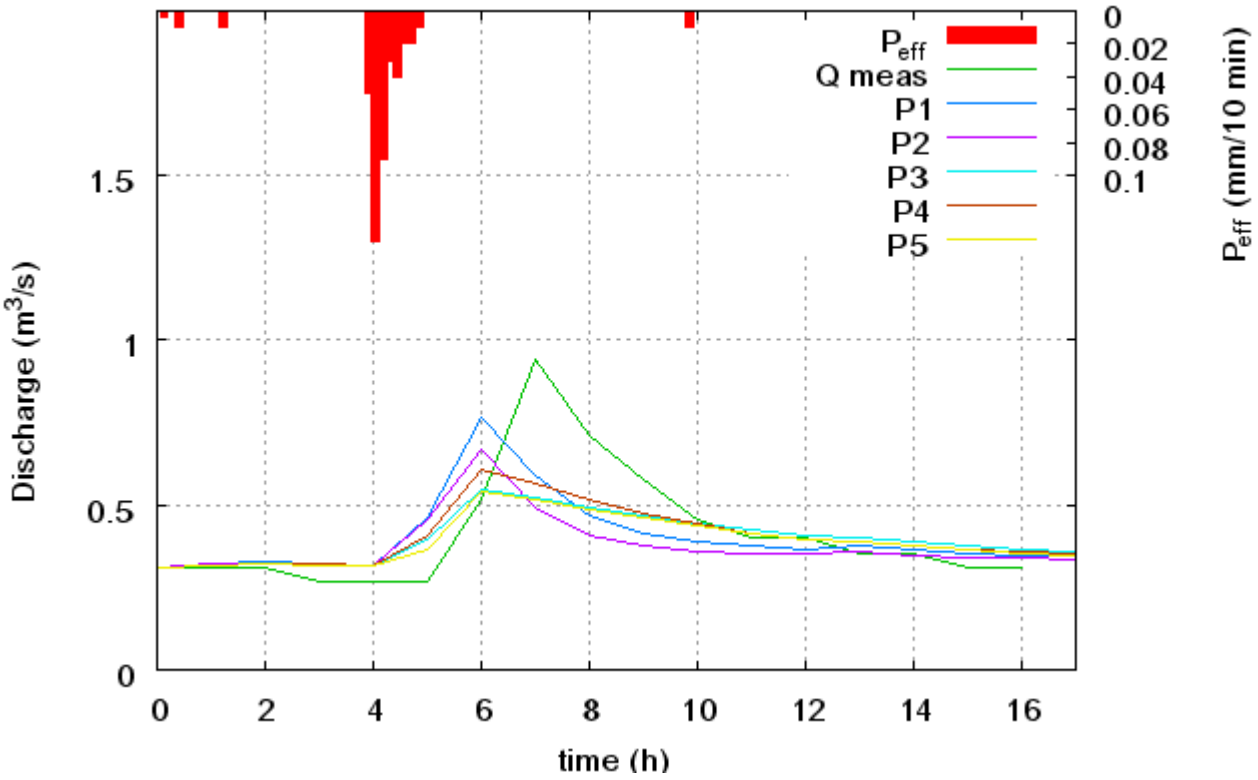

Figure 5.40 Effective precipitation, modelled and measured runoff of St. Wilhelmer Talbach for VE3.

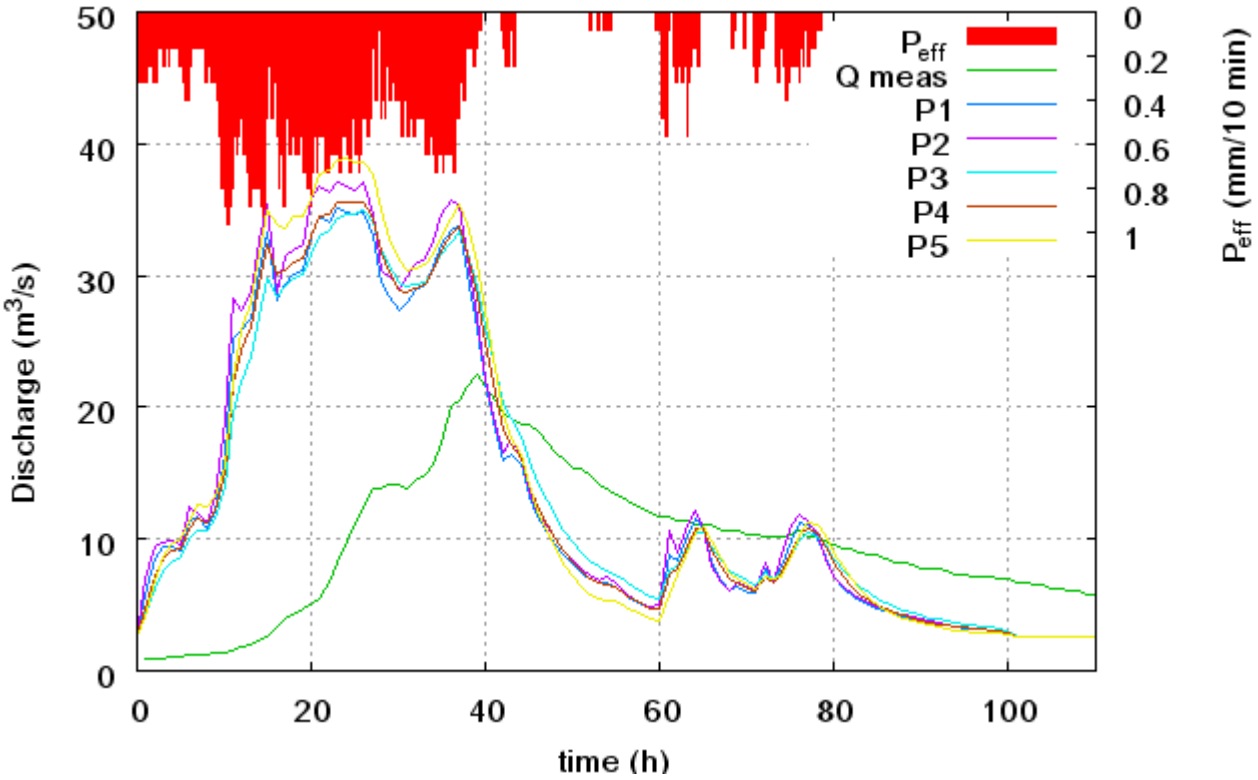

Figure 5.41: Effective precipitation, modelled and measured runoff of Brugga for VE4.

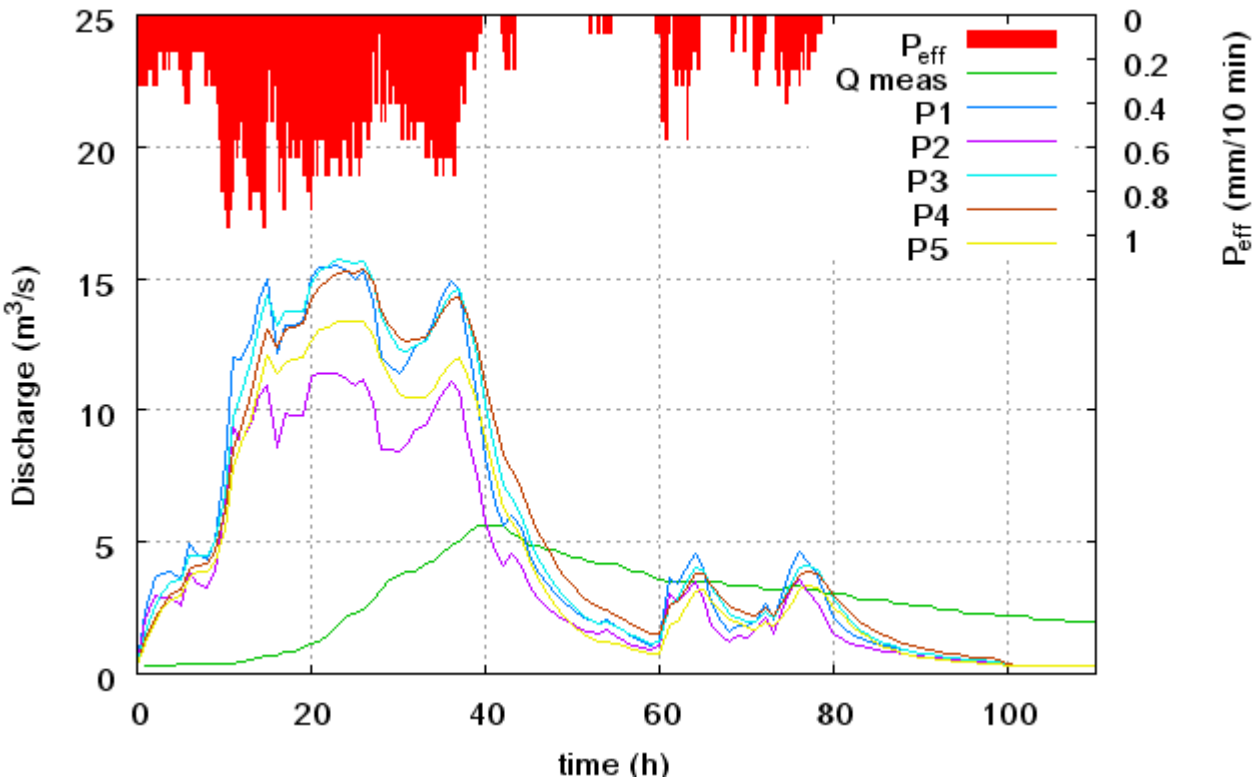

Figure 5.42: Effective precipitation, modelled and measured runoff of St. Wilhelmer Talbach for VE4.

The results of all validation runs are given in Table 5.7. VE1 and VE2 yield the highest efficiencies. The parameter sets with lower wave celerities (P3, P4 and P5) outperform those with higher celerities (P1 and P2) for the Brugga and the St. Wilhelmer Talbach.

Better results are achieved with patterns of effective precipitation calculated with an exponential decrease of losses than with a constant runoff value.

Table 5.7: Performance of validation events for validation parameter sets.

Catchment	Parameter Set	Eff. prec. Pattern	Runoff model efficiency R_{eff} (-)/ R^2 (-)			
			VE1	VE2	VE3	VE4
Brugga	P1	const	0.64 /0.65	0.44 / 0.48	0.21 / 0.25	-1.8 / 0.29
		exp	0.68 / 0.63	0.49 / 0.52	0.29 / 0.32	-2.2 / 0.21
	P2	const	0.56 /0.57	0.34 /0.39	0.20 /0.22	-2.4 / 0.28
		exp	0.59 / 0.60	0.49 / 0.52	0.20 / 0.22	-2.7 / 0.20
	P3	const	0.77 / 0.84	0.67 / 0.77	0.37 / 0.59	-1.6 / 0.37
		exp	0.70 / 0.85	0.68 / 0.79	0.37 / 0.59	-2.2 / 0.24
	P4	const	0.77 /0.80	0.66 / 0.71	0.42 / 0.58	-1.9 / 0.31
		exp	0.73 / 0.85	0.69 / 0.75	0.58 / 0.43	-2.2 / 0.24
	P5	const	0.71 / 0.80	0.78 /0.79	0.51 / 0.57	-5.1 / 0.07
		exp	0.81 / 0.86	0.80 / 0.82	0.51 / 0.67	-2.9 / 0.23
St. Wilhelmer Talbach	P1	const	-	0.39 / 0.57	0.38 / 0.39	-8.9 / 0.01
		exp	-	0.50 /0.63	0.39 / 0.39	-5.7 / 0.02
	P2	const	-	0.40 /0.48	0.22 / 0.26	-5.7 / 0.02
		exp	-	0.47 / 0.53	0.22 / 0.26	-5.6 / 0.02
	P3	const	-	0.84 / 0.84	0.49 / 0.67	-10 /0.12
		exp	-	0.85 / 0.85	0.50 / 0.67	-11 / 0.07
	P4	const	-	0.79 / 0.82	0.56 / 0.68	-9.4 / 0.17
		exp	-	0.83 / 0.85	0.57 / 0.68	-6.8 / 0.11
	P5	const	-	0.85 / 0.86	0.50 / 0.72	-11.9/0.0
		exp	-	0.83 / 0.84	0.50/0.71	-7.7/0.45

5.8 Conclusions

The model GUHmod developed in this study is applied to two nested catchments, the Brugga catchment and its subcatchment St. Wilhelmer Talbach. Four events were used for calibration. Discharge and silica concentrations of the Brugga and discharge of the St. Wilhelmer Talbach are modelled. Fast and slow hillslope responses are modelled separately, based on the delineation of runoff-generating areas used in the TAC^D model. These hillslope responses are then routed through the channel network.

The three wave celerities for fast hillslope response (vhf), slow hillslope response (vhs) and the channel network (vc) are used as calibration parameters.

Two patterns of effective precipitation have been used for each event, one calculating effective precipitation with a constant runoff coefficient and one using an exponential decrease of losses.

In total, 72,000 Monte Carlo simulations have been made to determine validation parameter sets. Model efficiencies R_{eff} up to 0.9 for runoff and up to 0.8 for silica modelling have been achieved. For both catchments and both patterns of effective precipitation individual parameter sets have been identified, which yield successful runoff simulations and are used for model validation. The parameter sets for the Brugga, P1 using the constant runoff coefficient, and P2 using the exponential decrease of losses, have significantly higher values for vhf than the respective parameter sets for the Talbach, P3 and P4. The values for vhs and vc are close to each other for both catchments.

Another parameter set, P5, has been determined for the Brugga catchment considering goodness of fit of modelled runoff and modelled silica concentrations. Its wave celerities are close to those of parameter sets P3 and P4. Incorporating solute modelling as a means of multi-criteria calibration thus has a big influence on the determination of parameter values.

Both pattern of effective precipitations yield similar results, but celerities are slightly higher for the parameter sets P2 and P4, because most of effective precipitation occurs later if calculated with an exponential decrease of losses than with a constant runoff coefficient.

Equifinality complicates the identification of validation parameter sets. The subjective method of visual determination of parameter sets leads to arbitrary results, especially for channel wave celerity vc, which is poorly defined.

It is found that events where precipitation data from several gauging stations are regionalized to the catchment (CE1 and CE2) are modelled better than if only one climate station is considered. Also, the convective hail-storm event CE3 was modelled worse than the advective winter event CE4 (in both cases, precipitation from only one climate station is used). This stresses the problems which arise from the assumption of spatially uniform precipitation.

Isotope modelling is tested with deuterium data for CE4. However, measured δ-values of streamflow show hardly any reaction to input of heavy isotopes from precipitation. This is attributed to the large fraction of lighter pre-event water in storm runoff. As this is not considered in the GIUH approach, isotope modelling does not seem promising.

Four events are used for validation. R_{eff} values up to 0.85 are obtained. In both catchments, the “slower” parameter sets P3, P4 and P5 outperform the faster sets P1 and P2.

This is surprising, because P1 and P2 have been calibrated to the Brugga, whereas P3 and P4 have been calibrated to the Talbach. It leads to the conclusion that inter-event variability is higher than the variability of the two catchments. Apparently, the difference

in catchment size (40.0 km² for the Brugga versus 15.4 km² for the St. Wilhelmer Talbach) is too small to cause a scale-dependant difference in dominating runoff-generation processes. This is in line with the classification of BLÖSCHL (1996), in which both catchments belong to the lower meso-scale. Parameter sets may be much more catchment-specific if two separate catchments are considered, not nested ones like in this study.

The model fails to reproduce the snow-melt event (VE4). Runoff dynamics cannot be reproduced adequately, and peak discharge is seriously overestimated. A snow-melt routine is definitely needed to model this type of event.

6 Discussion

6.1 Evaluation of wave celerities

The best modelling results are achieved with values between one and 12 m/10 min for the celerity of slow hill response vhs and between five and 70 m/10 min for the fast hillslope response, although some higher values for the latter are also quite good. Flow velocity is approx. 3/5 of wave celerity (Eq. 3.17), which translates into a velocity between 3.6 and 43.2 m/h for the slow and between 18 and 252 m/h for the fast component. Channel wave celerities lie between 600 and 3600 m/10 min, without clear preference of a value of subset. Channel flow velocities therefore varied between 0.6 m/s and 3.6 m/s, and the validation parameter sets contain velocities ranging from 1.5 m/s to 2.4 m/s.

ARMBRUSTER (1997, p.37) gives mean hillslope velocities between 5 and 8.8 m/h and channel velocities between 0.2 and 0.4 m/s derived from tracer experiments. He assumed a celerity of 800 m/h to model runoff from saturated areas. FRITZ (2001, p.42) also measured channel flow velocities below 1 m/s for the Brugga catchment using salt-dilution-experiments. These were carried out during low-flow conditions. MESA AND MIFFLIN (1986) give velocities for Horton flow (10 to 500 m/h), subsurface flow (<0.0001 m/h) and saturation overland flow (0.3 to 100 m/h).

Channel velocities assumed in this study seem to be plausible for stormflow runoff, at least lying in the correct order of magnitude. Hillslope velocities are high, but within the range given for fast runoff components like Horton and saturation overland flow.

These high velocities are necessary to represent fast-responding runoff generation mechanisms based on pressure transmission like piston flow and ground-water ridging. Also the GIUH approach considers all areas to generate the same amount of runoff. In reality shorter flow paths will prevail, with most of the runoff generated near the stream. To compensate this error in conceptualization, higher flow velocities are needed.

The incorporation of solute modelling leads to a decrease in hill flow celerities for the Brugga catchment. Thus multi-criteria calibration yields parameter values closer to measured velocities than a calibration based on runoff alone.

6.2 Evaluation of goodness of fit

Runoff modelling with the validation parameter sets yields model efficiencies R_{eff} up to 0.95 for the calibration events and up to 0.85 for the validation events. For all calibration events parameter sets could be found which yield model efficiencies of 0.8 or higher. This

is a very good result and shows that it is possible to use the approach followed in this study.

But the limitations of this simple model are also clearly shown. A convective thunderstorm (Calibration Event 3) and a rain-on-snow event (Validation Event 4) could not be modelled adequately with any validation parameter set, model outputs always performed worse than the use of arithmetic mean runoff ($R_{eff} < 0$). If VE4 is disregarded, with the best parameter set P5 strong correlations (according to Table 3.1) for VE1 ($R^2=0.86$), VE2 ($R^2=0.82$) and VE3 ($R^2=0.67$) are obtained.

For silica modelling, model efficiencies up to 0.8 are achieved. This proves the possibility to model silica with the assumption of constant concentrations in each runoff component. Silica modelling is more demanding than runoff prediction regarding the co-domain of successful flow velocities. Thus it helps to determine a parameter set for one event, but finding a common set for many events is difficult.

ARMBRUSTER (1997, p. 61) modelled one event in the St. Wilhelmer Talbach catchment using the GIUH approach and flow velocities derived from tracer experiments. A good fit to the recession limb of the hydrograph was achieved, but peak flow is seriously underestimated. This is attributed to the missing conceptualisation of pressure wave mechanisms. Quantitative measures of goodness of fit are not given.

The wave celerities found in this study are higher than those used by ARMBRUSTER (1997) and enable a better fit of peak runoff, although it still is underestimated for most events. Parameter sets with which measured peak runoff is matched exist, but generally have worse overall goodness of fit. If a correct prediction of peak runoff is desired, the model should be calibrated using not R_{eff} but a comparison of measured and modelled peak runoff.

A comparison to other event-based models is difficult, as the catchment and event characteristics have a big influence on model performance and no event-based models have been applied to the Brugga. Exemplarily the results from another study are given:

JAIN AND INDURTHY (2003) compared event-based unit hydrograph models to regression models and artificial neural networks. The study site was the micro-scale (6.3 ha) Salado Creek catchment in Texas. 20 hours of runoff data were used for calibration and one single-peak event of three hours for validation. Runoff data were given in time steps of five minutes. The best lumped Unit Hydrograph model obtained a R^2 of 0.46 during validation, the best nonlinear multiple regression model got a R^2 of 0.90 and the best ANN achieved an R^2 of 0.93.

The comparison to other model applications in the Brugga catchment is far more interesting. SIEBER (2003) modelled the events CE1, CE2 and VE4 with the TAC^D model.

TAC^{D} is not event-based but continuous. Therefore stores were initialized using an initialization phase of at least 12 months for each event. If necessary, water content of stores was corrected manually (SIEBER 2003, p. 65). For all three events model efficiencies between 0.95 and 0.98 could be obtained, regarding runoff at Brugga. The best overall parameter set, regarding runoff of the St. Wilhelmer Talbach and runoff and silica concentrations of the Brugga, yielded values of R_{eff} of 0.83 for CE1, 0.52 for CE2 and 0.91 for VE4 (SIEBER 2003, p.115). Figure 6.1 shows the best simulated runoff for the three events, using the optimal parameter set for each event,

The best silica simulations reached coefficients of determination R^2 of 0.17 for CE1, 0.58 for CE2 and 0.73 for VE4 (SIEBER 2003, p. 76). These values, which are poor compared to goodness of fit for runoff, are attributed to a problem to correctly represent the contribution of each runoff component to total discharge (SIEBER 2003, p.117) and to the conceptual error made in assigning a constant silica concentration to each component (SIEBER 2003, p. 60). Furthermore, it was not the scope of the study to optimise silica modelling.

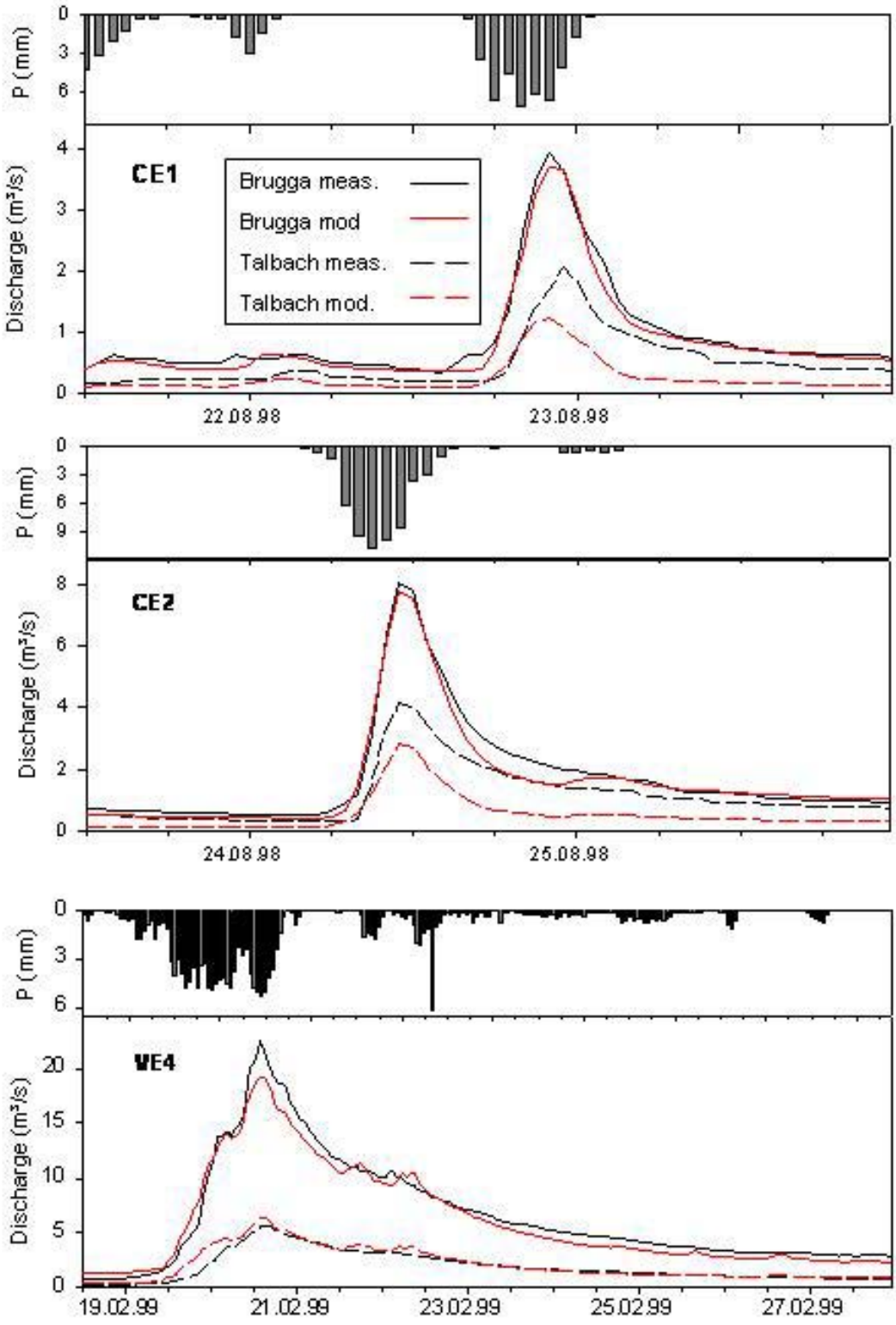

Figure 6.1: Simulated runoff for Brugga and St. Wilhelmer Talbach with TACD for events CE1, CE2 and VE4 (*SIEBER *2003, edited).

WISSMEIER (2005, p. 111) implemented distributed solute transport into TACD and found that, if data requirements are met, ^{18}O can be predicted within the analytical error.

A comparison of TAC^D to GUHmod leads to the conclusion that the more complex model structure of the former is much more suited to model complex rain-on-snow events like VE4 and for the simulation of natural isotopes. Surprisingly, the simpler conceptualization of GUHmod yielded better results for silica modelling (the best R_{eff} was 0.7 for CE1 and 0.8 for CE2).

It can be said that TAC^D proves more versatile and stable than GUHmod, but for some events, similarly good results can be achieved with both models.

6.3 Model structure and data preprocessing

Two methods to determine effective precipitation are used in this study. In both cases total volume of effective precipitation is given by the volume of storm runoff. The first method uses a constant runoff coefficient, thus keeping the pattern of measured precipitation but reducing the amount by a fixed percentage. The second method assumes an exponential decrease of losses, leading to an increase of runoff coefficient over time. Thereby much of precipitation is delayed compared to the first method.
The results for both methods are similar, but for the validation events the exponential approach works slightly better. It is also closer more realistic and can be recommended for further studies.

The assumption of constant baseflow works for the shorter events and the tailings of modelled hydrographs are reproduced quite well. For long events like CE3 this does not seem to work promisingly, especially if discharge does not recede to its initial value.

The use of two components for hillslope response is adequately. Adding further components does not seem promising, as parameterization will become more complex. If experimental proof for three or more fast-reacting runoff components should exist, it would however seem useful to model these separately.

The implementation of pre-event water seems difficult. Of course another parameter can be used to assign each component a certain percentage of *old* water.

6.4 Proposals for further research

Much time was needed to develop the modelling system. Therefore the model application was not very extensive and some things remain undone. The main problem is the identification of a common parameter set for all events. It will probably be more promising to develop a classification scheme for events accounting for factors like the meteorological type of event (advective / convective) and antecedent soil moisture. Then a parameter set for each class can be searched.

Effective precipitation may be determined assuming an initial loss. If exponential decrease of losses proves better than constant runoff, initial losses may be even more.

If several rainfall gauging stations exist, subcatchments can be modelled with a different precipitation for each one. This can help to minimize the error made by the assumption of spatially uniform precipitation and is not hard to implement.

Isotope modelling can be improved by introducing a parameter or function which gives the fraction of pre-event water for each component. This parameter may be determined by calibration to measured isotope signatures or determined by field experiments. But there are probably very few catchments for which these data are available.

Finally an application in arid zones will be interesting. Limited data availability often prevents the use of more sophisticate models. Influence of snow melt does not pose a problem in most arid regions. If flash-floods in non-perennial streams are to be modelled, an inclusion of transmission losses is advisable.

6.5 Final Conclusions

The model developed in this study has successfully been applied to the Brugga catchment and its subcatchment St. Wilhelmer Talbach. Nash-Sutcliff efficiencies up to 0.9 for runoff and 0.8 for silica concentration modelling can be achieved. With the parameter set P5 derived by multi-criteria validation, strong correlations between modelled and measured discharge for the three validation events without snow-melt are obtained. This parameter set outperforms the sets P1 and P2 determined by runoff of Brugga alone. Its wave celerities for hillslope response are closer to measured values than those of P1 and P2.

Despite the parsimony of the model, with only three calibration parameters, equifinality prevents the identification of an unambiguous parameter set for validation. Further research is needed to achieve reliable prediction of discharge for all events.

The transfer of the parameter sets P3 and P4, which are calibrated to runoff of the St. Wilhelmer Talbach, to the Brugga yields better results than the use of parameter sets P1 and P2. This shows the similarity in hydrological response of the two basins and the high inter-event variability.

A good estimation of areal rainfall is needed to obtain good predictions of discharge. For the events where data from several rainfall gauging stations are regionalized to the catchment higher model efficiencies are achieved than for those with data from only one station.

The model fails to predict runoff for the snow-melt event. Snow storage is difficult to implement into an event-based model. Therefore this model seems unsuited to model winter events with snow melt.

Isotope modelling is tested for one event. Results do not seem promising, because of the unconsidered influence of pre-event water on streamflow concentrations of natural isotopes. A parameter might easily be included to give the fraction of old water for each runoff component.

Compared to the more complex catchment model TAC^{D}, GUHmod lacks versatility and robustness of predictions. If limited data availability prevents the application of a complex continuous model, GUHmod may be used to answer event-related questions like the calculation of the probable maximum flood using synthetic precipitation data.

References

ANDERSON, M. G. AND BATES, P. D. (eds) (2001): Model validation: perspectives in hydrological science. Chichester ; Weinheim : Wiley, 2001. - XI, 500 S.

ARMBRUSTER, F. (1997): Integration künstlicher Markierversuche in die geomorphologische Impulsantwort. Diploma thesis at the Albert-Ludwigs-University Freiburg,Department of Hydrology, (unpublished).

BAND, L. E. (1993): Extraction of Channel Networks and Topographic Parameters from Digital Elevation Data, in Channel Network Hydrology, Edited by K. Beven and M. J. Kirkby, Wiley, pp. 13-42.

BARNES, C. J. AND BONELL, M. (1996): Application of unit hydrograph techniques to solute transport in catchments, Hydrological Processes, 10, pp. 793-802.

BECK, M.B. (1991): Forecasting environmental change. Journal of Forecasting, 10, pp. 3-19.

BERGSTRÖM, S. (1992): The HBV model – its structure and applications. SMHI, RH, 4. Norrköping, Sweden.

BEVEN, K. (2001a): Rainfall-Runoff Modelling. Wiley & Sons, Chichester.

BEVEN, K. (2001b): How far can we go in distributed modelling? Hydrology and Earth System Science 5, pp. 1-12.

BLÖSCHL, G. (1996): Scale and Scaling in hydrolgical modelling: a review. Hydrological Processes 9, pp. 251-290.

BOOLTINK, H.W.G. (2001): Soil water relations. In: ANDERSON, M.G. & BATES, P.D. (Hrsg.): Model Validation: Perspectives in Hydrological Science. John Wiley & Sons, Chichester, England, pp. 195-232.

CLARK, C.O. (1945): Storage and unit hydrograph. Transactions of the American Society of Civil Engineers 110: pp. 1416–1446; after BEVEN 2001a.

DAWSON, C.W. AND WILBY, R.L. (2001): Hydrological modelling using artificial neural networks. Progress in Physical Geography 25,1, pp. 80-108.

DIDSZUN, J. (2004): Experimentelle Untersuchungen zur Skalenabhängigkeit der Abflussbildung, Ph. D. thesis at the Albert-Ludwigs-University Freiburg,Department of Hydrology, Freiburg i. Br..

DINGMAN, S.L. (1984): Fluvial Hydrology. W.H. Freeman and Company, New York.

DOOGE, J.C.I. (1959): A general theory of the unit hydrograph. Journal of Geophysical Research, 64, pp. 241–256.

DYCK, S. AND PESCHKE, G. (1989): Grundlagen der Hydrologie. Verlag für Bauwesen, Berlin (in German).

FORREST, S. (1996): Genetic Algorithms. ACM Computing Surveys, 28 (1), pp. 77–80.

FRITZ, A. (2001): Experimentelle Untersuchung der Abflusskonzentration in Bächen des Bruggaeinzugsgebiets. Diploma thesis at the Albert-Ludwigs-University Freiburg, Department of Hydrology, (unpublished), Freiburg i. Br..

GANDOY-BERNASCONI, W. AND PALCIOS-VELEZ, O. (1990): Automatic cascade numbering of unit elements in distributed hydrological models, Journal of Hydrology, 112, pp. 375-393.

GLA (1981): Erläuterungen zur geologischen Karte von Freiburg im Breisgau und Umgebung 1 : 50000. Landesvermessungsamt Baden-Württemberg, Stuttgart.

GOSLING, J. AND MCGIBBON, H. (1996): The Java Language Environment, A White Paper. Available at http://java.sun.com/docs/white/langenv/ (last visited 12/2004).

GUPTA, V.K. WAYMIRE, E. AND WANG, C.T. (1980): A representation of an instantaneous unit hydrograph from geomorphology, Water Resource Research, 16, pp. 855-862.

GUPTA, V.K. AND WAYMIRE, E. (1983): On the Formulation of an Analytical Approach to Hydrologic Response and Similarity at the Basin Scale, Journal of Hydrology, 65 (1/3), pp. 95-123.

HÄDRICH, F. & STAHR, K. (1992): Die Böden in der Umgebung von Freiburg i. Br.. In: MÄCKEL, R. AND METZ, B.: Schwarzwald und Oberrheintiefland. Freiburger geographische Hefte, Heft 36. Institut für Physische Geographie der Universität Freiburg i. Br..

HAINES, T.S. AND LLOYD, J.W. (1985): Controls on silicia in groundwater environments in the United Kingdom. Journal of Hydrology, 81, pp. 277-295.

JAKEMAN A., LITTLEWOOD, I.G. AND WHITEHEAD, P.G. (1990): Computation of the instantaneous unit hydrograph and identifiable component flows with application to two small upland catchments. Journal of Hydrology, 117, pp. 275-300.

JAIN, A. AND INDURTHY, S.K. (2003): Comparative Analysis of Event-based Rainfall-runoff Modelling Techniques—Deterministic, Statistical, and Artificial Neural Networks. Journal of Hydrologic Engineering ASCE 82, pp. 93-98.

KÄSS, W. (1992): Geohydrologische Markierungstechnik. Lehrbuch d. Hydrogeologie Band 9. Editor Mathess, G. Gebrüder Bornträger, Berlin.

KIRKBY, M.J. (1993): Network Hydrology and Geomorphology, in Channel Network Hydrology, Edited by K. BEVEN AND M. J. KIRKBY, Wiley, pp.1-11.

MELCHING, C.S. (1995): Reliability Estimation. in: V.P. SINGH (1995): Computer Models of Watershed Hydrology. Water Resources Publications, Colorado, USA, pp. 69-118.

MEHLHORN J. (1998): Tracerhydrologische Ansätze in der Niederschlags-Abfluss-Modellierung. Ph. D. thesis, Universität Freiburg, Freiburg i. Br..

MESA, O. J. AND MIFFLIN, E. R (1986): On the relative role of hillslope and network geometry in hydrologic response. In GUPTA, V. K., RODRIGUEZ-ITURBE I. AND WOOD, E. F. (eds). Scale Problems in Hydrology, pp. 1-18.

MOSER, H. & RAUERT, W. (1992): Lehrbuch der Hydrogeologie - Isotopenmethoden in der Hydrologie. 2. Auflage, Gebr. Bornträger, Berlin, Stuttgart.

NASH, J.E. (1958): The form of the instantaneous unit hydrograph. Intl. Assoc. Sci. Hydrology, Pub 42, Cont. Rend. 3, pp. 114-118.

NASH, J.E. (1959): Systematic determination of unit hydrograph parameters. Journal of Geophysical Research, 64, pp. 111-115.

NASH, J.E. AND SHAMSELDIN, A. Y. (1998): The Geomorphological unit hydrograph- a critique. Hydrology and Earth System Science, 2, pp. 1-8.

NASH. J.E. AND SUTCLIFFE, J.V. (1970): River flow forecasting through conceptual models 1. A discussion of principles. Journal of Hydrology, 10, pp. 282-290.

NELDER, J.A. AND MEAD, R. (1965): A simplex method for function minimization. Computer Journal, 7, pp. 308-313.

O'CALLAGHAN, J. F. AND D. M. MARK (1984): The Extraction of Drainage Networks From Digital Elevation Data, Computer Vision, Graphics and Image Processing, 28, pp. 328-344.

O'CONNEL, P. E. (1991): A Historical Perspective. In BOWLES, D. S. AND O'CONNEL, P.E. (Eds) Recent advances in the Modelling of Hydrologic Systems, Kluver, Dordrecht. pp. 3-30.

O'LOUGHLIN, E. (1986): Prediction of surface saturation zones in natural catchments by topographic analysis. Water Resources Research, 22, pp. 794-804.

ORESKES, N. AND BELITZ, K. (2001): Philosophical Issues in Model Assessment. In ANDERSON AND BATES (2001).

OTT, B. (2002): Weiterentwicklung des Einzugsgebietsmodells TAC^D und Anwendung im Dreisameinzugsgebiet. Diploma thesis at the Albert-Ludwigs-University Freiburg, Department of Hydrology, (unpublished), Freiburg i. Br..

PCRaster Manual (2001): available at: http://pcraster.geog.uu.nl/documentation /pcrman/book1.htm (last visited 03/2005).

QUINN, P. F., BEVEN, K. J., CHEVALIER, P., AND PLANCHON, O. (1991): The prediction of hillslope flow paths for distributed hydrological modelling using digital terrain models. Hydrological Processes, 5, pp.59-79.

REFSGAARD, J. C. AND STORM, B. (1995): MIKE SHE. IN SINGH V.P. (ed.) Computer Models of Watershed Hydrology. Water Resource Publication, Highland Park, CO, pp. 809-846.

RODRIGUEZ-ITURBE, I. AND VALDES, J. B. (1979): The geomorphological structure of hydrological response. Water Resources Research, 31 (4), pp. 1119-1127.

RODRIGUEZ-ITURBE, I. (1993): The geomorphological unit hydrograph. In BEVEN, K. J. AND KIRKBY, M. J. (eds) Channel Network Hydrology. John Wiley, Chichester, pp. 43-68.

ROSER, S. (2001): Flächendetaillierte Weiterentwicklung des prozessorientierten Einzugsgebietsmodells TAC und Visualisierung der Modellergebnisse in einem dynamischen GIS. Diploma thesis at the Albert-Ludwigs-University Freiburg, Department of Hydrology, (unpublished), Freiburg i. Br..

ROSS, C. N. (1921): The calculation of flood discharge by the use of time contour plan isochrones. Transactions of the Institute of Engineers, Australia, 2, pp. 85-92.

ROSSO, R. (1984): Nash model relation to Horton ratios. Water Resources Research, 20, pp. 914-920.

SCANLON, T.M., RAFFENSPERGER, J.P., HORNBERGER, G.M. (2001): Modeling transport of dissolved silica in a forested headwater catchment: Implications for defining the hydrochemical response of observed flow pathways. Water Resources Research, 37 (4), pp. 1071-1082.

SCHLITTGEN, R. (2000): Einführung in die Statistik. 9. Auflage, R. Oldenbourg Verlag, München.

SHAMSELDIN, A. Y. AND NASH, J. E. (1998): The geomorphological unit hydrograph—A critical review. Hydrology and Earth System Sciences, 2, pp. 1-8.

SHERMAN, L. K. (1932): Streamflow from rainfall by the unit-hydrograph method, Eng. News Rec., 108, pp. 501-505.

SEIBERT, J. (2000): Multi-criteria calibration of a conceptual runoff model using a genetic algorithm. Hydrology and Earth System Sciences 4 (2), pp. 215-224.

SEIBERT, J. AND MCDONNELL, J. (2002): On the dialog between experimentalist and modeler in catchment hydrology: Use of soft data for multicriteria model calibration. Water Resources Research, 38 (11), pp. 1-23.

SIEBER, A. (2003): Parameterstudien und Unsicherheitsanalysen mit dem Einzugsgebietsmodell TAC^{D}. Diploma thesis at the Albert-Ludwigs-University Freiburg, Department of Hydrology, (unpublished), Freiburg i. Br..

SINGH, V.P. (1995): Computer Models of Watershed Hydrology. Water Resources Publications, Colorado, USA.

SIVAPALAN, M. (2003): Process complexity at hillslope scale, process simplicity at the watershed scale: is there a connection? Hydrological Processes 17 (5), pp. 1037-1041.

SNELL, J.D. AND SIVAPALAN, M. (1994): On geomorphological dispersion in natural catchments and the geomorphological unit hydrograph, Water Resources Research, 30, pp. 2311-2324.

SOROOSHIAN, S. AND GUPTA, V.K. (1995): Model calibration. In Singh V.P. (ed.) Computer Models of Watershed Hydrology. Water Resource Publications, Highlands Ranch, CO, pp. 23-68.

STOBER, I. (1995): Die Wasserführung des kristallinen Grundgebirges. Ferdinand-Enke-Verlag, Stuttgart.

STRAHLER, A. N. (1957): Quantitative analysis of catchment geomorphology. Trans. Am. Geophys. Union 38, pp. 913-920.

UHLENBROOK, S. (1999): Untersuchung und Modellierung der Abflussbildung in einem mesoskaligen Einzugsgebiet. Freiburger Hydrologische Schriften, Band 10, Institut für Hydrologie der Universität Freiburg, Freiburg i. Br..

UHLENBROOK, S., FREY, M., LEIBUNDGUT, C. AND MALOSZEWSKI, P. (2002): Hydrograph separations in a mesoscale mountainous basin at event and seasonal timescales, Water Recourses Research, 38 (0).

UHLENBROOK, S., ROSER, S., TILCH, N. (2004): Hydrological process representation at the meso-scale: the potential of a distributed, conceptual catchment model. Journal of Hydrology, 291, pp. 278-296.

TETZLAFF, D. AND UHLENBROOK, S. (2005): Effects of spatial variability of precipitation for process-oriented hydrological modelling: results from two nested catchments. Hydrology and Earth System Sciences, in press.

Todini, E. (1988): Rainfall – runoff modelling – past, present, and future. Journal of Hydrology, 100, pp. 341-352.

WALKER, J.P. AND WILGOOSE, G.R. (1999): On the effect of digital elevation model accuracy on hydrology and geomorphology. Water Resources Research, 35 (7), pp. 2259-2268.

WARD, R.C. AND ROBINSON, M. (2000): Principles of hydrology. McGraw-Hill, London.

WEILER, M., MCGLYNN, B.L., MCGUIRE, K.J. AND MCDONNELL, J.J. (2003): How does rainfall become runoff? A combined tracer and runoff transfer function approach. Water Resource Research, 39. (11), 1315.

WENNINGER, J., UHLENBROOK, S., TILCH, N. AND LEIBUNDGUT, CH. (2004): Experimental evidence of fast groundwater responses in a hillslope/floodplain area in the Black Forest Mountains, Germany. Hydrological Processes, 18, pp. 3305-3322.

WISSMEIER, L. (2005): Implementation of distributed solute transport into the catchment model TAC^{D} and event based simulations using oxygen-18, Diploma thesis at the Albert-Ludwigs-University Freiburg, Department of Hydrology, (unpublished), Freiburg i. Br..

XU, M. AND ECKSTEIN, Y. (1995): Use of weighted least-squares method in evaluation of the relationship between dispersivity and scale. Groundwater, 33 (6), pp. 905-908.

YOUNG, P. C. (2002): Advances in real-time flood forecasting. Philosophical Transactions of the Royal Society London A360, pp. 1433-1450.

Appendix

Data Formats for model input

- Flow path distributions
  FPDs are stored in .csv (comma separated value) files. The separator char (delimiter) is the semicolon (";").
  The meta data in the first line gives the class size in meters, the total number of cells in the FPD and the number of classes. The second line is blank, then each line contains the lower class bound and the number of cells in the class.
  Example (113 cells in 5 classes of 50 meters):

```
50;113;5

0;39
50;41
100;20
150;9
200;4
```

- Precipitation
  Effective precipitation is stored in .csv (comma separated value) files. The separator char is the semicolon (";").
  The first line contains the meta data, namely the data, starting time (in hours), the duration of one time step used (in minutes) and the number of data points. The second line is blank, then each line contains one data point.
  Example (data starting on the 12th of April 01, at three o'clock p.m., containing 12 data points in steps of ten minutes):

```
12.04.01;15;10;12

0.2
0.4
...
```

- Input function for isotopes
  Each line contains the δ-value of effective precipitation for one time step. Meta data are not given.
  Example:

  −34. 2
  −42. 2
  −17. 5
  ….

EHRENWÖRTLICHE ERKLÄRUNG

Hiermit erkläre ich, dass die Arbeit selbständig und nur unter Verwendung der angegebenen Hilfsmittel angefertigt wurde.

Freiburg i. Br., März 2005